Master's Thesis

Master Earth, Surface and Water

Utrecht University

Hydrogeological Study of the Assasuni Region in Coastal Southwest Bangladesh –

A combined fieldwork and modelling approach to understand changing flow directions

Jan Dirk Smidt

Utrecht, June 2018

Author: **Jan Dirk Smidt**

Student number: **3670945**

University Supervisor:

dr. Amir Raoof (A.Raoof@uu.nl)

Internship Organization:

DeltaMAR project

Internship supervisors:

dr. Paul Schot (P.P.Schot@uu.nl)

Floris Naus, MSc (F.L.Naus@uu.nl)

30 ECTS

Earth Surface and Water
Faculty of Geosciences, Utrecht University
Utrecht, June 2018

Abstract
The Bengal basin in Bangladesh is an area with a large variety in groundwater salinity. To improve freshwater security in the dry season the DeltaMAR project is set up to investigate the implementation of MAR-systems in the region. To improve the sustainability prediction of these MAR-systems it is important to know how different factors in a region are connected and what their implications are regarding the groundwater flow. This thesis combines results of a fieldwork and a modelling study to define the main connections between surface elevation, clay thickness, salinity, infiltration capacity and groundwater flow. This is done by defining distributions of the above-mentioned characteristics within a representative case study area of approximately 40 km^2 (the Assasuni region). The study first confirmed that high elevated areas imply thin clay layers with relative fresh aquifer water due to recent rainwater infiltration. Low elevated areas can contain thin clay layers with saline aquifer water or thick clay layers with brackish aquifer water. Second, regarding the groundwater flow, elevation (including rivers) and pumping are found to be the main drivers. Surprisingly, it is found that groundwater flow reverses direction from high to low elevation during the wet season towards flow from low to high elevation during the dry season because of extensive pumping. Third, the fieldwork conclusions show the net yearly groundwater flow to currently be from the fresh elevated areas towards saline low region. This indicates that the fresh aquifers are not salinizing and the pumping is sustainable. Model results however show the instability of this flow and emphasize the possibility of aquifer salinization when pumping quantities increase or fresh recharge quantities decrease. This emphasizes the importance of quantifying the consequences of irrigation pumping with respect to fresh recharge when predicting the sustainability of a MAR-system.

Acknowledgements

First, I would like to thank dr. Paul Schot and Floris Naus for the opportunity they gave me to contribute in this interesting research project during which I learned a lot and was able to enjoy a fieldwork in Bangladesh. Thereby the meetings we had were very useful. Floris' door was always open and the large amount of knowledge of the region was of great help. The way Paul could simplify complex problems always helped me to look at things from another angle which helped me a lot in the process.

Second, I want to thank Ken Burer, Luc Essink and Ruth Wijland for the great time we had in Bangladesh.

And last a great thanks to all the members of the Delta-MAR project in Khulna and Dhaka University for assisting during the fieldwork. With a special thanks to Abir Zaman and Mahfuzur Rahman with whom I spend the most time.

Table of Contents

1. Introduction 1
1.1 Previous research 2
1.2 Problem definition and aim of this research 6
1.3 Research questions 6
1.4 Hypotheses 7
2. Methods 8
2.1 Data collection from the field 8
2.1.1 Tube well examination 9
2.1.2 Piezometers 9
2.1.3 Gauging groundwater levels 11
2.1.4 Levelling 13
2.1.5 Infiltration experiments 14
2.1.6 Augerhole drillings 14
2.1.7 Interviews regarding the use of mechanical pumps 15
2.1.8 Extra observations 15
2.2 Coupling of field data to conclusions and model 15
2.2.1 Field data to field conclusions 15
2.2.2 Field conclusions to model 22
2.3 Modelling study 22
3. Results & Discussion 24
3.1 Fieldwork 24
3.1.1 Topography 24
3.1.2 Lithology 26
3.1.3 Soil characteristics 29
3.1.4 Pumping 32
3.1.5 Salinity variation 35
3.1.6 Groundwater flow 39
3.2 Coupling of field data to model 51
3.2.1 Modelling goal and research questions 51
3.2.2 Initial model setup 51
3.3 Model 55
3.3.1 Calibration and model performance 55
3.3.2 Model outcomes 57
4. Conclusions and recommendations 64
References 66
Appendix 68

List of Figures

Figure 1-1:	Introduction to location and setting of study area with piezometers and transect used during previous studies within the PhD research	-2-
Figure 1-2:	SRTM map indicating the elevation of the study area. It does not match with the real elevation where the difference between high (orange/red) and low elevated (blue) is between 1 and 2 meters	-3-
Figure 1-3:	Land use map based on satellite interpretation (Naus, 2018)	-3-
Figure 1-4:	Soil map of the study area (FAO, 1959)	-4-
Figure 1-5:	Cross-section of the lithology from N1 (north) to P14 (south) on the transect (van Broekhoven, 2017)	-5-
Figure 1-6:	Cross-section of the electrical conductivity of the groundwater indicating the salinity on the transect (van Broekhoven, 2017). Again, from N1 (north) to P14 (south)	-5-
Figure 2-1:	Locations of previously installed piezometers (of which a part is levelled already) and examined tube wells	-8-
Figure 2-2:	Locations of current fieldwork activities	-9-
Figure 2-3:	Hand-flapper method: A) by placing the hand on the tube a vacuum is created and soil is sucked up. B) The hand is released and soil together with drilling fluid blows out of the pipe. (Horneman et al., 2004)	-10-
Figure 2-4:	A) top view of the double ring infiltrometer (location I3) and B) stick to measure the decrease in water level in the inner ring	-14-
Figure 2-5:	Flow diagram of the construction of the conclusive elevation map	-16-
Figure 2-6:	Flow diagram of the construction of the conclusive clay thickness map	-17-
Figure 2-7:	Flow diagram of the estimation of saturated conductivity values	-18-
Figure 2-8:	Flow diagram of the estimation of a range of representative pumping rates	-19-
Figure 2-9:	Vertical salinity profile for different a-factors and customized distribution Z1 and Z2	-20-
Figure 2-10:	Flow diagram of the constructed salinity distribution	-21-
Figure 2-11:	Flow diagram of the concluded groundwater flow	-22-
Figure 3-1:	Measured elevations during the levelling procedure relative to zero-point N1	-24-
Figure 3-2:	Boxplots representing the topography data obtained by levelling	-25-
Figure 3-3:	Conclusions regarding the surface elevation	-25-
Figure 3-4:	Well-screen depths of piezometers and tube wells indicating the thickness of the clay layer	-27-
Figure 3-5:	Graph to display correlation between surface elevation (measured in levelling procedure) and clay thickness. Piezometers indicate measured clay thickness based on lithology classification and tube wells indicate well screen depths representing the maximum top of the aquifer	-27-
Figure 3-6:	Soil map (FAO, 1959) with depths of the clay layer based on piezometers and tube wells. It must be noted that the soil map is referenced manually so the exact location of different units can differ, the map can only be used as indication of the different units	-28-
Figure 3-7:	Conclusions regarding the clay thickness	-29-
Figure 3-8:	a) Results of the five infiltration experiments: cumulative infiltration in cm versus time in minutes. b) Result of the auger drilling at location A2: Water level measured from surface versus time	-30-
Figure 3-9:	Overview of mechanical pumps found in the selected study area	-33-
Figure 3-10:	Areas with mechanical pumping for rice and combined irrigation	-34-

Figure 3-11:	Spatial salinity variation expressed in electric conductivity (EC) [mS/cm] of the groundwater. Color indicates the EC-value and the shape indicates the depth of the groundwater sample	-36-
Figure 3-12:	An overview of the EC-measurements compared to a) the clay thickness b) the land use and c) relative elevation in comparison with N1. The red text in b and c represents low elevated aquaculture which are expected to by saline	-37-
Figure 3-13:	Conclusions regarding the salinity distribution based on A-factor (see figure 2.9)	-39-
Figure 3-14:	Spatial distribution of equivalent freshwater heads on the 17th of January 2018	-40-
Figure 3-15:	Temporal overview of part of the logger data. The black loggers written in black in the legend represent the loggers in the elevated homestead area and the ones written in red those in the low-elevated aquacultural region	-40-
Figure 3-16:	Boxplots of all logger data for the period February 2017 to April 2018. The piezometers in red are the ones situated at lower elevation in aquacultural ponds	-41-
Figure 3-17:	Cross-sectional profiles of head data measured in the field on the 17th of January and by be the loggers in the dry and wet period	-42-
Figure 3-18:	Weekly averages of daily variation of all loggers. Computed by subtracting the daily minimum from the daily maximum value before averaging all these values for one week	-43-
Figure 3-19:	Hydraulic head variation for 3-day periods a) in the wet season with a lot of rain b) in the wet season with 3 dry days c) between dry and wet without rain during the fieldwork and d) in the dry season. The loggers located in low-elevated qquaculture are shown in red and for locations with 2 well screen depths the vertical flow direction is indicated next to the legend	-44-
Figure 3-20:	Isohypses map and flow directions during the period with most data (between dry and wet); the thickness of the flow lines roughly indicates the amount of groundwater flow	-50-
Figure 3-21:	Isohypses map and flow directions during the wet period; the thickness of the flow lines roughly indicates the amount of groundwater flow	-50-
Figure 3-22:	Isohypses map and flow directions during the dry period; the thickness of the flow lines roughly indicates the amount of groundwater flow	-51-
Figure 3-23:	Boundaries chosen for the model	-52-
Figure 3-24:	Top: Surface of the Modflow model with in blue the constant head cells, grey the inactive cells and in white the active cells. Bottom: Cross section of the indicated row to present the different layer thicknesses	-55-
Figure 3-25:	Observed head versus calculated head for the loggers in the last month of a) the wet period and b) the dry period	-56-
Figure 3-26:	Head distribution of layer 6 calculated in PMWIN by SEAWAT in a) wet period and b) dry period. The circle indicates the area of most severe pumping and the arrows show the flow vectors where the thickness indicates the speed.	-57-
Figure 3-27:	Domains used to analyze the flow in north-south direction with the surface elevation of the model as background	-58-
Figure 3-28:	Cross sectional head profiles of the wet (a and c) and dry (b and d) model. The black circle again indicates an area of mechanical pumping. The scale of b is the same as a and of d the same as c	-59-
Figure 3-29:	Results of the sensitivity analysis regarding the flow between zone A and B for a) the wet model and b) the dry model	-60-

List of Tables

Table 2-1:	Conversion from Electrical conductivity to Chloride concentration (Bot, 2011)	-19-
Table 3-1:	Overview of infiltration experiments with Ks representing the calculated vertical saturated conductivity based on the infiltration experiments	-30-
Table 3-2:	Information obtained for the mechanical pumps shown in figure 3.7	-33-
Table 3-3:	Overview of groundwater extraction rates found in the field	-35-
Table 3-4:	Filter depths of piezometers with logger devices	-39-
Table 3-5:	Observations from the resulting graphs and figures	-45-
Table 3-6:	Overview of initial parameter applied to the model	-53-
Table 3-7:	Initial head values of the rivers	-54-
Table 3-8:	Parameter changes after calibration	-56-
Table 3-9:	Water balance wet and dry model. Values in m^3/day for the whole model domain	-58-
Table 3-10:	Absolute values used in the sensitivity analysis of the models	-60-
Table 3-11:	Calculated flow distances of the groundwater for model and measurements	-63-

1. Introduction

Water availability in southwestern Bangladesh shows a great annual fluctuation with 82% of the annual precipitation (1500 to 3000 mm) falling in the monsoon period (June to October). This is a period with a high amount of river flooding and plenty available water for drinking and agriculture (Mukherjee, Fryar, & Thomas, 2009). However, this abundance of water stops during the dry period in which drinking water options are scarce and groundwater becomes an important source. The area consists of the world's largest and most densely populated delta, the Ganges-Brahmaputra-Meghna (GBM) Delta. The delta is inhabited by 130 million people and comprises an area of 100.000 km^2 (1300 inhabitants/km^2).

The general lithology of the region consists of a clay layer at the surface overlying one or two silty to sandy aquifers of which the first aquifer can reach a depth of about 150 meters (Adhikary, Das Gupta, & Babel, 2011). The thickness of the superimposing clay layer varies regionally between 5 to 45 meters (M. Shamsudduha, Chandler, Taylor, & Ahmed, 2009).

A decrease in fresh water supply during the dry period causes the fresh-salt water interface to move upstream in tidal rivers which results in salinization of large amounts of surface water. As a consequence, areas become unfit for irrigation and drinking purposes (Acacia Water, 2015). Due to the occurrence of these tidal flooding events in combination with low precipitation during the Holocene the main salinity of the groundwater is brackish but has a large spatial variance with patches of fresh water (Ayers et al., 2016; George, 2013; Naus, 2018; Worland, Hornberger, & Goodbred, 2015). The expected sea level rise and extension of the dry period further increases the occurrence of saline flooding and salinization of the water in the region (Acacia Water, 2015; Auerbach et al., 2015).

To increase the freshwater availability and security, UNICEF set up a project with Dhaka University and Acacia Water. The project resulted in the implementation of about 100 Managed Aquifer Recharge (MAR) systems that store fresh water in confined saline or brackish aquifers. During the dry period with high water demand, the water can be pumped up without being affected by surface pollution or salinization. The quality and effectiveness of the implemented MAR-systems varies from great successes to failures, indicating knowledge gaps in their construction (NWO, 2016). To decrease those knowledge gaps, the DeltaMAR project, a collaboration of Utrecht University, Delft University of Technology and Dhaka University was set up in the form of four PhD researches.

The current study is part of the PhD research of Floris Naus that aims at developing a method to predict the performance of MAR-systems in the southwest region of Bangladesh (Future Deltas, 2016). For this MSc thesis a detailed study area, the Assasuni region (figure 1.1) is investigated by a combined fieldwork and groundwater modelling study. This first chapter will discuss the previous research done in the area (parts of the PhD research of Floris Naus), the problem definition and goals of this MSc thesis, followed by the research questions and hypotheses of the thesis.

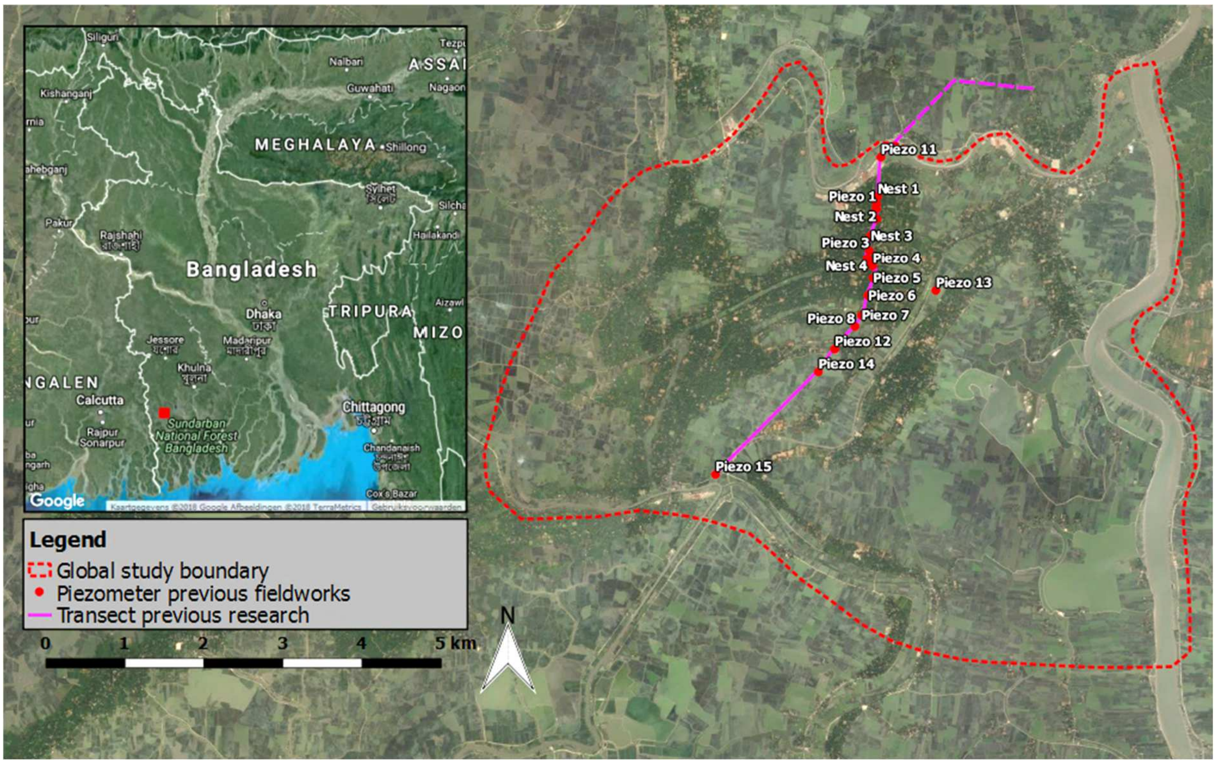

Figure 1-1. *Introduction to location and setting of study area with piezometers and transect used during previous studies within the PhD research*

1.1 Previous research

Within the PhD research of Floris Naus several fieldworks have been conducted to study the southwestern area of Bangladesh. As a first result of these fieldworks, the Assasuni area is chosen to be investigated in further detail because the large variation in land use makes it a complex and interesting region. The overall topography is flat (figure 1.2) with some slightly elevated villages and agricultural fields between lower lying areas with aquaculture in the form of shrimp and fish ponds (figure 1.3). It must be noted that the elevation in the SRTM map (figure 1.2) has an error is the actual elevations and can only be used to roughly indicate regions of relatively high or low elevation (Naus, 2018), the real maximum elevation differences are between 2 and 3 meters. The agricultural fields are divided in areas with clear rice agriculture and areas with a combination of rice and other crop agriculture. Multiple streams surround the Assusuni area: the Morirchap river in the north, the Guntiakhali river in the south and the Kholpetua river in the east. These streams all show to be under tidal influence and vary in salinity through the year with low salinities during the monsoon period that increase during the dry period (Naus, 2018). The variation of the upper soil is mapped by a regional soil study of the FAO (1959), shown in figure 1.4. It generally indicates the higher elevated areas to consist of fluvial silts and the lower lying areas of tidal flat clays.

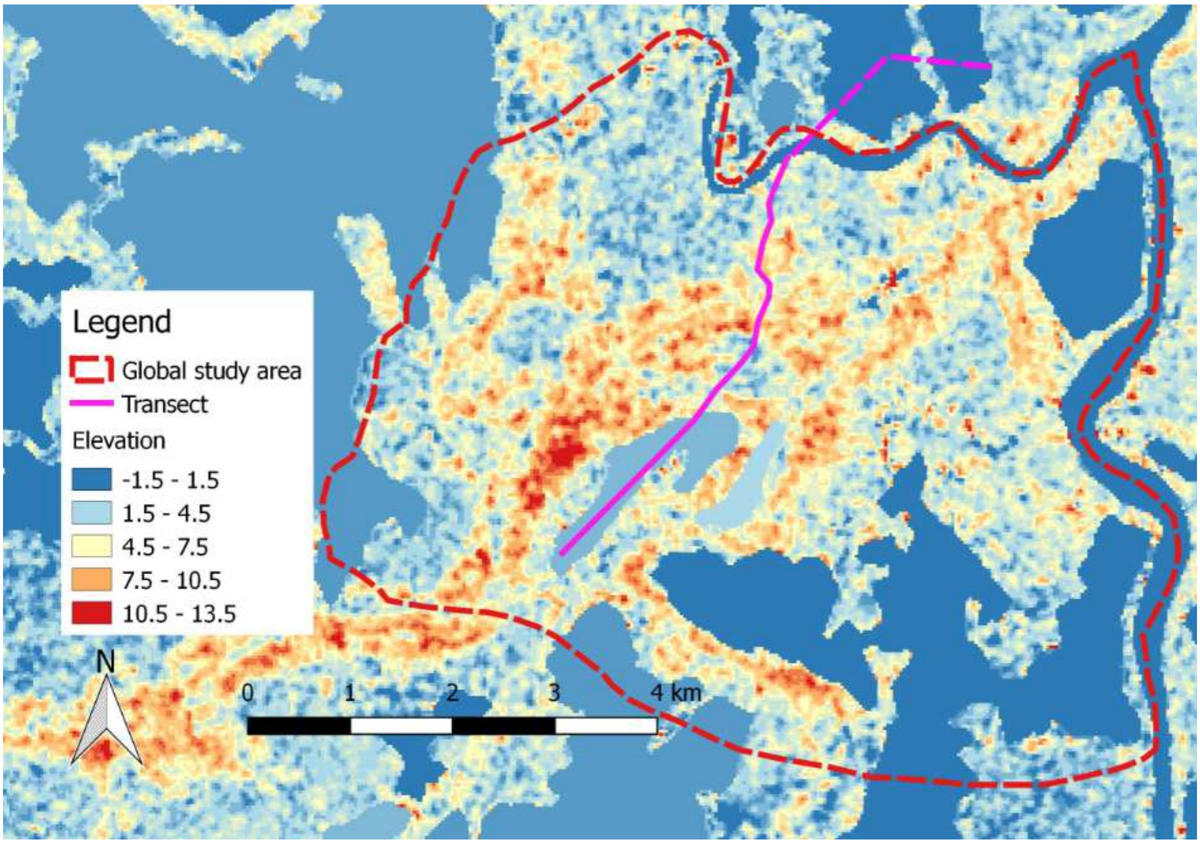

Figure 1-2. *SRTM map indicating the elevation of the study area. It does not match with the real elevation where the difference between high (orange/red) and low elevated (blue) is between 1 and 2 meters.*

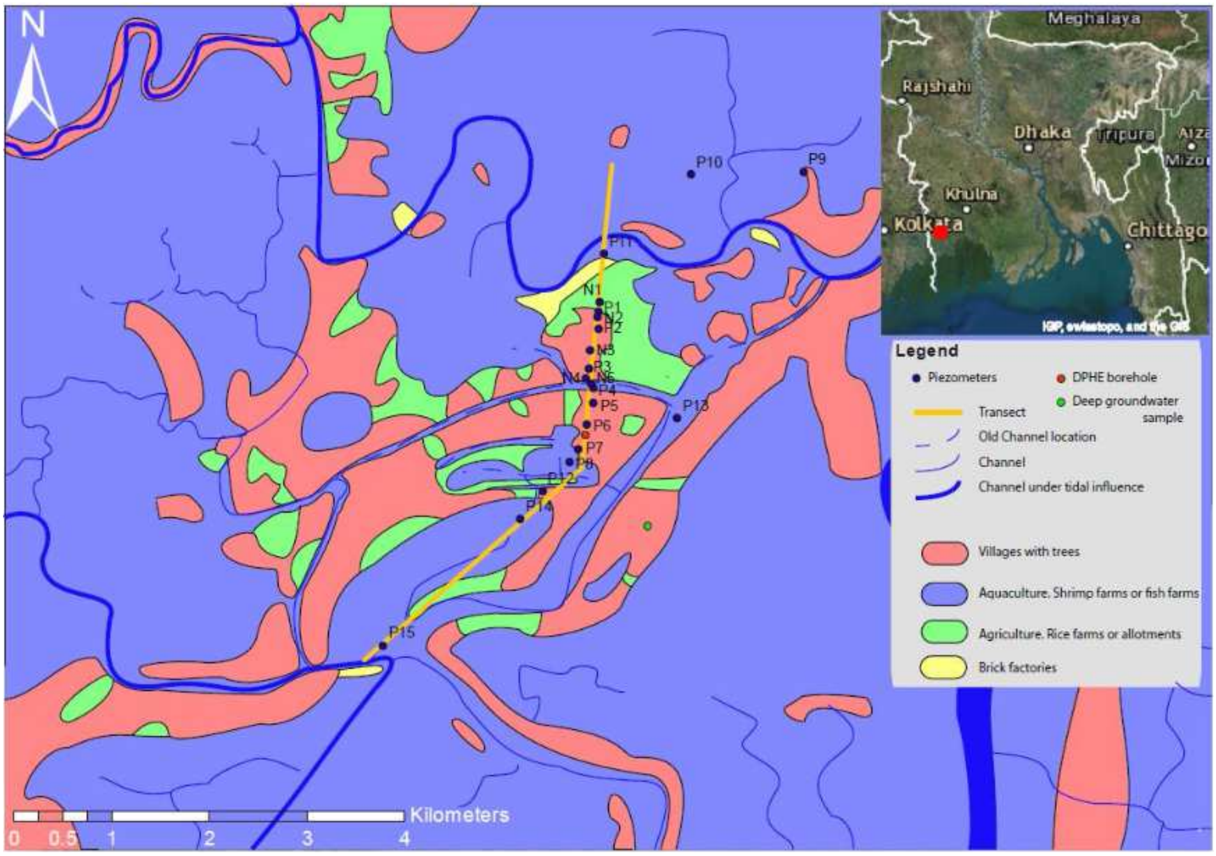

Figure 1-3. *Land use map based on satellite interpretation (Naus, 2018)*

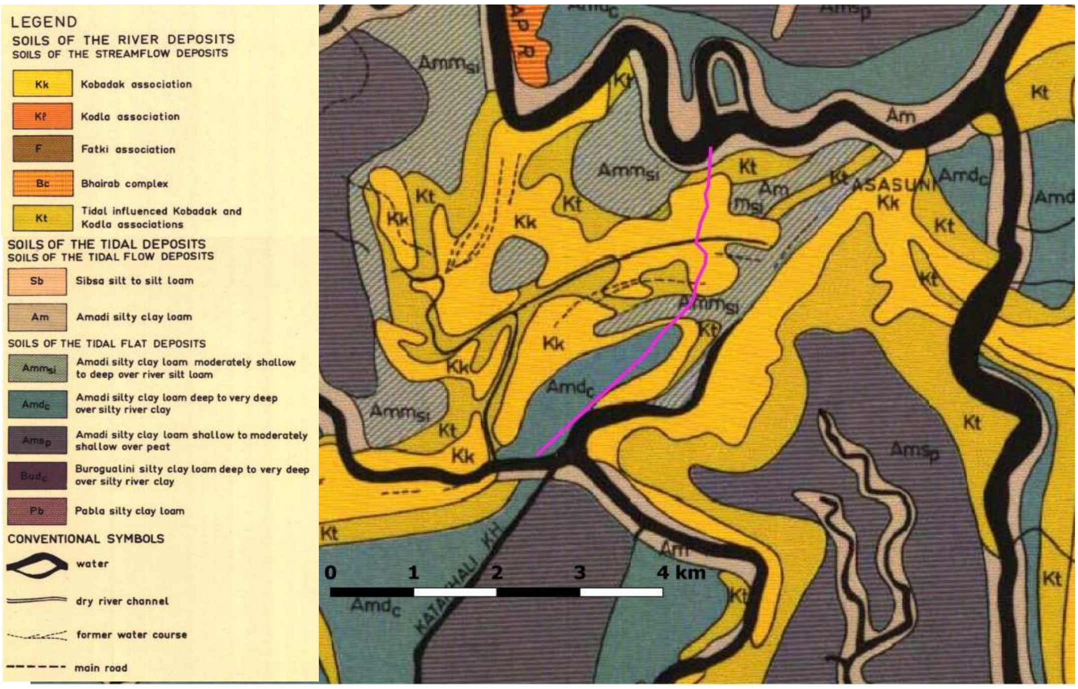

Figure 1-4. *Soil map of the study area (FAO, 1959)*

The Assasuni region is studied in further detail by focusing on a transect situated in the center of the region. Along this transect, multiple piezometers are placed to map the lithology and salinity of the groundwater (shown in figures 1.1). An extensive fieldwork and 2D model of the transect resulted in several conclusions regarding the geologic origin of the connections between elevation, land use, soil and salinity (Naus, 2018; van Broekhoven, 2017) which are explained via the following theoretical reconstruction (Naus, 2018).

1. **Pleistocene fresh conditions**: Deposition of fresh riverine deposits during the Pleistocene.
2. **Transgression in the Holocene**: High sedimentation rates during the transgression in the first part of the Holocene followed by a salinization of the depositional environment due to sea level rise.
3. **Migration of Ganges**: Increase in deposition of silts and clays under brackish to saline conditions due to migration of the Ganges.
4. **Compaction and freshening**: Compaction of especially areas with a thick clay cover and high amount of organic matter. Due to this compaction, the lower lying areas experience more saline flooding and the elevated areas less, resulting in freshening of the groundwater under elevated areas. The rate of salinization of the lower elevated areas increases with decreasing clay thickness.
5. **Erosion and salinization**: Erosion by tidal creeks causing lowering of several areas and salinization of the floodplains. Some of these areas were part of the elevated areas and thus show patches of fresh groundwater.
6. **Human influence and land use influence**: Finally, human influence in the form of saline shrimp farms, construction of polders with dikes and increased pumping for irrigation can have a major influence on the spatial distribution. This influence is currently investigated.

This reconstruction results in the general conclusions that: 1) Elevated areas are underlain by thin clay layers and relatively fresh groundwater (0-300 mg chloride/L) since the elevation protects them from saline flooding and only fresh rainwater infiltration occurs. 2) Non-elevated areas consist of both thin and thick clay layers of which the thick layers caused the lowering of the surface by compaction and the low-elevated thin clay layers originate from erosion of high-elevated areas. 3) The non-elevated regions with thin clay layers consist of saline water (1000-4000 mg chloride/L) due to extensive saline water infiltration during flooding events. In the areas where those clay layers are thick, the groundwater salinity is comparable to the deposition environment (brackish, 300-1000 mg chloride/L) because the thick clay layer acts as a protection from saline water infiltration. The expected lithology and salinity distributions along the part of the transect with a relatively thin clay layer are shown in figures 1.5 and 1.6.

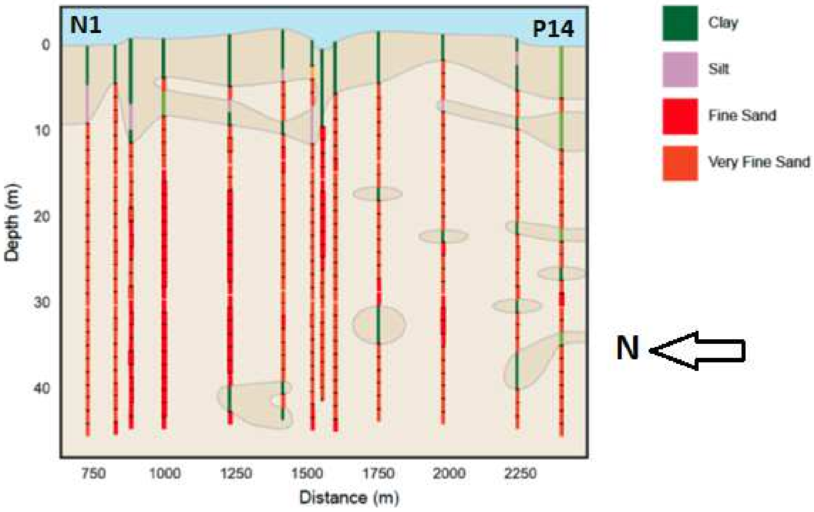

Figure 1-5 Cross-section of the lithology from N1 (north) to P14 (south) on the transect (van Broekhoven, 2017)

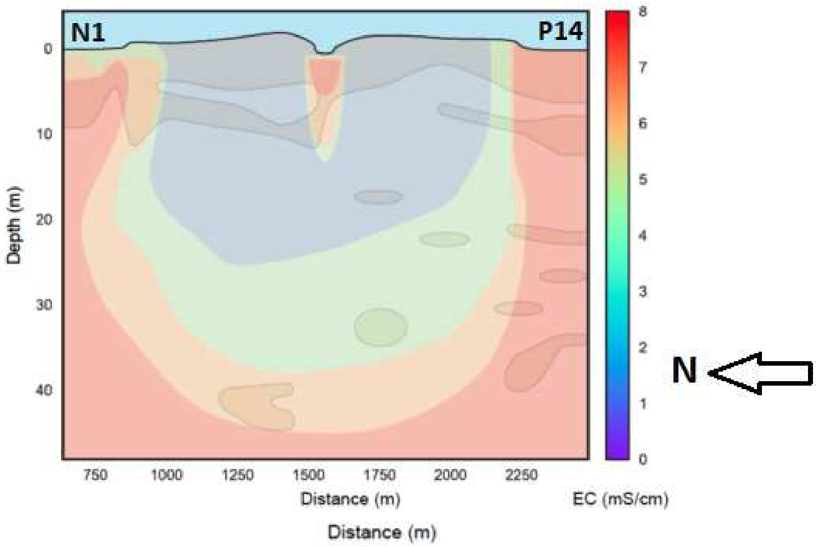

Figure 1-6 Cross-section of the electrical conductivity of the groundwater indicating the salinity on the transect (van Broekhoven, 2017). *Again from N1 (north) to P14 (south).*

The elevation differences shown on the figures are mapped by local levelers. According to the DEM (figure 1.2) and landcover map (figure 1.3) homesteads and agricultural fields are situated at higher elevation since they are highly vulnerable to saline floods. Regions with aquaculture on the other hand need brackish to saline water from the tidal rivers and are situated in lower lying areas.

1.2 Problem definition and aim of this research

As presented above, hydrological changes can strongly alternate the spatial salinity variation. For the prediction of the performance of MAR-systems it is there for very important to understand the impact of current and future scenarios on the groundwater and salinity distribution. Only by acquiring this knowledge it is possible to predict the performance of MAR-systems. Regarding the current situation it is therefore important to understand the hydrogeological flow conditions and drivers behind this flow. Two important aspects when regarding the future scenarios are climate change and anthropogenic influences. The first is represented by an expected extension of dry spells and increased sea level rise (Auerbach et al., 2015). The anthropogenic influences mainly consist of increased groundwater extraction (Mukherjee et al., 2015; Mohammad Shamsudduha, Taylor, Ahmed, & Zahid, 2011) but also decreasing conductivity as a result of ploughing (Neumann et al., 2009) can be important for the future hydrogeological situation. Currently, there is no knowledge of the existing flow conditions or drivers in the region which makes it impossible to predict the future situation.

The aim of this MSc thesis can be divided in two different parts. With at first the aim to map and understand the current conditions of the groundwater flow and salinity. And secondly, to predict how these current conditions may change in the future. Since the Assasuni region has a large diversity with respect to land use and elevation the results can be used in the PhD research of Floris Naus for the prediction of MAR-system performance in southwest Bangladesh.

1.3 Research questions

To reach the objectives stated in the previous section, two research questions and sub-questions are formulated. Again, these are separated in questions regarding the current situation and questions regarding future scenarios.

- **What are the current conditions and drivers of the groundwater-flow and salinity distribution in the Assasuni region?**

  <u>Current situation</u>
  - What is the current topography of the area?
  - What is the current lithological structure of the area?
  - What is the current salinity distribution of the area?
  - What are the current groundwater flow conditions?
    - What are the drivers for groundwater flow?
    - What is the infiltration capacity of the upper clay layer?
    - What is the horizontal/vertical conductivity of the clay and sand?

  - What is the relation between topography, lithology, soil, salinity and groundwater flow?

- **How do the current groundwater conditions evolve in the future under varying scenarios?**

  <u>Future</u>
  - What are important factors that can change the future groundwater situation?
  - What is the influence of these factors on the groundwater situation?
  - At what rate is the hydrogeological situation expected to change?

1.4 Hypotheses

Many location specific hypotheses were formed to determine the required methods throughout the study area during the fieldwork. For convenience, only four of the main hypotheses regarding the fieldwork and modelling study are presented below.

<u>Hypothesis 1: Elevation, clay thickness, land use and groundwater salinity are correlated and elevation is a driver for groundwater flow.</u> First, the effect of elevation on clay thickness and groundwater salinity is based on the theoretical construction presented in section 1.1 (Naus, 2018). Second, elevation differences are known to induce flow, so in this situation with a probable low interaction between surface- and groundwater it is expected that the small elevation differences can induce flow from the higher elevated homestead areas to lower elevated aquacultural pond areas.

<u>Hypothesis 2: Rivers are driving forces groundwater flow.</u> From previous research (Goswami, 2014) it is concluded that the eastern river in the area is in contact with the aquifer and drains groundwater in both the dry and wet season. It is expected that clay depth varies along the river and connection with the aquifer is only the case in areas where the clay layer is thin and the river depth is high, such as the meander halfway the eastern river. Since previous fieldwork in the region (Naus, 2018; van Broekhoven, 2017) found groundwater flow from south to north along the transect, the northern and/or southern river could also act as a driver.

<u>Hypothesis 3: Infiltration rates are low but do influence the hydrogeological situation.</u> The top layer of the whole region consists of clay which is known to have low infiltration capacities. Thereby, several studies conclude that there is no significant infiltration or mixing of water under ponds (Neumann et al., 2009; Sengupta et al., 2008). On the other hand, infiltration of fresh and saline water is regarded as one of the possible processes that result in the current salinity distribution (Ayers et al., 2016; George, 2013; Worland et al., 2015). Combining these two, results in the hypothesis that water does infiltrate with low velocities and is thus an important factor in future scenarios. The effect of infiltration in the current situation is expected to be minimal.

<u>Hypothesis 4: Groundwater extraction in the form of pumping influences current groundwater flow and decreases future groundwater heads.</u> In parts of the region, mechanical pumps extract groundwater to supply agricultural fields during the dry season. Thereby, in total three brick factories are situated in the north of the region and one in the south. These factories also use water for the production process and could extract substantial amounts of groundwater. Whether these groundwater extractions contribute to the hydrogeological situation strongly depends on the extracted quantities. Previous studies (Mohammad Shamsudduha et al., 2011) suggest that the increase in storage capacity due to pumping can limit the effects on future hydraulic heads if the potential recharge is high enough. Since potential recharge is expected to be relatively low (Mohammad Shamsudduha et al., 2011) it is hypothesized that the pumping will decrease the groundwater levels in the future.

2. Methods

For this research the methods are subdivided in three different parts. The first part is a fieldwork with the duration of 24 days (8/1/18 – 31/1/18) to gain supplementary data of the Assasuni area. Extra focus is placed on the areas east- and westwards of the central transect which are not yet extensively investigated by Floris Naus, Msc (2017) during previous fieldworks (section 1.1). The second part of this section explains how the fieldwork results are interpreted and conclusions are drawn regarding the first research question. Thirdly, the general approach and calibration of the modelling study will be discussed.

2.1 Data collection from the field

In this section the different methods used in the field will be discussed together with the reasoning behind the choice of locations for these methods. The fieldwork for the current study was preceded by a fieldwork conducted in 2017 by Floris Naus. From this fieldwork, installed piezometers and EC-measurements of tube wells are especially of great importance. An overview of these previously conducted activities (figure 2.1) is presented below.

Since the exact study area was not known before the start of the current project the first step was to define its boundaries. Here for the northern and eastern rivers are chosen together with the elevated area in the west and the extended river in the south. All of them are expected to represent no or very slow flow conditions. The activities of the current fieldwork are carried out within these boundaries (figure 2.2).

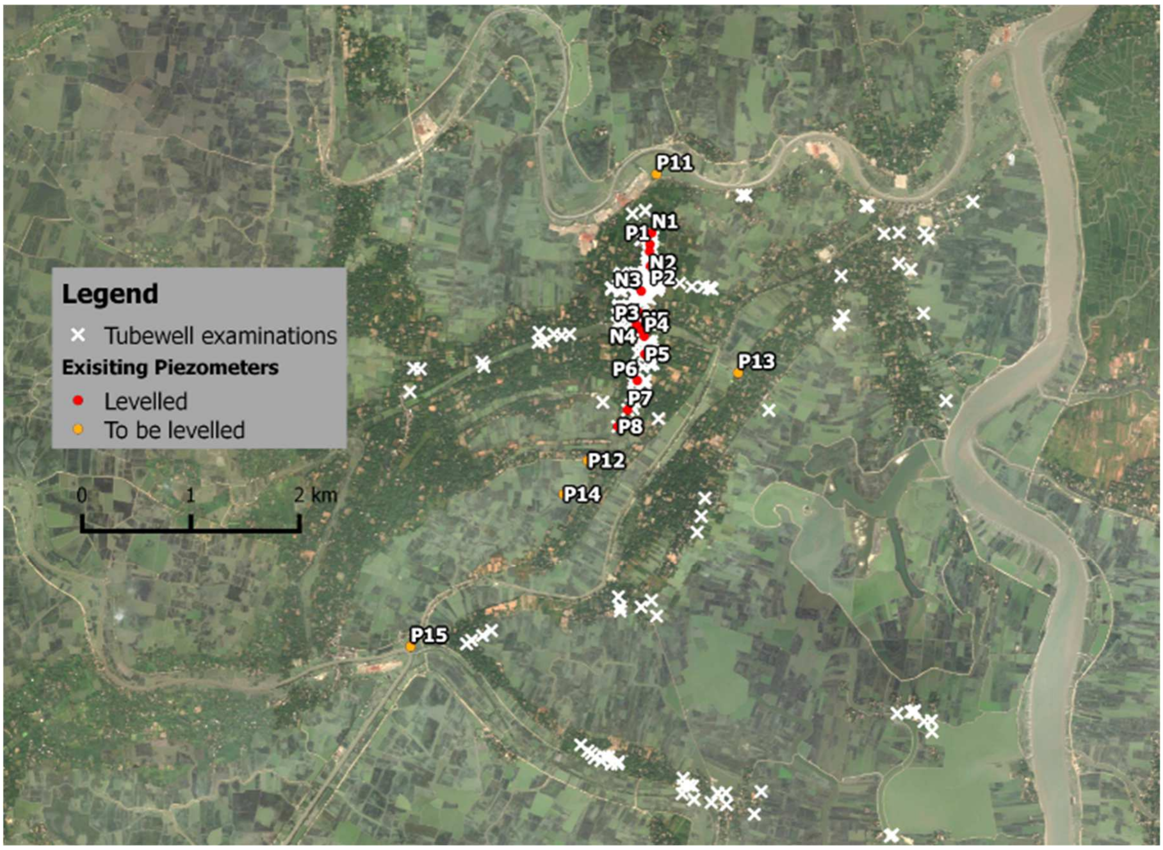

Figure 2-1. *Locations of previously installed piezometers (of which a part is levelled already) and examined tube wells*

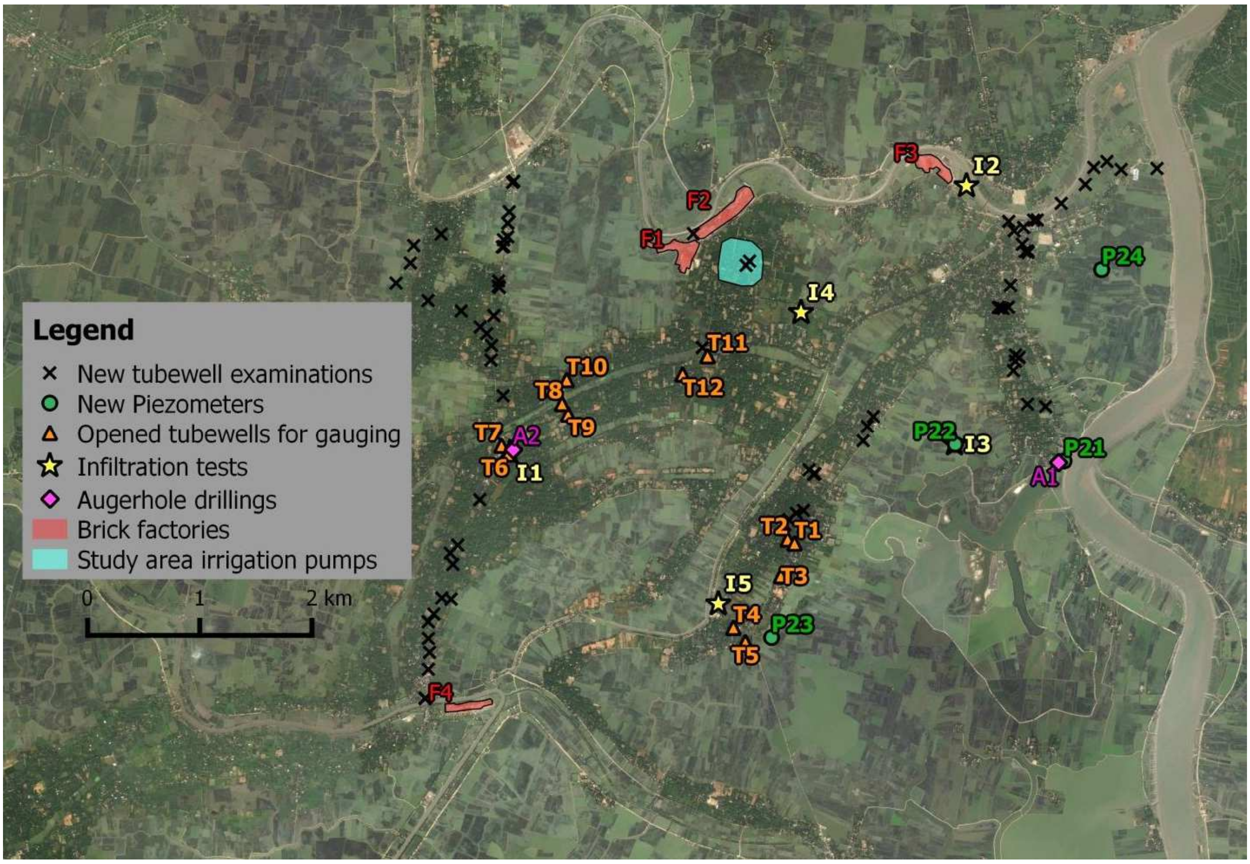

Figure 2-2. Locations of current fieldwork activities

2.1.1 Tube well examination

A simple and fast way to get information about aquifer depth and its salinity is the examination of tube wells. The locations of these tube well inspections were concentrated on both the homestead areas on the western boundary as well as east of the main transect. The wells in the west were primarily used to verify the possible connection between lithology, elevation and groundwater salinity (section 1.1; Naus (2018)). Second, the salinity distribution in east-west direction of this boundary could be used to check the hypotheses of this boundary being a no-flow boundary. The eastern tube well areas were chosen because the database of EC measurements (Naus, 2018) lacked a significant amount of points in this region. As tube wells are almost exclusively present in the homestead areas, only in the northeast some tube wells in between aquacultural ponds close to the river were studied. It was hoped that these tube wells could give some more insight in the interaction between the northern river and the sandy aquifer. In practice all tube well examinations were done by first asking the depth of the well before measuring the EC with an HANNA HI 9829 (Hanna Instruments, USA). With the depth of the shallowest wells per area estimations could be made of maximum clay thickness. It must be noted that this method is very time-efficient but the certainty of well depths is questionable since the owner's memory is the only source of information and many wells are placed some time ago. It is hoped that the fact that the high density examined tube wells decreases this uncertainty.

2.1.2 Piezometers

2.1.2.1 Measurement procedure

For the drillings the traditional 'sludger' or 'hand flapper' method was used (Horneman et al., 2004). This method is common in Bangladesh for the drilling of wells and is done by a team of three drillers. With a bamboo pole construction, a lever is constructed to move a hollow pipe up and down into the drilling hole accompanied by drilling fluid from a nearby pond. During the shaking movement, soil is sucked out of the ground by creating a vacuum in the pipe. This vacuum is created by closing the top of the pipe with the hand during the upward movement, during the downward movement the vacuum is released by opening the top of the pipe (figure 2.3). At this stage, soil with drilling fluid will blow out of the pipe and is collected in a bucket. The total depth of all four drillings is 46 meters (150 feet) and a soil sample from the bucket is collected every 1.52 meter (5 feet) to create a complete soil stratigraphy. After drilling, the filter is placed at the depth where more information is required. This was in all cases the top of the first (and only) sand layer.

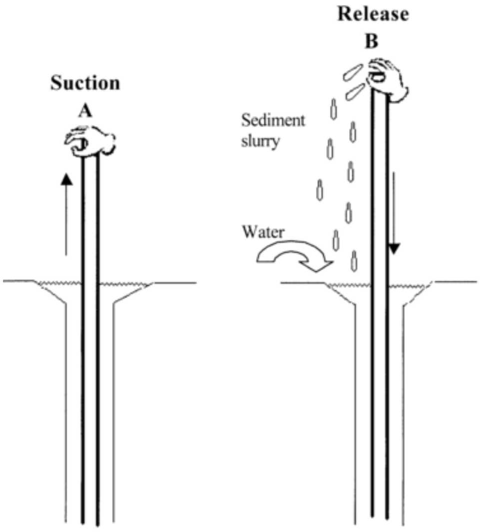

Figure 2-3. *Hand-flapper method: A) by placing the hand on the tube a vacuum is created and soil is sucked up. B) The hand is released and soil together with drilling fluid blows out of the pipe. (Horneman et al., 2004)*

2.1.2.2 Locations

In areas without tube wells, such as regions of aquacultural ponds, tube well examinations are not possible. Since the drilling of a piezometer gives a detailed insight in the lithology and can be easily used for head measurements their placement a very important and useful source of information. Regarding the available time of the fieldwork four locations were chosen to place a piezometer.

All four piezometers are placed on the eastern side of the model. This choice is made because the eastern region consists of a large area of aquacultural ponds and thus a shortage of tube wells. Thereby, it is hypothesized that the eastern river could be an important driver of the study areas flow conditions and that it contains a variation in clay thickness (hypothesis 2). These two factors together resulted in the decision to investigate this part in more detail instead of spreading the piezometer constructions over the west and east.

Piezometer 21 next to the meander in the eastern river is not necessarily placed on a location without any tube wells but is chosen for its position next to the eastern river where it is hypothesized the river and aquifer could be in connection (hypothesis 2). It is valuable for both the lithology and for logging the head conditions during a day or tidal cycle. The other three piezometers are placed in between aquacultural ponds where no tube wells are present. West of the meander in the eastern river piezometer 22 is especially useful to learn about the lithology and determine the connection between the river and elevated homestead areas in the central area. Piezometer 23 in the south is also suitable for the lithology but is mainly installed to monitor the daily cycle of the groundwater level so this can be used to interpret head measurements of the tube wells (discussed later in this section). At last piezometer 24 in the northeast is placed near the connection of the northern and eastern river to examine whether old river paths influenced the lithology of this area. During the process of choosing locations for the piezometers, the fact that piezometer 21, 22 and 23 had to be levelled and thus should be easy to reach by foot was also considered. The levelling process will be explained later in this section and is necessary to determine the relative height of the piezometer and thus groundwater level. It would have been useful to place a piezometer on the western transect as well to test whether it indeed acts as a no-flow boundary, unfortunately this was not possible in the available time.

2.1.3 Gauging groundwater levels

2.1.3.1 Measurement procedure

As mentioned, it was not possible to place many piezometers. However, for the construction of the model it is important to test some hypotheses on the overall and local flow patterns. Here for twelve tube wells were disassembled by a mechanic to measure their head with a water level sensor. During these measurements the time was notated so the level could be referred to head measurements that are done during a daily cycle in nearby piezometers. This way the chance of measuring temporal instead of spatial differences is decreased to a minimum. Strict care had to be taken during the choice of tube wells since extensive pumping in the vicinity could highly influence the measurements. Also the use of the water level sensor causes some uncertainty (± 5 cm) since it was difficult to exactly determine the water level.

The hydraulic head measurements over a daily cycle were conducted with 'Keller' logger devices that measure the exerted pressure every 20 minutes. Eleven of these devices are being used to measure the year-round head values of previously placed piezometers in the region (Naus, 2018). These loggers provide pressure data from February 2017 up to the end of April 2018. For the duration of about 8 hours (from ± 9:00 AM to ± 5:00 PM) three of them were displaced to the newly installed piezometers (see section 2.1.2) 21, 22 and 23 to gain some insight in their short-term temporal variance. This variance was compared to the head measurements from disassembled tube wells and was used for the analysis of the groundwater flow patterns. To summarize, the head data consists of long-term pressure head data from eleven previously installed piezometers, short-term pressure head data for the three newly installed piezometers (P21, P22, P23) and single water level data for the 12 opened tube wells and for piezometer 12. For analysis of the groundwater flow it is important that all these measurements are corrected for their density differences due to salinity, this procedure is explained in the next section.

2.1.3.2 Density corrections

As stated above, the obtained data must be corrected for density differences. Thereby, to compare the pressure heads measured by the loggers with the water levels measured in the tubes and piezometer 12 it is necessary to equally express both variables. In this case the hydraulic head is chosen to represent both measurement techniques. A method presented by Essink (2001) is used for these conversions. First the conversion of the water level measurements will be explained.

Since hydraulic heads are influenced by density differences, the method uses a fictive freshwater head to present the hydraulic head values independent of water density and thus salinity. The equation for the fictive freshwater hydraulic head is:

$$\varphi_f = h_f + z \quad \text{[equation 2.1]}$$

With φ_f as fictive freshwater hydraulic head in meters, z as elevation of the well screen in meters and h_f as fictive freshwater pressure head in meters calculated with:

$$h_f = \frac{\rho}{\rho_f} h \qquad \text{[equation 2.2]}$$

Where ρ represents the density of the groundwater in kg/m^3, ρ_f the density of fresh water (1000 kg/m^3) and h the pressure head of the groundwater in meters. This pressure head of the groundwater is calculated with the general equation for the hydraulic head:

$$\varphi = h + z \qquad \text{[equation 2.3]}$$

This hydraulic head φ is the value that is measured as the water level in the tube wells and piezometer 12 and z is the elevation of the well screen that is either measured or asked. By rearranging the above equations, the equation shown below can be used to convert the measured hydraulic head to the fictive fresh water hydraulic head.

$$\varphi_f = z + \frac{\rho}{\rho_f}(\varphi - z) \quad \text{[equation 2.4]}$$

The only unknown in this equation is the density of the groundwater ρ, this is obtained via a lookup table relating the electric conductivity of the groundwater to the density (Bott, 2011).

The procedure for the logger data is different since the loggers provide the exerted pressure instead of the water level in the well. Nevertheless, the overall method for the procedure is the same as for the head measurements. First, the pressure exerted by the water (P_w) is calculated by subtracting the atmospheric (P_{atm}) pressure from the measured pressure (P_{meas}), all in unit Pascals:

$$P_w = P_{meas} - P_{atm} \quad \text{[equation 2.5]}$$

The atmospheric pressure in this equation is represented by the atmospheric pressure measured by logger 3. This is the case for all logger data because large atmospheric pressure variances within the relatively small area are not expected. The water pressure (equation 2.5) is used to calculate the length of the water column above the logger, y in meters:

$$y = \frac{P_w}{\rho g} \qquad \text{[equation 2.6]}$$

Where g represents the gravitational acceleration of 9.81 m/s^2 and ρ is again obtained via measurements of the electric conductivity (Bott, 2011). This water column length in turn is converted to hydraulic head of the groundwater by using the length of the logger L and the elevation of the top of the pipe, x, where the logger is adjusted:

$$\varphi = x - L + y \qquad \text{[equation 2.7]}$$

From this groundwater hydraulic head, the fictive freshwater head of the loggers is calculated by subsequently computing the pressure head with equation 2.3, the freshwater pressure head with equation 2.2 and the fictive freshwater head with equation 2.1. By substitution of the above equations the general formula to obtain the fictive freshwater head from the measured logger pressure becomes:

$$\varphi_f = \left(\frac{\rho}{\rho_f} - 1\right) z + \frac{\rho}{\rho_f}\left(\frac{P_w}{\rho g} - L\right) + x \quad \text{[equation 2.8]}$$

Since the logger data consist of series of measurements per location, a python script is used to calculate each single fictive freshwater head. The period during which the tube well measurements were performed (17th of January between 9:20 AM and 16:40 PM) is extracted from the logger data and maximum, minimum and average values within this period are obtained. Since the range of these values is relatively small, the average of the logger data within the time period of tube well measurements is used to compare the two measurement types.

2.1.3.2 Locations

The locations of the tube wells are based on the areas where more information on the flow was required. Thereby it is important that the tube well is not located near any operating (mechanical) pumps that would influence the temporal groundwater level in the well. In general, three regions were chosen, all consisting of a group of measurements to visualize the local differences and to decrease the possibility of wrongly interpreting local deviations or errors during the measurements.
The first group of five tube wells is situated in the southeast of the study area because the model boundary at this location does not exist of a natural river so it is not possible to assume a no-flow boundary. There also had not been any previous measurements in the vicinity so these head measurements together with the piezometer information were the only information available from the field.
The second group of tube wells is west of the main transect and consists of seven well measurements. It is firstly chosen to gain insight in the possible flow from the western boundary towards the east, secondly to measure possible flow from the east-west orientated homestead area towards the northern or southern aquacultural ponds and thirdly to detect a possible east-west oriented flow component near the main transect.

2.1.4 Levelling

To couple and interpret the water levels found in both the piezometers and tube wells it was important to know the relative height of each gauging point. This was measured by a team of three levelers using a leveling stick and a digital leveling station of the type TopCon ES series. In short, the procedure worked with the station first measuring the height of the stick backward, after which the stick was moved to a point further on the route. When this height was measured the station would be replaced to a point further on the route to calibrate itself to the last leveled point where the stick is still placed.

During a previous fieldwork (Floris Naus, 2017) this leveling procedure was already conducted for the piezometers P1,P2,P3,P4,P5,P6,P7 and P8 and nests N1, N2, N3, N4 and N5. Here for nest N1 was used as zero-point. For this reason, the leveling team used nest N1 as zero-point again this year to level the existing piezometers P11, P12, P13, P14, P15, new piezometers P21, P22 and P23 (P24 was not levelled due to is remote location) and tube wells T1 to T12. The leveling procedure was supervised to make sure the right points were measured. During a check near the end of the leveling process the deviation at the zero-point showed to be 0.3 mm, at this moment T1, T2, T3, T4, T5 and P12, P13, P14, P15 were leveled. During this leveling procedure the water levels of the eastern, northern and southern river were also measured. The points in between the piezometers and tube wells are saved as well to gain an overview of the topography of the region. This levelling method is very time-consuming but has a high accuracy which is required since head differences are expected to be low.

2.1.5 Infiltration experiments

The infiltration of water through the clayey soil towards the underlying sandy aquifer is one of the important yet challenging aspects of this study. Therefor some experiments were performed to learn more about the rate and process of infiltration. Knowing the full infiltration process and rate is beyond the scope of this research and would require more time and extensive experiments in the field. Nevertheless, four infiltration experiments with a double ring infiltrometer (figure 2.4a) were performed at different locations throughout the area. The two rings were both part of PVC pipes and had diameters of respectively 13.5 and 23 cm. During the measurement the two tubes were placed in the soil to a depth of 7 cm after which first the outer tube was filled with water to a reference height of 25 cm above soil level. Subsequently the inner tube was filled with water to the same height, from this point on the time was measured until the water level dropped with 1.5 cm, at this point water in both the outer and inner tube was added to the initial level. Water in the outer ring was measured with a line on the inside of the ring and of the inner ring with a stick inside the ring (figure 2.4b). A plastic bag was placed over the two rings to decrease evaporation. The method of measuring the rate of decrease is prone to error because it is done by human eye and could have been performed more precise with a Mariotte's bottle but this was not available and for the scope of this research this method is sufficient. Also, the time of the experiments was limited (1-2 hours) which decreases the certainty of the measured values but since the aim of the experiments is to better understand the different behaviors this is not a problem.

The locations of these infiltration experiments are based on the different land uses. I1 is situation next to the northern river in recent deposited clay, I2 is based on clayey silt and clay in an elevated homestead area which is deposited longer ago, I3 and I4 are both located on lower lying areas with I3 in an empty aquacultural pond with wet clay and I4 in a rice field with dry clay. Experiment I5 is conducted in an unused rice field within an area of elevated homestead.

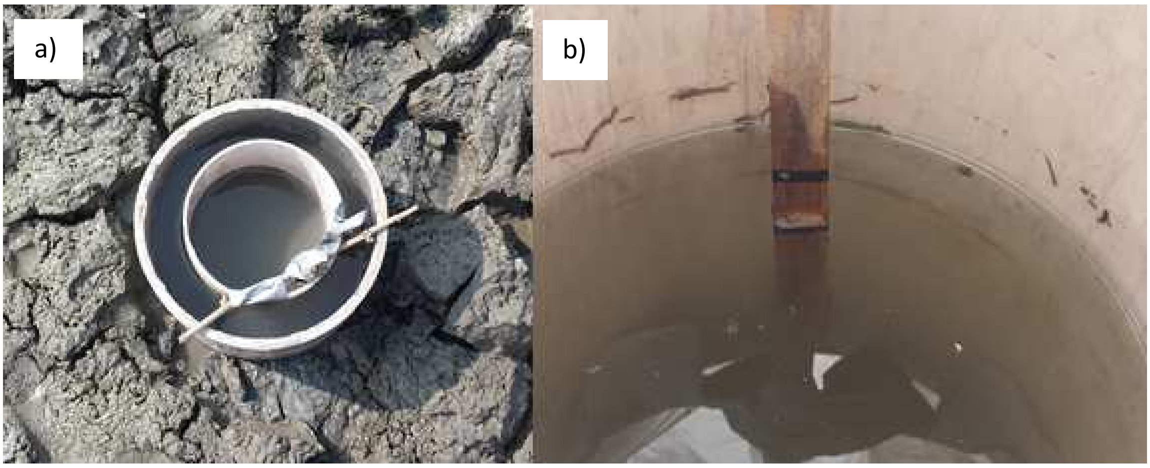

***Figure 2-4**. A) top view of the double ring infiltrometer (location I3) and B) stick to measure the decrease in water level in the inner ring*

2.1.6 Augerhole drillings

Some shallow hand drillings with an Edelman hand auger were performed to get more insight in the behavior of the top layer of the soil. Due to available time and the high demand of the hand auger during the fieldwork only two auger drillings were achieved. During an auger drilling the focus was on the presence and movement of water into or out of the drilling hole. Thereby the soil was classified after being drilled up. The two locations were chosen in such a way that they covered both an area of relatively young soil close to the river as well as older soil in the homestead area. After drilling, the increase or decrease of water is closely monitored to learn more about the suction behavior of the fine top layer. This way it was hoped some more insight was gained in the behavior of the clayey topsoil.

2.1.7 Interviews regarding the use of mechanical pumps

Since mechanical pumps are expected to influence the groundwater flow their use cannot be neglected. Two types of land uses were expected to use mechanical groundwater pumps and thus influence the groundwater flow; brick factories and rice fields (hypothesis 4). The brick factories in the research area are mostly situated in the north with only one located in the south. They were all visited and with the use of interviews, observations and some simple bucket tests the number of pumps together with the timing and quantity of pumping was obtained. Mechanical pumps used for irrigation of rice fields and other agriculture were less straightforward to investigate. An area of 0.13 km^2 in the northern part of the research area was chosen as representative area for rice field agriculture. In this area the number of mechanical pumps together with again their timing and quantity of pumping was obtained by interviews. Thereby, the area of rice fields irrigated by one pump was roughly estimated by interviewing the local population. This was however challenging because the owner wasn't present at all pumps and different estimations were given for pumping frequency and area of irrigation. This makes the pumping analysis only a rough estimate rather than an exact examination of the pumping quantities. To increase the estimates literature values for crop demands are compared to the results.

2.1.8 Extra observations

Besides the above-mentioned activities, observations regarding the landcover and salinity of surface water (rivers, fish ponds, irrigation areas and village ponds) in the region were closely documented. With this information it was possible to verify the landuse-map based on the combination of satellite imagery (figure 1.3). The monitoring of the surface water salinity is important for the analysis of the salinity distribution of the region.

2.2 Coupling of field data to conclusions and model

After collecting field data, conclusions regarding the first research question are formed *('What are the current conditions and drivers of the groundwater-flow and salinity distribution in the Assasuni region?'*). These fieldwork conclusions are used for a modelling study. This section provides the methods used for the coupling of the field data to the field conclusions as well as the methods to couple these field conclusions to the model. The accuracy of this method is limited since the amount of data is small compared to the area of the region. The created maps and flow patterns will provide information on the general situation but will not be able to correctly represent all the small-scale processes.

2.2.1 Field data to field conclusions

The field data are obtained by point measurements while the conclusions regarding the fieldwork are required in the form of area-covering maps. Therefor the field data was combined with area-covering maps as the SRTM-map (figure 1.2), landuse-map (figure 1.3) and soil map (figure 1.4) to extrapolate the obtained point data. This section will cover the different methods used to obtain the conclusions regarding the fieldwork and show flow diagrams of these methods in which black boxes indicate available data and red boxes information created by interpretation of data during this study.

2.2.1.1 Topography

The concluding figure representing the surface elevation is constructed by manually extrapolating the point measurements obtained by the levelling procedure to planes with equal elevation in QGIS. For this extrapolation the different land use categories (figure 1.3) are taken as reference for equal elevation. These are checked with the SRTM-map (figure 1.2). Boxplots of the relation between land use and measured elevation are constructed to validate the method of using the land use as indicator for the surface elevation. A flow diagram of this methods is presented in figure 2.5.

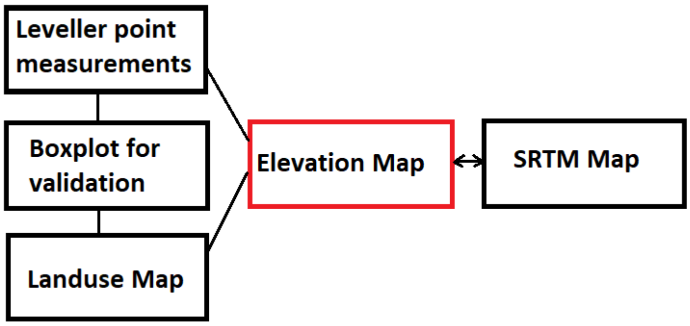

Figure 2-5. *Flow diagram of the construction of the conclusive elevation map*

2.2.1.2 Lithology

The measured point data (tube well depths and borehole logs) must be extrapolated to obtain an area covering conclusive map. Here for extra predictive elements for clay thickness are used. Previous fieldwork and modelling studies (Naus, 2018; van Broekhoven, 2017) suggest a connection between the thickness of the clay layer and the surface elevation (section 1.1). Since this connection originates from changes in depositional environment it is hypothesized that besides the elevation, the FAO soil map is an indication for clay thickness as well.

To check the correlation between the surface elevation and clay thickness, a scatter plot is created. For the piezometers the clay thickness is measured by soil classification and for the tube wells the depth to the well screen is used as indication for the clay thickness. The surface elevations from the levelling procedure are used for this graph of which the outcomes are presented in section 3.1.2.

The overall conclusion regarding the clay thickness is obtained by manually extrapolating the point measurements of tube wells and piezometers to areas of equal thickness in QGIS. Here for the created elevation map and soil map are combined to create clay thickness-areas based on the theory of sedimentation if this is confirmed by the data. In practice this means that first areas of equal clay thickness are created, based on the formation theory. Hereafter the exact values of these areas are chosen based on the field measurements which are also used to check the appointed areas (figure 2.6).

Figure 2-6 Flow diagram of the construction of the conclusive clay thickness map

2.2.1.3 Soil Behavior

The investigation of the soil behavior is intended to learn about water movement in the superimposing clay layer in horizontal and vertical direction. The fieldwork was used to calculate and get a feeling with conductivity values based on infiltration experiments, auger hole drillings and an analysis of tidal influence on the groundwater level. Via a combination of these fieldwork activities, previous fieldwork campaigns and literature, values are estimated for the horizontal and vertical saturated hydraulic conductivity of clay and sand.

First the vertical saturated hydraulic conductivity of clay is regarded by analyzing the infiltration measurements. The results of the experiments are analyzed using the Phillip equations (Philip, 1969):

$$i(t) = St^{\frac{1}{2}} + At \qquad \text{[Equation 2.9]}$$

$$v(t) = \frac{1}{2}St^{-\frac{1}{2}} + A \qquad \text{[Equation 2.10]}$$

With i(t) being the cumulative infiltration over time, S the sorptivity, t the time and v(t) the infiltration rate over time. A is a parameter that is described with equation 2.3:

$$A = Km \qquad \text{[Equation 2.11]}$$

where K is the hydraulic conductivity in unit length per time and m is a constant equal to $\frac{2}{3}$. By plotting the cumulative infiltration and infiltration rate, values for A and S are estimated which results in a value for K. The different values found via this procedure are compared to literature to decide whether they are reliable or not. Based on this comparison a rough estimate of the Ks-value is obtained.

For the horizontal hydraulic conductivity of clay, the water table in the auger drilling is analyzed with the method of Beers (1983):

$$k = C\frac{\Delta y}{\Delta t} \qquad \text{[equation 2.12]}$$

Where k is the conductivity in m/day, Δy is the water level rise [cm] over time Δt [seconds]. The value C is based on the average water level in the auger hole and the depth of the hole in comparison to the groundwater level and can be found via a graph (van Beers, 1983). The outcome of this procedure is again compared with literature before it is decided if it is a reasonable estimate.

For the horizontal hydraulic conductivity of sand two measurements are used. The first is a pumping test performed at a MAR site in the Assasuni region (Acacia Water & Dhaka

University, 2015). Second, a combination of logger data next to the eastern river at piezometer 21 and river level measurements of this eastern river is used to indicate the horizontal sand conductivity as a check of the value obtained from the pumping test. With known values for the tidal period of oscillation (τ [0.536 days]) and distance (x [15.5 m]) between the river and piezometer combined with an estimate of the specific yield (S [-]) and measurements of the amplitude attenuation of the river (A [-]), the transmissivity T [m^2/day] of the aquifer can be calculated with the following equation (Rotzoll, Gingerich, Jenson, & El-Kadi, 2013):

$$T = \frac{x^2 S}{ln(A)^2 \tau} \qquad \text{[equation 2.13]}$$

With the known thickness of the aquifer (d) from piezometer 21 the conductivity (K) can then be calculated (K=T/d) to check if the value found at the pumping test is representative. Since there were no measurements regarding the vertical conductivity of sand this is estimated via literature.

An overview of the methods used for the estimation of the different conductivity parameters is presented in figure 2.7.

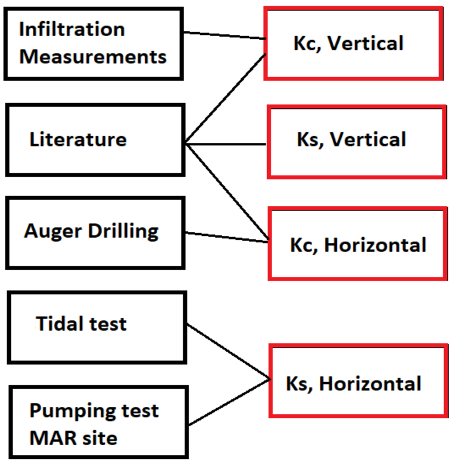

Figure 2-7 *Flow diagram of the estimation of saturated conductivity values*

2.2.1.4 Pumping

The research on the pumping focused on mechanical wells for brick factories and for irrigation purposes. Because the latter was not possible to record for the whole area, a region of about 13 hectares (0.13 km^2) was chosen to investigate the pumping frequency and intensity. The locations of these factories and irrigation study area are shown in figure 2.2. In this region of 13 hectares the goal was to obtain pumping durations, operation months, pumping rates and areas of irrigation for all mechanical pumps present. With these values it is possible to calculate the annual pumping rate in m^3/m^2. This is done by taking the average of all the above-mentioned parameters and multiplying the pumping rate [L/s] with the annual operation time (months in operation x 30.5 days per month x pumping hours per day) before dividing this total value by the average irrigation area. This value is then compared to literature values for the demand of dry-season rice to estimate a realistic range of pumping values. It must be noted that this final estimation is based on interpretation and not on any calculations. Figure 2.8 shows the flow diagram of this method.

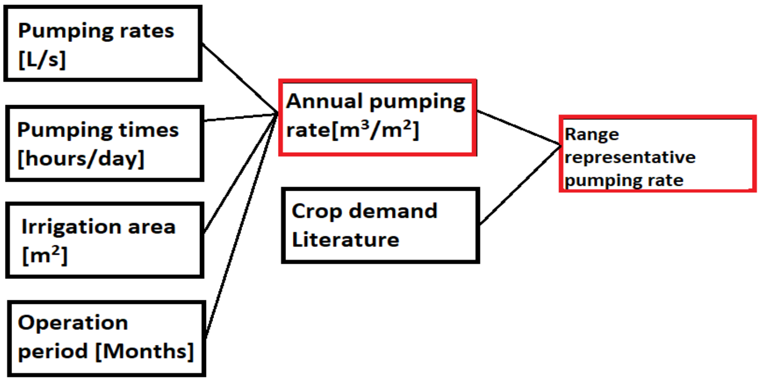

Figure 2-8 Flow diagram of the estimation of a range of representative pumping rates

2.2.1.5 Salinity variation

Previous research (Naus, 2018; van Broekhoven, 2017) concluded elevation and lithology to be indicators of salinity (*hypothesis 1* and explained in section 1.1). For the current salinity distribution this hypothesis is first tested before applying it in the current method of constructing the salinity distribution.

This testing is done by analyzing tube well measurements (section 2.1.1), samples from piezometers (section 2.1.2), surface water measurements and surveys to create a spatial overview of the water salinity in QGIS. During these measurements the salinity is represented by the EC of the water sample. The vertical extent of the region is divided in surface water (rivers, fish ponds, irrigation areas and village ponds), water in the confining clay layer and water in the sandy aquifer. For the resulting maps chloride concentration is used to represent the salinity of the groundwater because seawater is the main source of water salinity in the region and chloride contributes most to the salinity of seawater (Bot, 2011). The conversion table used from EC-value to chloride concentration is shown in table 2.1.

Table 2-1 Conversion from Electrical conductivity to Chloride concentration (Bot, 2011)

Electric conductivity [mS/cm]	Cl^- [mg/L]
0	0
1.350	500
2.700	1,000
5.400	2,000
8.100	3,000
13.400	5,000

For the surface water analysis self and previously conducted EC-measurements (van Broekhoven, 2017) are combined with interviews with local inhabitants. The latter is used as main source for the investigation because surface water in aquacultural ponds, village ponds and on agricultural fields can be highly time variable and is influenced by anthropogenic behavior.

Unfortunately, it was not possible to perform any tests on the salinity of the confining clay layer. Here for the conclusion from the previous fieldwork (van Broekhoven, 2017) must be used in this study as well. That is, that the distribution is like that of the surface- and groundwater.

In the case of the groundwater, many EC-measurements of water originating from the depth of the well or piezometer filter are conducted (section 2.1.1 and 2.1.2). The spatial overview is statistically (boxplots and line graphs) compared to the elevation and clay before deciding if the hypothesis can be used for the construction of the salinity distribution. This salinity distribution is then manually constructed in QGIS by using the proven or a newly confirmed theory. For example, in the case of proving *hypothesis 1*, elevated areas with thin clay layers would be assigned with thick fresh water layers.

Since the groundwater salinity varies in both lateral as vertical direction a method is constructed to visualize these different depth profiles. This method comprises a factor (the a-factor) which indicates the distribution of salinity layers of subsequently 150, 500, 1500, 2500 and 4000 mg/L. These values are based on *Oude Essink, van Baaren, & de Louw* (2010) with 150 mg/L representing fresh water between 0 and 300 mg/L, 500 mg/L representing brackish water between 300 and 1000 mg/L and the higher values all representing saline water in the range that it is found in field measurements. The advantage of this method is that it represents the 3-D salinity variation on a 2-D map and that it can also be implemented in a model relatively easy. In the method it is assumed that deep water is all very saline (4000 mg/L) since there are no measurements at this depth and it is salinized after brackish to saline deposition by density driven flow. Whether this is a correct representation is highly uncertain, but especially the top 70 meters are investigated so this uncertainty is manageable.

The distribution is based on the theory that the groundwater is salinizing downwards between 0 and 70 meters depth due to infiltration of fresh water at the surface (section 1.1) The a-factor determines to what extent this distribution is skewed. For a=1 the 70 meters are equally divided in 4 layers of 17.5 meters where this distribution shifts towards thicker layers of fresh water if *a* is decreased and thicker layers of saline or brackish water when a is increased. Figure 2.9 shows the vertical salinity distribution for the different a-factors that are used. Because some zones could not be created with an a-factor, two customized vertical salinity distributions are created (Z1 and Z2). This vertical distribution is very rough since spatial salinity measurements only represent the salinity at one particular depth.

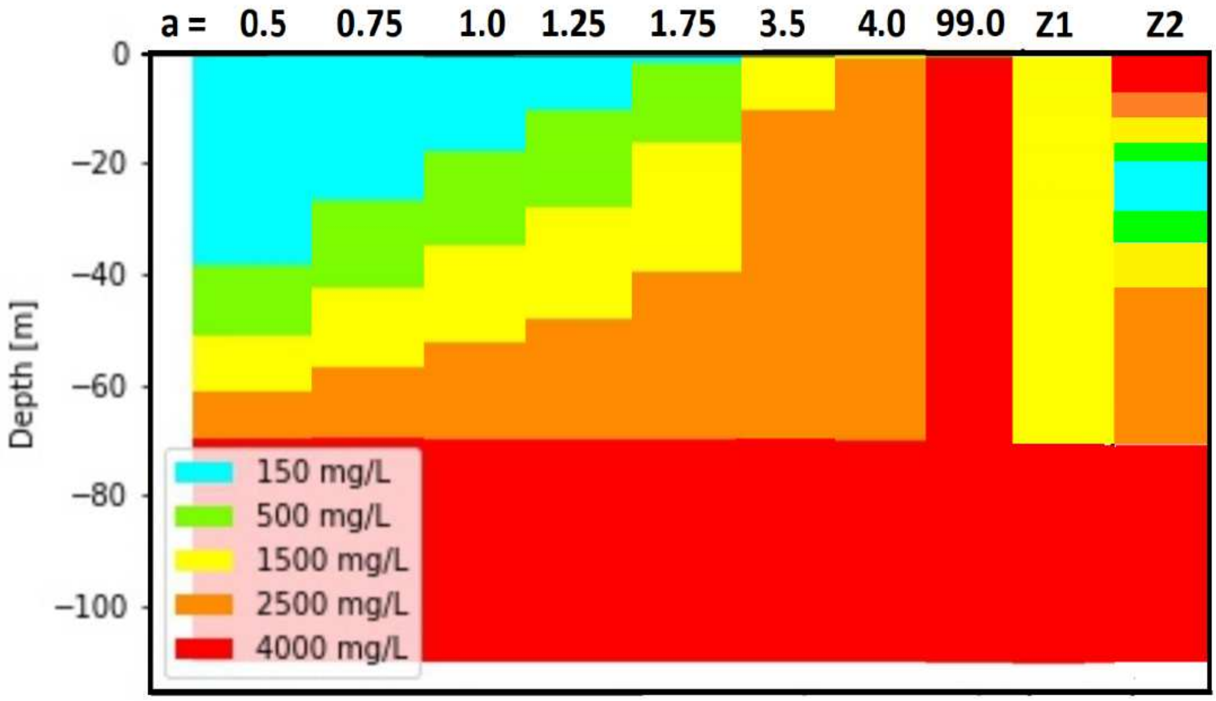

Figure 2-9 *Vertical salinity profile for different a-factors and customized distribution Z1 and Z2.*

To conclude the methods on creating the 3-D salinity distribution, figure 2.10 shows a flow diagram of the processes.

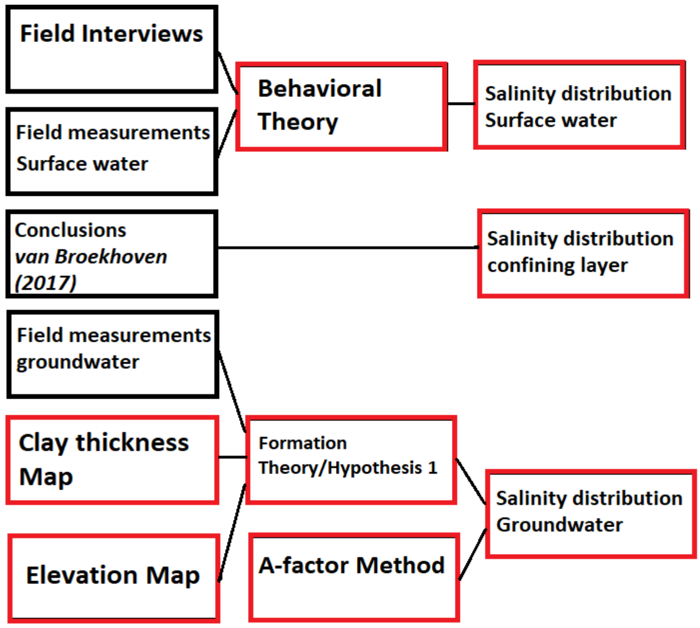

Figure 2-10 *Flow diagram of the constructed salinity distribution*

2.2.1.6 Groundwater flow

To obtain knowledge of the flow patterns of the study area, the hydraulic head variation is investigated. Section 2.1.3 discussed that fictive hydraulic head values must be used to compare the measured water levels in tube wells to the water pressures measured by logging devices with all different salinities. For clarity the term 'heads' will be used to refer to those fictive hydraulic freshwater head values in the rest of this report. The tube well measurements are all obtained on the 17^{th} of January and corrected for any daily changes by comparing them to nearby logger data so temporal variation does not influence the results. With the combination of this tube well and logger data, a wide, fixed in time, spatial head variation is conducted in QGIS. To clarify these head data, two cross-sectional head profiles are created in north-south and east-west direction. It must be noted that the 17^{th} of January is in between the dry and wet period.

It is important to mention that the terms dry period, wet period and period in between will be frequently used in this report. The dry period represents the period with minimum groundwater levels before the beginning of the rains (April-May), the wet period is the period with maximum groundwater levels during and at the end of the heavy rains (August-October) and the period in between is the period between this maximum and minimum during which there are no rains and the heads are falling (January-February).

Since the logger data consists of measurements between February 2017 and April 2018 it consists of both dry as well as wet data. Therefor the logger data are used to investigate the temporal changes in head distribution. Unfortunately, these loggers are almost all (except for P13) placed on the north-south transect making it impossible to use them for any east-west directed head variations. Nevertheless, they are very useful because the variation between dry and wet season is expected to be important. The logger data for 11 October 2017 and 11 April 2018 are used to visualize the wet and the dry period on the satellite map and on the north-south cross-section. They are also used to construct boxplots for all loggers to investigate the variation, plot data for periods of 3 days in the different seasons to investigate what happens during a day and to plot the daily variations (maximum minus minimum head on a day) to find out what the main flow directions and drivers are.

Those maps, cross-sections and graphs mentioned above are used to test hypotheses 2, 3 and 4 and define new conclusions regarding the groundwater flow if necessary. This is done by analyzing what drivers of certain head differences and thus flow directions could be. The fact that the data is plotted in many ways helps in this analysis. Hypotheses are checked by searching for similar results in literature. After this step the hypotheses will be referred to as defined fieldwork conclusions.

Finally, after defining fieldwork conclusions regarding the drivers of the groundwater flow, isohypses-maps are created manually in QGIS. This is consecutively done for the dry period (11th April 2018), wet period (11th October 2017) and period in between (17th January 2018). For the latter this is mainly based on measurements and complemented by the created conclusions. For the dry and wet period, less data is available and the maps are based on the conclusions and corrected with the logger measurements. A flow diagram summarizing the methods in analyzing the groundwater flow is presented in figure 2.11.

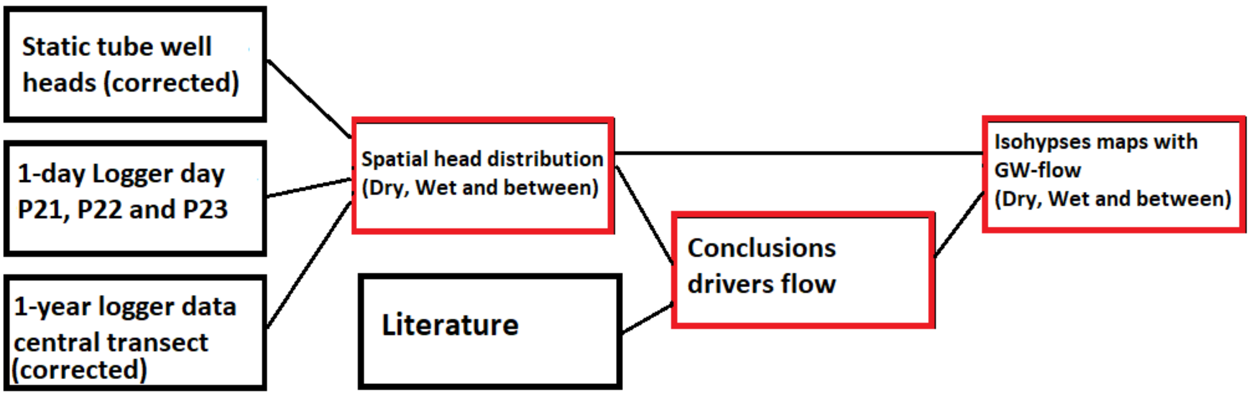

Figure 2-11 Flow diagram of the concluded groundwater flow

2.2.2 Field conclusions to model

The field conclusions are first used to define the exact aim of the modelling study by analyzing what is learnt from the fieldwork and what is useful for the PhD research of Floris Naus. Secondly, the fieldwork results are used to construct the model and define the different parameters. And finally, measurements performed by logger devices in the field together with the concluded flow patterns are used to calibrate the model performance.

2.3 Modelling study

To answer the second research question ('How do the current groundwater conditions evolve in the future under varying scenarios?') a groundwater model of the area is constructed. Here for the MODFLOW and SEAWAT packages are used to simulate groundwater flow and salinity as chloride concentration within the interface of Processing Modflow (PMWIN 5.3). Chloride concentration is chosen to represent the salinity of the groundwater because it is expected to represent the salinity best (section 2.2.1.5). Thereby, chloride is a conservative element which simplifies the modelling processes and enhances the focus on the physical developments.

Based on the conclusions drawn from the fieldwork the aim of the model is defined first, after which these conclusions are used to build up the model by defining grid- and cell sizes, elevation differences and boundary- and initial conditions for the hydraulic head and salinity distribution. Thereby, parameter values for conductivity, porosity, specific storage and specific yield are estimated by a combination of field- and literature data. The same is done for extra flow inputs in the form of surface recharge and groundwater extraction by pumping. This build-up of the model is presented in section 3.2.2 as it requires the fieldwork results.

In total two models are constructed, one representing the dry period with pumping (approximately November to March) and one for the wet period with precipitation (April to October). The initial conditions of the dry model are based on the concluded isohypses from the fieldwork study at the end of the wet period. For the dry period this is done with the end of the wet period. After constructing the model, it is important to calibrate it to verify that the modelled results are a realistic representation of the real situation. Here for the temporal logger data on the north-south transect are compared to the modelled values at implemented observation nodes in PMWIN. Thereby the overall flow patterns of the model are compared to the expected pattern based on the fieldwork study. These comparisons are done manually and the optimal situation will be chosen for the modelling study.

Since the amount of data is scarce and some outcomes of the fieldwork study will be uncertain (e.g. pumping quantitiy, conductivity values and vertical salinity distribution) it will be difficult to correctly calibrate the model. Based on the time that is left the performance of the model can be improved before deciding for which purposes it is useful.

3. Results & Discussion

Like the previous section, the results will be provided in three parts: First a fieldwork section to present and discuss the measurement outcomes of the fieldwork, second a section to couple these fieldwork outcomes to the aim and input of the model and third a section about the modelling outcomes.

3.1 Fieldwork

The fieldwork results presented in this section are divided in different parts that consist of separate objectives. Consecutively the results will be provided for the topography, lithology, soil characteristics, pumping behavior, salinity variation and hydraulic head variation.

3.1.1 Topography

To compare the head measurements and find influences of topography on flow and salinity this section provides an overview of the results obtained from the fieldwork measurements and combines them with maps of the region (SRTM and soil map (FAO,1959)) to create a conclusive relative elevation map.

3.1.1.1 Results

The relative elevation measurements resulting from the leveling procedure (section 2.1.4) are shown in figure 3.1. It must be noted that the measured points in the aquacultural ponded areas (light green) are generally situated on the dykes and not in the ponds, of which the base is on average situated about 1 to 2 meters below the surface of the dyke.

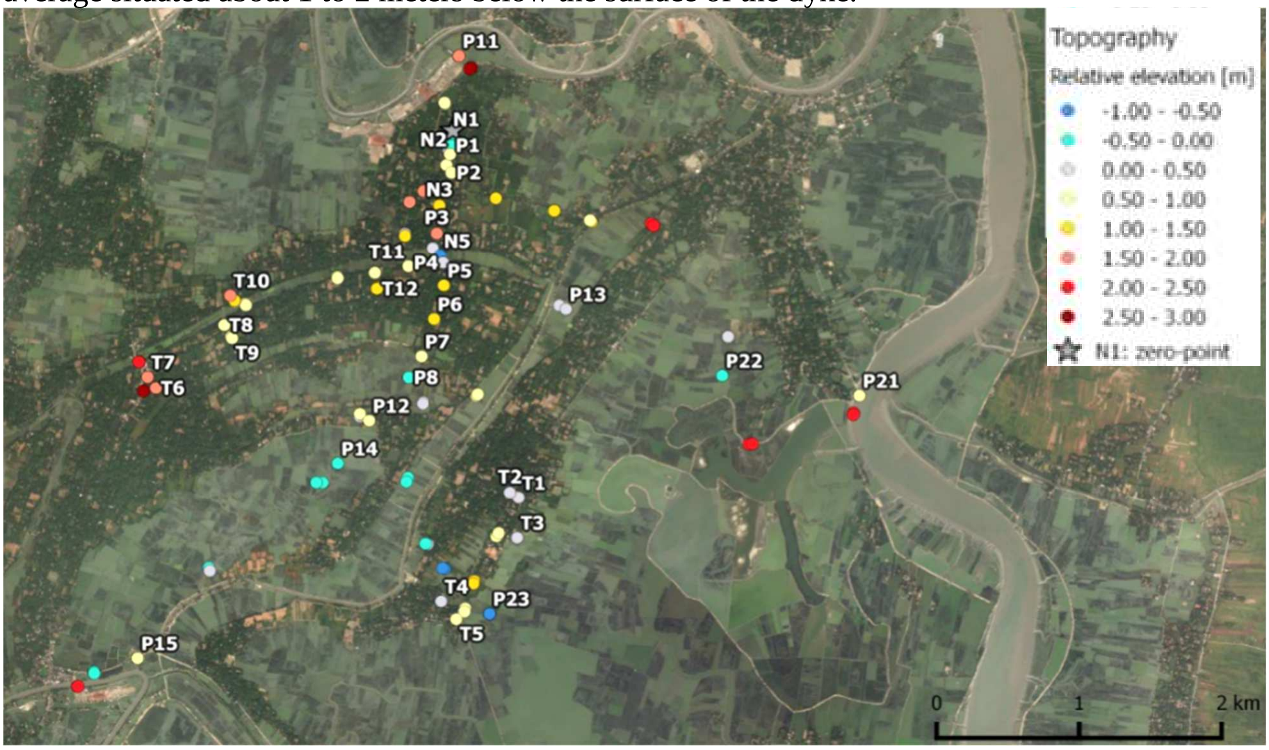

Figure 3-1 *Measured elevations during the levelling procedure relative to zero-point N1.*

3.1.1.2 Discussion

Figure 3.1 showed the elevation distribution relative to the zero-point at nest N1. This figure, together with the SRTM map (figure 1.2), observations in the field and the landuse map (figure 1.3) indicates a correlation between the land use and elevation. With the village or homestead areas (dark on the satellite imagery due to vegetation) higher elevated than the areas with aquaculture (light green on the satellite imagery). Boxplots to test this hypothesis are shown in figure 3.2.

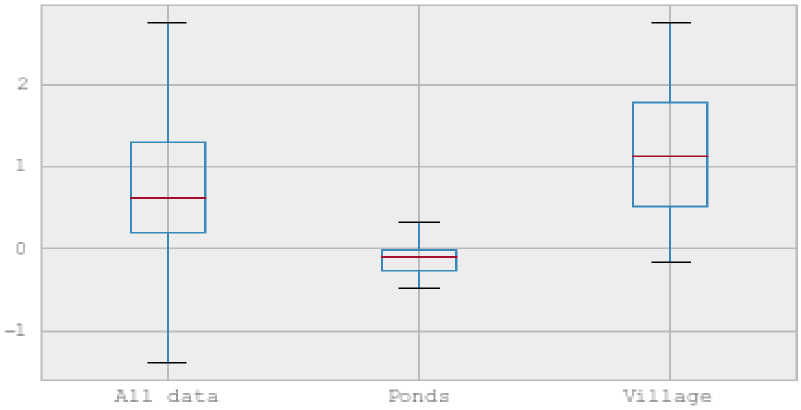

Figure 3-2. Boxplots representing the topography data obtained by levelling.

As expected, this shows the aquacultural areas (ponds) to be situated lower than the village areas. The average values of the three are 0.79 meters for all the data, -0.09 for the aquacultural ponds and 1.11 for the village areas. Since the aquacultural pond values are measured on dykes, it is expected that inhabited areas in the region have an elevation of 1.5 to 2.0 meter higher than the aquacultural ponded areas. Furthermore, the western village area is clearly higher than the other village areas, this is presented by both the SRTM map (figure 1.2) and the fieldwork results (figure 3.1). The low-lying aquacultural ponded areas show less fluctuation than the elevation village areas. A figure with these conclusions regarding the surface elevation is presented in figure 3.3.

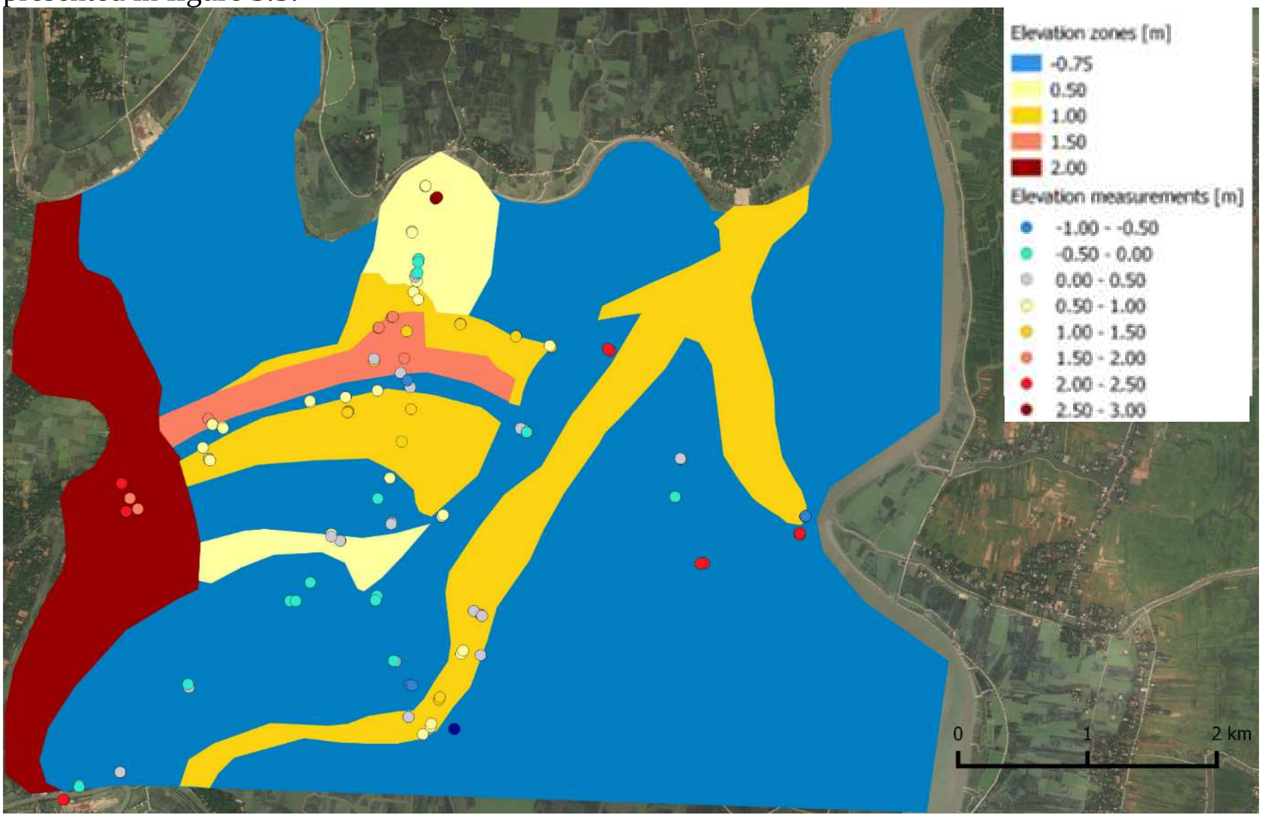

Figure 3-3. Conclusions regarding the surface elevation

In the figure it is visible that the areas with aquaculture (light green on satellite imagery, figure 3.1) are all assigned the same low elevation of -0.75 relative to the zero-point. This is partly due to the lack of data in these regions which forces values to be based on the SRTM map and interpretation. Besides the fact that the SRTM map indicates the low elevation, the field observations clearly showed the elevation difference between the areas of aquacultural ponds and villages. So, even though there are no clear measurements the assigned elevation of the low-lying aquacultural areas is regarded as reliable. The rest of the elevation differences are based on elevation measurements, the SRTM-map and the landuse map as discussed in section 2.2.1.1 and shown in figure 2.5.

The pattern can be explained by the soil map (FAO, 1959; figure 1.4) which indicates river deposits (yellow) on most parts of elevated village areas and tidal deposits (grey/blue) in aquacultural areas. The pattern of the riverine deposits follows the course of past rivers from the northwest to the south and east. In the areas next to these rivers, tidal clays were deposited causing a thick clay layer to arise. This results in the subsidence of the currently lower elevated areas (as explained in section 1.1). It is expected that after this subsidence further shifting of the rivers caused some of the lower elevated areas (the region connecting the current eastern river with the higher elevated area, P22 to P6) with thick clay layers to be eroded and covered by riverine deposits as currently visible on the soil map.

Because the levelling process was time consuming it was not possible to level the whole region. The lack of data in several areas does decrease the reliability of the study. Thereby, the thickness of the dykes is only measured at some locations making the estimation of 0.5 to 1.0 meters uncertain. Nevertheless, the measurements in the field relatively correspond to the zones visible on the SRTM map (figure 1.2) indicating that the combination of the two is sufficient to construct the elevation input for the model and use the relative elevation differences in the analysis of the groundwater flow.

3.1.2 Lithology

Since the overall lithology consists of a sandy aquifer overlain by a clayey aquitard, the aim of the lithology investigation is to find the distribution of this clay thickness within the region. This thickness is of high importance for the system as thick clay layers decrease the infiltration of recharging water to the aquifer. The lithology explained in this section is based on tube well measurements (section 2.1.1), logging the sediment during installation of piezometers (section 2.1.2) and analyzing the soil map (FAO, 1959; figure 1.4).

3.1.2.1 Results

The logging of the boreholes results in more reliable lithology data but for the overall thickness of the clay layer the tube well depths are useful since they are placed in the first sandy aquifer and investigated in large quantities. An overview of the well-screen depths indicating the thickness of the clay layer is presented below (figure 3.4).

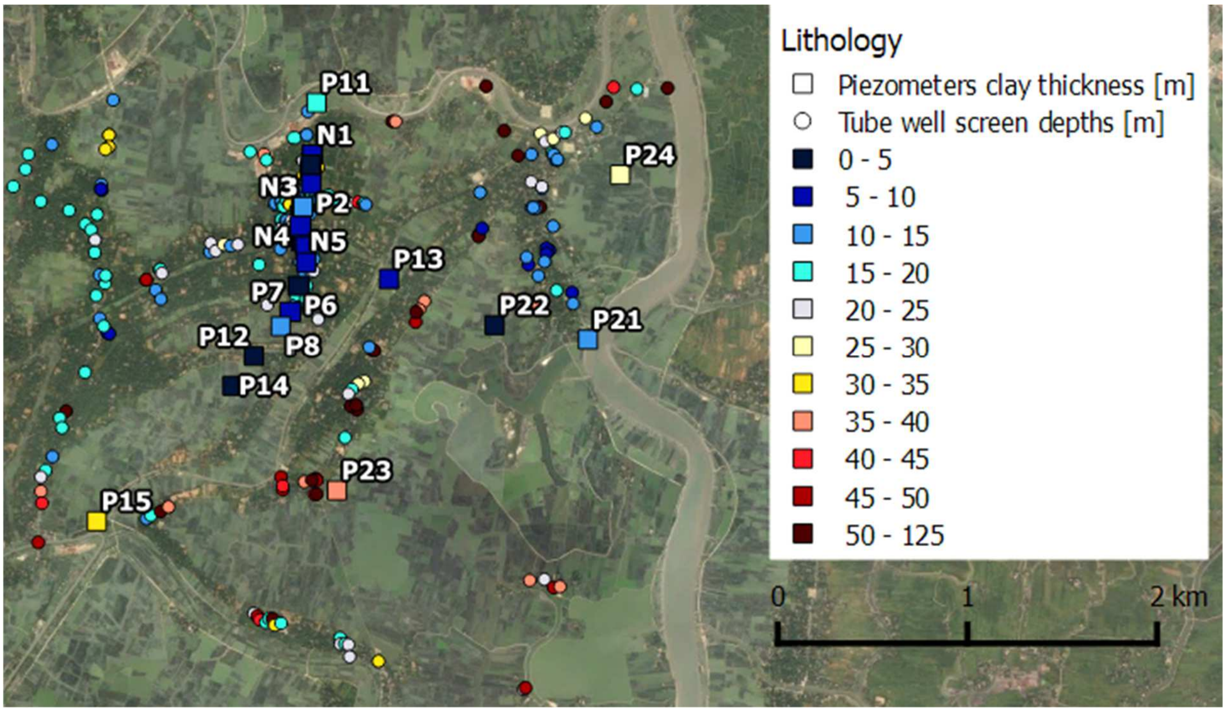

Figure 3-4. Well-screen depths of piezometers and tube wells indicating the thickness of the clay layer

3.1.2.2 Discussion

As explained in the introduction, the sandy aquifer is supplemented by patches of clay in it. For this study however, the situation is simplified to only a clay layer with varying thickness on top of the sandy aquifer. This is done because the amount of data is insufficient to provide more detail. As explained in section 2.2.1.2 the elevation (figure 3.3) and soil map (figure 1.4) are expected to indicate clay thickness. Hereby riverine deposits indicate thin clay layers. For the higher elevated areas this is explained by the fact that they were protected from flooding and deposition of clay. The lower elevated riverine deposits also indicate thin clay layers due to erosion of originally elevated areas after the subsidence had taken place (as explained in section 3.1.1).

The relation between the surface elevation and clay thickness is shown in a scatter plot to test the hypothesized negative correlation (figure 3.5).

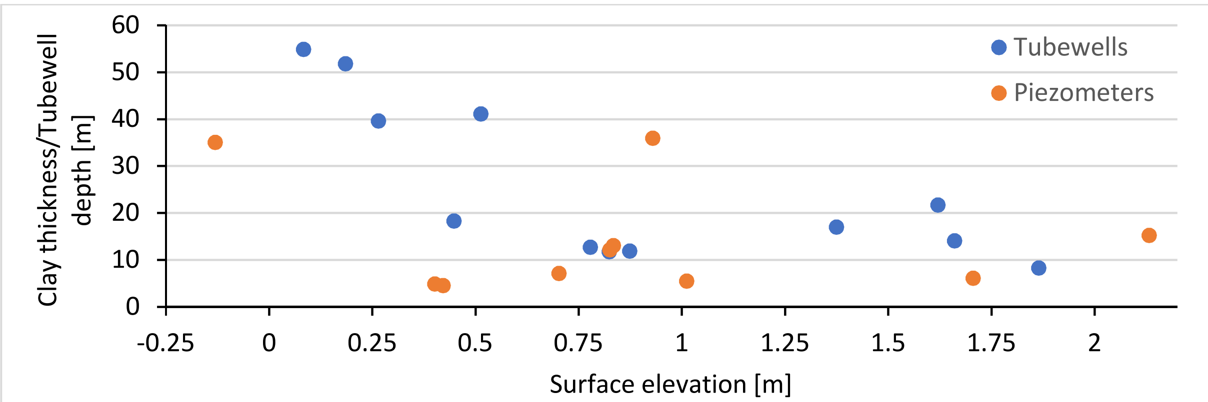

Figure 3-5. Graph to display correlation between surface elevation (measured in levelling procedure) and clay thickness. Piezometers indicate measured clay thickness based on lithology classification and tube wells indicate well screen depths representing the maximum top of the aquifer.

The graph does indeed show thinner clay layers for increasing surface elevation. However, between elevations of 0.25 and 1 meter no correlation is visible. Especially the piezometers with a surface elevation between 0.25 and 0.75 meter (P22 in the east and P14 and P13 near the central transect) have thin clay layers. These piezometers are all placed in areas of aquaculture (figure 3.2) at low elevation with riverine deposits (figure 3.6) indicating erosion of previously elevated areas. Regarding the tube wells, it is important to interpret the shallowest tube wells in a region, it is not uncommon that tube wells are placed deeper than the beginning of the aquifer. All tube wells between 1.25 and 2.0 m elevation are placed in the same region (area with T6 to T10) indicating that the lowest thickness can be taken as reference for this area.

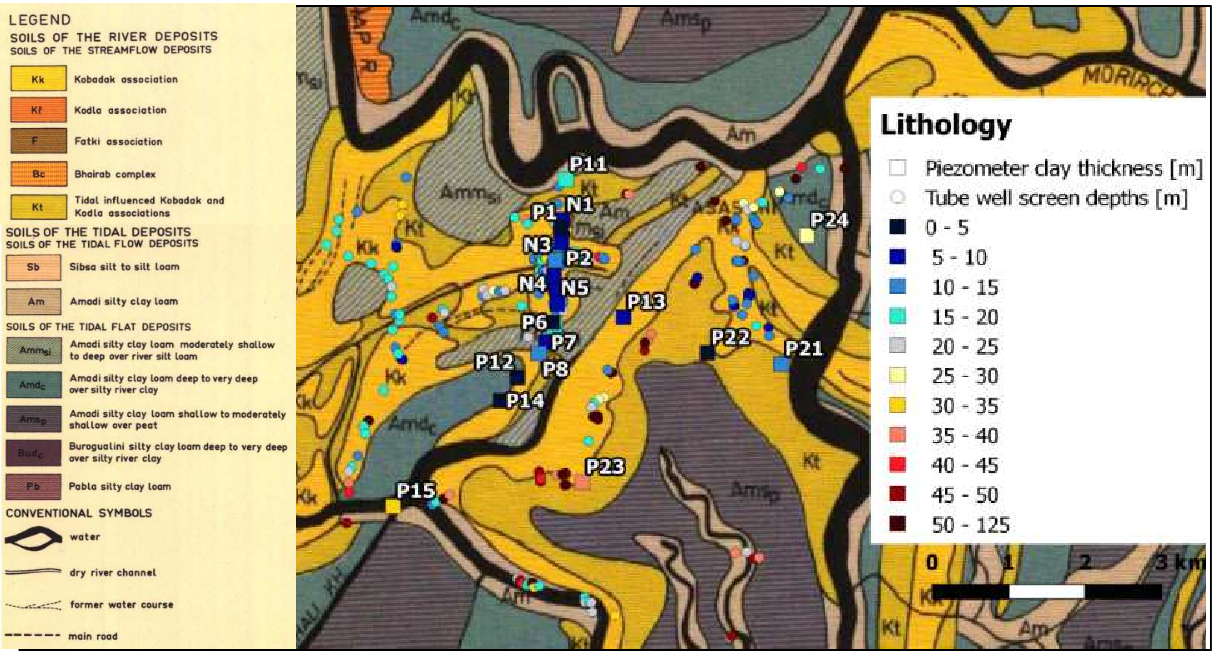

***Figure 3-6**. Soil map* (FAO, 1959) *with depths of the clay layer based on piezometers and tube wells. It must be noted that the soil map is referenced manually so the exact location of different units can differ, the map can only be used as indication of the different units.*

It must be noted that the locations of the regions in the soil map (figure 3.6) can differ slightly because it is a scanned hardcopy map that has manually been georeferenced. Here for the different zones are not used as absolute locations but more as indications for soil classes being present in the area.

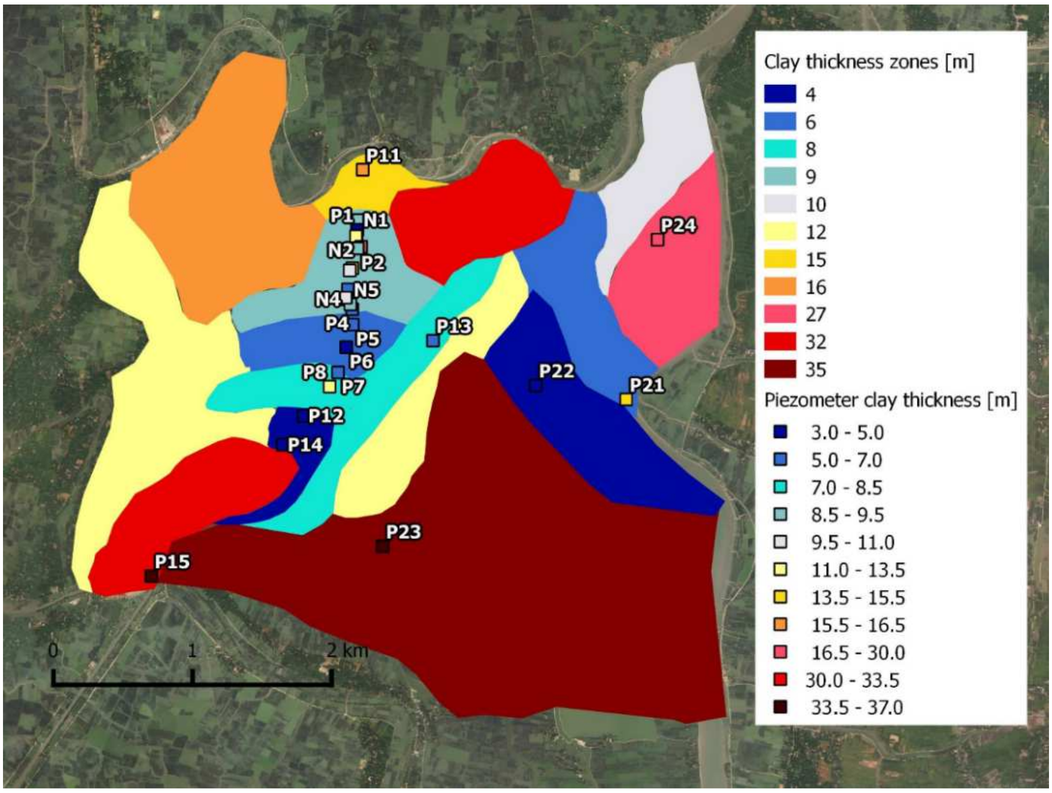

Figure 3-7. *Conclusions regarding the clay thickness.*

The conclusive figure with zones of roughly equal clay thickness (figure 3.7) does show most of the elevated areas to be underlain by a thin clay layer (region along the central part of the transect). However, some of the lower elevated areas are appointed with thin clay layers. The biggest difference between the elevation map and clay thickness is the area in the east around P21 and P22 which is indicated as riverine deposits in the FAO soil map. As explained this is expected to be due to erosion of the clay after subsidence. A different situation occurs for the regions in the northwest and the line of aquacultural ponds where P13 is situated. These parts of the region are classified as tidal flat deposits by the FAO soil map, however still erosion of the top clay layers is expected since interviews during the fieldwork indicated recent (up to 50 years) flow of a river through the area of P13 causing the current tidal clay classification to be deposited recently. The same is expected for the area in the northwest.

The clay thickness presented in figure 3.7 is quite reliable for areas where many tube wells or piezometers were present. The hypothesized relation between elevation and clay thickness is visible in these measured data and supported by the soil map. Nevertheless, the data is severely scaled up in regions without tube wells, making the exact clay depths highly uncertain. This is especially the case for aquacultural areas like the northwest, northeast and southeast.

3.1.3 Soil characteristics

It is hypothesized that infiltration rates in the region are low but that they do influence the groundwater situation through time (hypothesis 3). To learn more about this infiltration rates and their variance for different land uses, this section treats the research done in the field to investigate the behavior of the soil.

3.1.3.1 Results

The soil behavior is studied by performing several infiltration experiments and auger drillings. An overview of the locations of these experiments is presented in table 3.1 and figure 2.2.

Table 3.1. Overview of infiltration experiments with Ks representing the calculated vertical saturated conductivity based on the infiltration experiments.

	Landcover	Location	Soil	Ks [m/day]
A1	Grass	Next to river dyke (homestead)	Wet clay	**-**
I1 & A2	Trees	Homestead area	Dry clayey silt	**0.173**
I2	No landcover	On tidal riverbank	Wet clay	**1.944**
I3	Fish pond (not in use)	1 km from river	Wet clay	**0**
I4	Rice field (not in use)	Homestead area	Wet clay	**0**
I5	Rice field (not in use)	Homestead area	Dry clay	**0.0245**

For each infiltration experiment a saturated conductivity is calculated as explained in section 2.1.5 and an infiltration curve is plotted to compare the cumulative infiltration through time (figure 3.8a). The two auger drillings are mainly used to improve the understanding of the soil behavior, for drilling A2 the increase in water level in the auger hole through time is recorded (figure 3.8b).

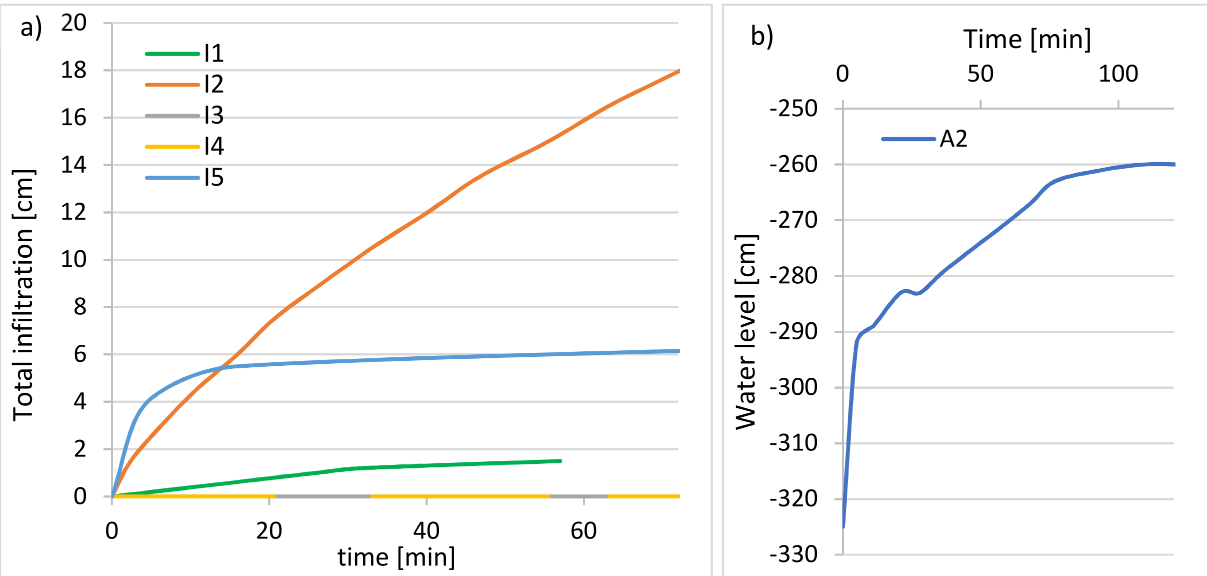

Figure 3-8. a) Results of the five infiltration experiments: cumulative infiltration in cm versus time in minutes. b) Result of the auger drilling at location A2: Water level measured from surface versus time.

First it is clearly visible that the infiltration experiments located in wet aquacultural ponds (I3 and I4) do not record any infiltration for over one hour. Second, the test on the wet river bank (I2) shows by far the highest infiltration rate followed by I5 in a dry rice field and I1 on a dry patch of homestead.

Regarding the two auger drillings, A1 was unfortunately not recorded in detail but auger drilling A2 was closely recorded. The vertical profile comprised of 40 cm of dry clayey silt that became moist clayey silt between 40 and 295 cm, from here on the texture was wet silty clay until the bottom of the drilling at 390 cm. No water was subtracted from the auger hole before recording the water level increase.

3.1.3.2 Discussion

The vertical conductivity values of clay (table 3.1) show a large variation, with an unrealistic high value (1.94 m/day) found next to the northern river and lower values (0-0.173 m/day) in homestead and aquacultural pond areas. The area with trees in the homestead area is high as well while the other low conductivities are comparable to values found by previous studies in the same region [0.002 m/day (Michael & Voss, 2009) and 0.1 m/day (Mukherjee, Fryar, & Howell, 2007)]. The high values are expected to be a result of not measuring long enough. This causes the measured infiltration to only reach a maximum of 18 cm which is not representative for the clay layer and could be still a result of unsaturated flow. Especially for the region at the northern river it is expected that underneath the freshly deposited clay next to the river (with high conductivity) a more compacted clay layer is present with a much lower conductivity than measured. Regarding the experiments with 0 infiltration, this could represent very low infiltration rates that were not possible to measure, but it can also be explained by the fact that there is no downward gradient in the clay. The clay was wet while the measurements were in the dry season so the only probable gradient was upward due to evaporation. However, these infiltration measurements clearly showed a difference between measured conductivity values in the homestead area and in (semi-)permanent saturated clays in rice fields and aquacultural ponds. Here for it is concluded that infiltration in these ponded areas is low and can be represented by a value of 0.007 m/day (in between *Michael & Voss (2009*) and own measurements) where the saturated vertical conductivity in homestead areas is expected to be around 0.15 m/day because this is somewhat lower than the infiltration measurement but still substantially higher than the measurements in aquacultural ponded regions. It must be noted that these values are not exactly calculated but determined by estimations based on literature and experiments.

As explained in section 2.2.1.3 the horizontal conductivity of the clay is obtained with the method of *Beers* (1983).This resulted in a k-value of 0.052 m/day which is within the ranges of reasonable values for clay (Fitts, 2002; Hendriks, 2010). So, even though it is the only successful measurement, it can be used for the model.

The horizontal conductivity of sand is found to be 11.25 m/day at a MAR site in the Assasuni region (Acacia Water & Dhaka University, 2015). When analyzing the measurement of the eastern river and piezometer 21 besides it, a transmissivity of 175.5 m^2/day is found for an amplitude attenuation of 0.223 and an estimated specific yield of 0.25 (estimated porosity of the sand). For an aquifer thickness of 23 meters this results in a horizontal conductivity of 8.2 m/day for the sandy aquifer which is comparable to the value found by the pumping test at the MAR site. This pumping test value is expected to be more reliable. The vertical conductivity of sand was not measured in the field and was assumed 1/10th of the horizontal conductivity (Bot, 2011).

In general, the analysis of the soil behavior results in the conclusion that indeed infiltration plays a role in the groundwater movement and composition since relatively high values were found by the infiltration experiments. At homestead areas infiltration is expected to recharge the aquifer during the wet periods which is much less in areas with ponds. This is as expected since settlement of small clay particles decreases the conductivity of the clay in ponds (Sengupta et al., 2008).

The different values obtained for the conductivity are highly uncertain. The vertical and horizontal conductivity values for clay are only based on one measurement in combination with literature values. For the hydraulic conductivity of sand, the value found via the pumping test is expected to be more certain but there can still be a variation within the region which is not regarded.

3.1.4 Pumping

As stated in hypothesis 4, *groundwater extraction is expected to influence the current groundwater flow and decreases future groundwater heads*. The first part of this hypothesis is severely investigated in the field. The second part regarding the future heads can only be verified in the modelling part of this study but requires input of the current data. Therefor this section focusses on the outcomes and interpretation of the knowledge acquired in the field by surveys and measurements of extraction rates.

3.1.4.1 Results

The locations of the factories and irrigation study area are shown in figure 2.2. First, it is found that factory F4 in the south of the region does not use any groundwater, factory F1 northwest of the central homestead area has 1 mechanical groundwater pump, factory F2, situated directly east of F1, has 5 mechanical groundwater pumps and F3, further to the east has 3. The pumping periods range from 1.5 to 2.5 hours per day for 5 to 6 days a week during the dry period (roughly October-March). Pumping rates between 4.5 and 5.5 liters/second are found.

Regarding the irrigation area, in total 8 mechanical pumps were found in the area but most of them were not running and it was difficult to learn which areas they supplied since it was not possible to speak to many owners of the pumps. An overview of the 8 pumps that were found is provided in figure 3.9 and table 3.2.

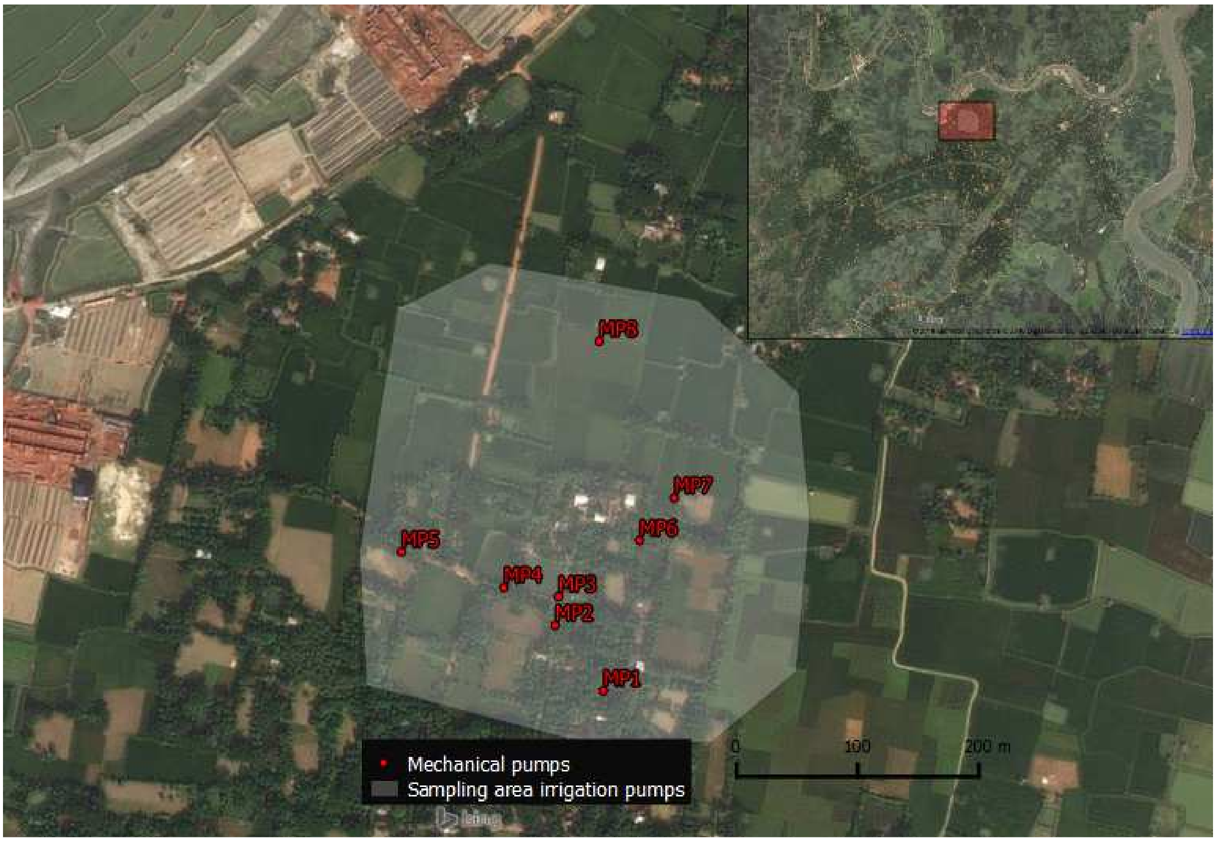

Figure 3-9. Overview of mechanical pumps found in the selected study area

Table 3-2. Information obtained for the mechanical pumps shown in figure 3.7

Pump	Irrigation area	Pumping time [hours]	Months in operation	Pumping rate [L/s]
MP1		7 per day	Feb – Apr	
MP2		6 in 48	Jan – Mar	
MP3	8,000 m^2	12 in 48	Jan – Mar	5
MP4				
MP5		2.5 per day		
MP6	12,000 m^2	4.5 per day	Sep – Mar	15
MP7	3,500 m^2	3 per day	Oct – Feb	
MP8				

Besides the analysis of extraction quantities in the small test area, a general overview of locations with mechanical pumping for both rice and other crop irrigation (figure 3.10) is constructed by documenting the land use during the fieldwork (section 2.1.8).

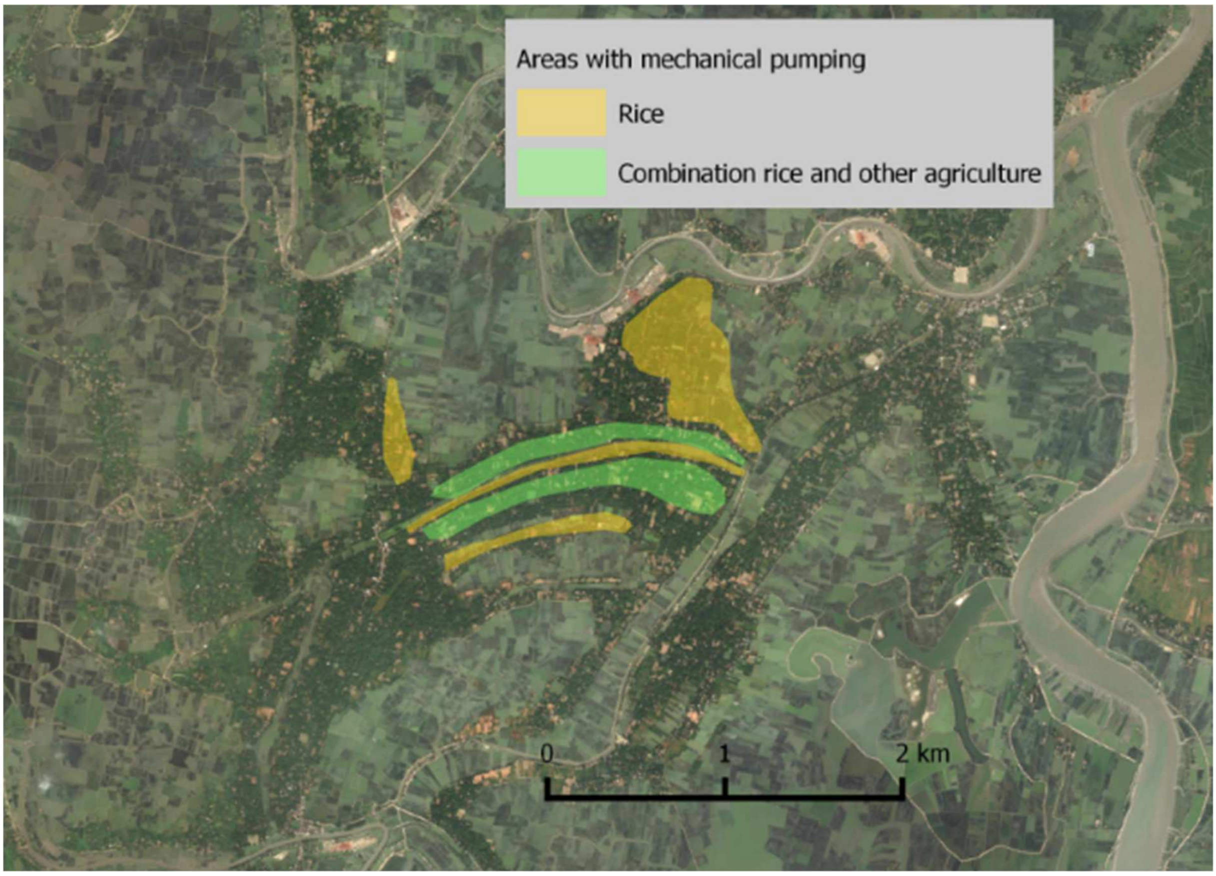

Figure 3-10. Areas with mechanical pumping for rice and combined irrigation

3.1.4.2 Discussion

During the fieldwork it proved to be challenging to accurately define pumping quantities by interviewing the local farmers. To define reliable extraction amounts, this section compares results found in the field with water demands found in literature. The influence of the pumping rates on the groundwater flow will be discussed later in section 3.1.6.

First the fieldwork results show that the pumping quantities of the brick factories are neglectable in comparison to the pumping for agriculture. Second, summarizing the results (table 3.2) shows the average groundwater extraction to be about 15,000 m^3/year divided over the months January to April (on average 7.5 L/s, 4.3 hours/day, 4.2 months a year) for an average irrigation area of 7,833 m^2. The average of 7.5 L/s is used instead of 10 L/s because the pumping rate of 15 L/s was measured at a pump that was substantially bigger than most of the other pumps that were observed. This results in an extraction of 1.91 m^3/m^2. The water demand is 0.4-1.5 m for the rice grown during the dry season in this area (Shahid, 2011; M. Shamsudduha et al., 2009). Since the irrigation is completely groundwater-fed these literature values can be compared to the field value. The field measurements show a small overestimation of the water extraction in combination with the literature values. This difference occurs because the values obtained from the field are based on an average of several pumps which is not so accurate. The fact that the field values overestimate the literature values could be due to the fact that the interviewed farmers overestimated their water use or possibly due to an increase in water demand for the rice as a result of increasing dry spells (Acacia Water, 2015). It is important that the pumping is regarded as significant parameter in the rest of the study and model when testing the sensitivity of the system.

For the areas with a combination of rice and other crops it is difficult to find specific extraction rates and exact distributions of crops. One field observation of a mechanical well in the west of the northern region of combined rice and agriculture (see figure 3.10) resulted in an extraction rate of about 36.000 m^3 per year (6 L/s, 5.5 months, 10 hours per day). This extracted groundwater was used to irrigate an area of about 0.05 km^2. Hereby it must be said that this is only one observation and the amount of pumping and area for irrigation are prone to error since they are obtained from only one survey. An overview of the irrigation for areas with rice and combined areas of rice and agriculture is provided in table 3.3 below.

***Table 3-3**. Overview of groundwater extraction rates found in the field*

	Rice	**Combination Rice & Agri**
Mean irrigation area [m^2]	7,833	31,000
Average daily pumping time [hours/day]	4.33	10
Average Months in operation	4.2	5.5
Average pumping rate [L/s]	7.5	6
Annual extraction [m^3/year]	15,000	36,000
Annual extraction per m^2 [m/year]	**1.91**	**1.16**

The locations of the different areas of dry-season rice and other agricultural irrigation (figure 3.10) were obtained during the fieldwork and are to a large extent reliable. They are all situated at or near areas of higher elevation or homestead because these areas generally overly fresher groundwater than regions of lower elevation which is necessary for the cultivation. The map also largely corresponds to the landuse map created by *Naus (2018)*. It must be noted however that the map shown in figure 3.10 does not take small areas of agriculture into account since it was not possible to define these during the fieldwork, only clear regions with predominantly agriculture are assigned. The pumping rates however have high levels of uncertainty since they were difficult to obtain in the field. Therefor it is important to create a model in which the pumping rates can be varied and the different effects on the groundwater distribution can be analyzed.

3.1.5 Salinity variation

Since understanding the current and future salinity distribution in the groundwater is one of the aims of this study it is important to start with the current distribution. As explained in section 2.2.1.5, this is done by first testing the formation theory and *hypothesis 1* before assigning vertical salinity profiles to the region. The terms relatively fresh, brackish and saline will be used to define water with EC-values in the ranges of 0-1.0, 1.0-3.0 and 3.0-22.0.

3.1.5.1 Results

As explained, the measured salinity is represented by EC-values at different depths. Figure 3.11 shows the measured EC-value for different depth ranges.

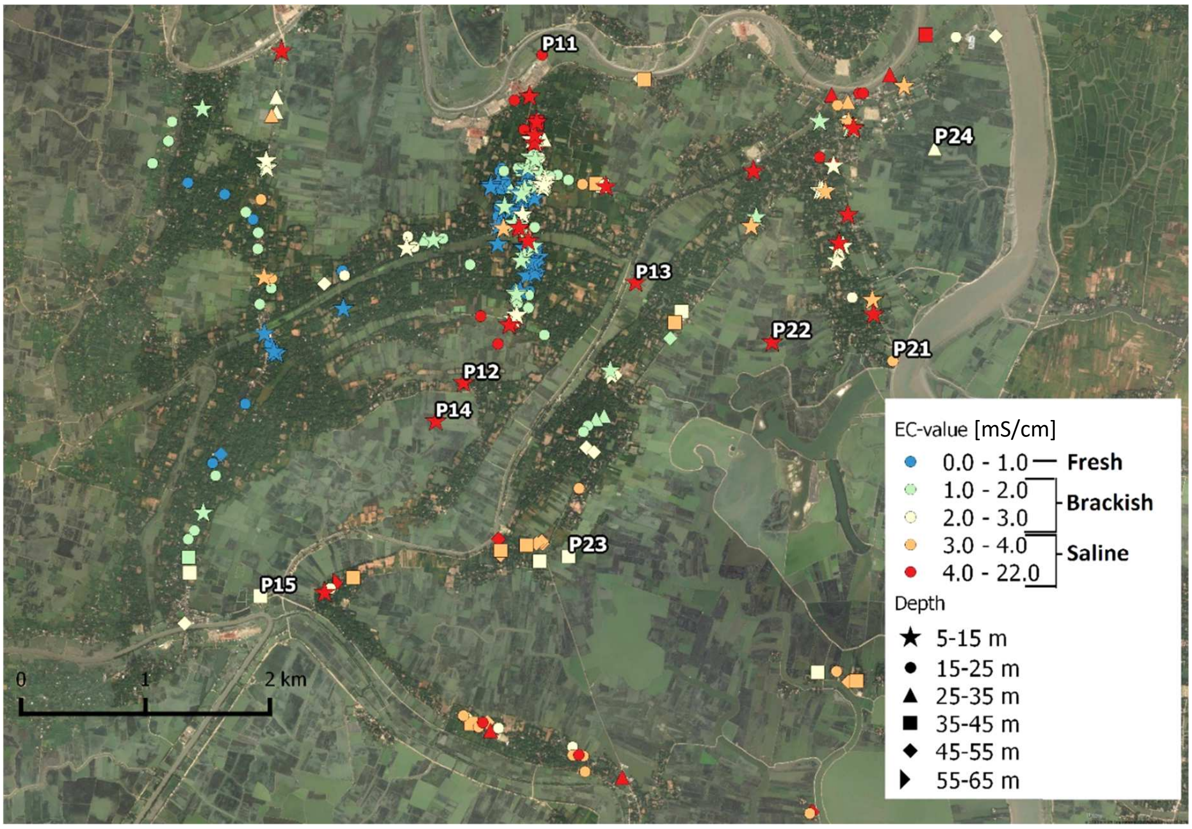

***Figure 3-11**. Spatial salinity variation expressed in electric conductivity (EC) [mS/cm] of the groundwater. Color indicates the EC-value and the shape indicates the depth of the groundwater sample.*

This figure comprises of a combination of data from previous fieldwork activities (Naus, 2018; van Broekhoven, 2017) and data from the current fieldwork. Especially the large amount of data in the center of the study area was available before the start of this study.

3.1.5.2 Discussion

For the salinity distribution it is important to separately regard the surface, confining clay layer and the sandy aquifer. As stated in *hypothesis 1*, the salinity of all layers is expected to be influenced by the surface elevation, land use and lithology (Naus, 2018; van Broekhoven, 2017).

Regarding the ponded surface water, it indeed seems that hypothesis 1 is true since interviews learned that Aquacultural ponds are filled with saline river water where agricultural fields and village ponds are preferably filled with water that is as fresh as possible (precipitation or groundwater). The field measurements confirmed this behavior with many saline aquacultural ponds at low elevation, brackish surface water in low-lying areas with rice cultivation and relatively fresh to brackish water in the few ponds that were present in the villages.

As stated in section 2.2.1.5 the conclusion from the previous fieldwork (van Broekhoven, 2017) is used to confirm that salinity distribution in the confining clay layer is comparable to that of the surface water.

For the groundwater, many extra measurements are performed (figure 3.11). These measurements are analyzed and combined with theories on the relation between elevation, lithology, land use and salinity, figure 3.12 gives an overview of these comparisons.

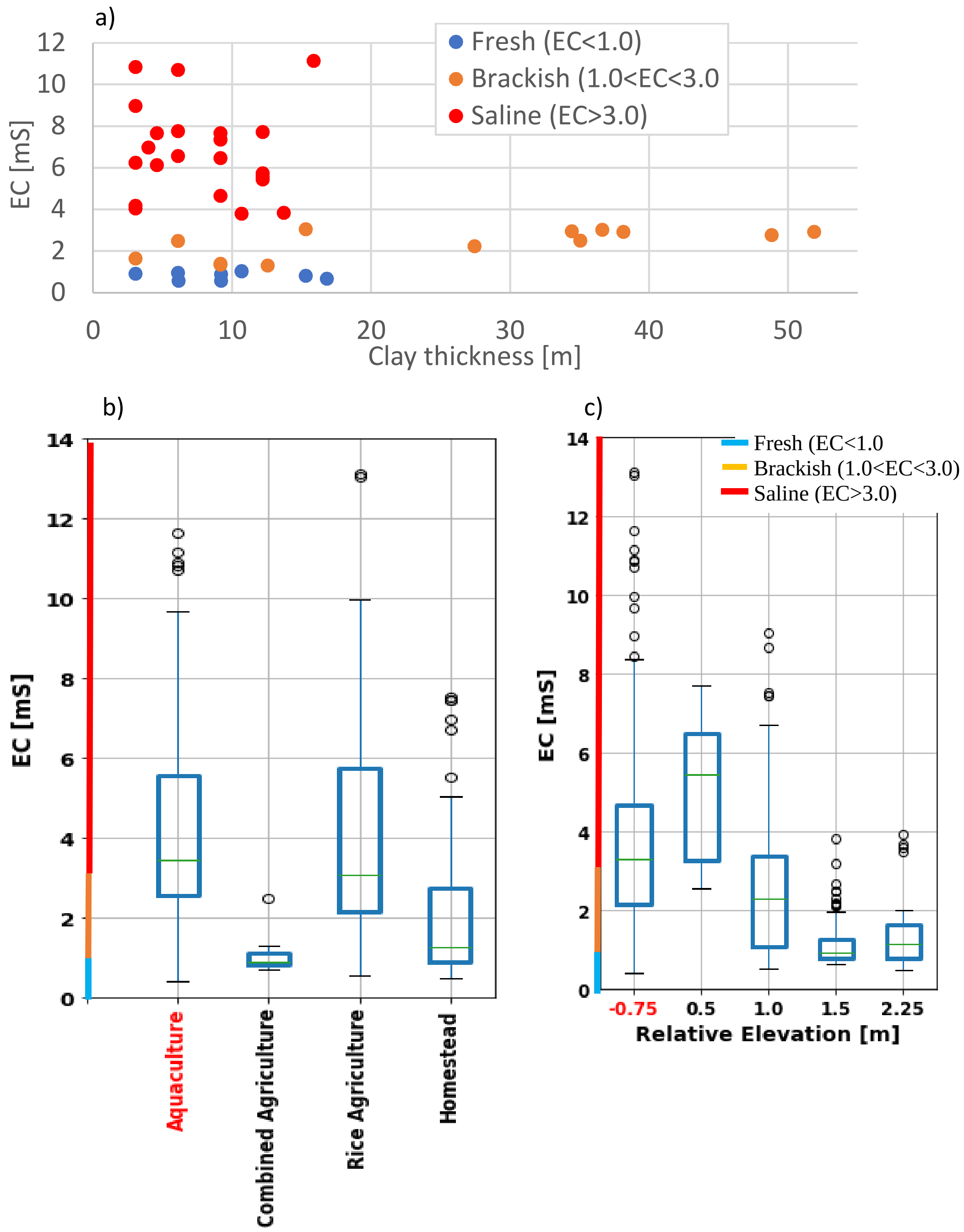

Figure 3-12 *An overview of the EC-measurements compared to a) the clay thickness b) the land use and c) relative elevation in comparison with N1. The red text in b and c represents low elevated aquaculture which are expected to by saline*

Figure 3.12a clearly shows a higher amount of saline measurements under clay thinner than 20 meters, this confirms the hypothesis that thick clay layers protect the groundwater from salinization. Figure 3.12b and 3.12c show the landcover and elevation versus salinity measurements. The low elevated aquacular regions are represented by higher salinity values in comparison to the high elevated (1.5-2.25 m) homestead area. This is as expected since the first are vulnerable to saline flooding. Thereby, rice agriculture and areas with an elevation of 0.5 meters also show high salinity values, this is due to the fact that a large part of the studied rice agriculture is situated at low elevated areas near aquacultural ponds and a region of 0.5 meters height is situated close to the northern river making it vulnerable to saline flooding as

well. In general, these graphs confirm the formation theory which is used in *hypothesis 1* and lead to the decision to use this theory to define the salinity distribution as explained in section 2.2.1.5. Some examples from the spatial measurements (figure 3.11) are presented below to further confirm this theory:
1) On the measured transect on the western partly elevated area, higher elevated (dark green) regions which are expected to have thin clay layers show fresh to brackish groundwater measurements due to fresh water infiltration.
2) The group of brackish to saline measurements in the south near piezometer 23 are situated at relatively high elevation under which relatively fresh groundwater would be expected. However, it is underlain by a thick clay layer protecting the aquifer from infiltration of saline flooding or fresh rainwater. This way the groundwater in these regions remains as brackish/saline as it was during deposition. Since the measurements north on the same elevated area are fresher while being situated on a thinner clay layer this is expected to be a feasible explanation.
3) In the northeast of the region many salinity variations at similar depths are visible. A reason for this could be the position between the two rivers with possibly different salinity values in the past causing the groundwater salinity to become very complex. Again, in this region the area with a thick clay cover (aquacultural area with piezometer 24) consists of brackish groundwater due to the protection from saline infiltration.
4) An area where the groundwater is very saline is the eastern aquacultural area near P22 where the clay layer is thin and elevation low. This area is also known for saline flooding that salinizes the groundwater.

The conclusive overview of the salinity distribution (figure 3.13) is thus largely based on the following theory: After deposition of brackish to saline sediments and the evolution of differences in elevation (section 3.1.1) and clay thickness (section 3.1.2), low elevated areas with thin clay covers were prone to salinization due to tidal floods. High elevated areas with thin clay covers were freshened by rainwater infiltration since they are protected from saline flooding. Areas with thick clay covers are protected from infiltration which results in similar brackish groundwater conditions as during deposition.

To further analyze the salinity distribution in the area more field data are required. Especially for the lower elevated aquacultural pond areas that do not contain any tube wells. For the current study however, the available field data in combination with the formation hypothesis is enough to create a 3D salinity distribution that can also be used in the model.

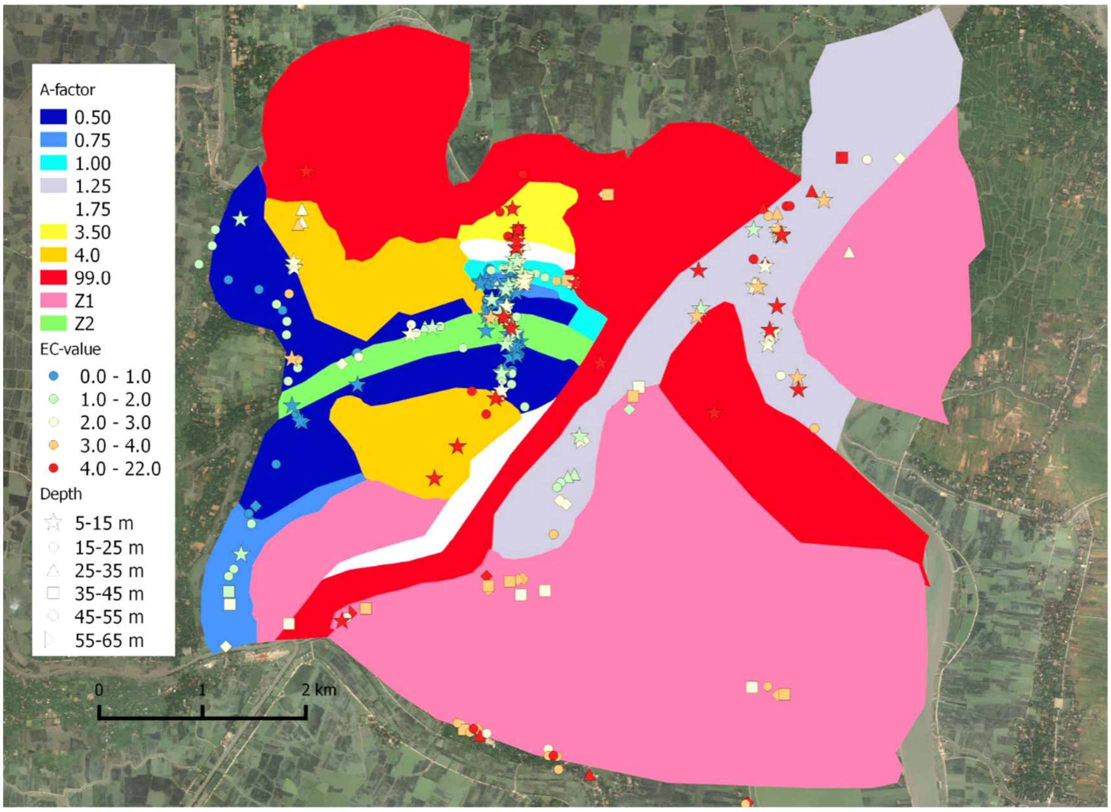

***Figure 3-13**. Conclusions regarding the salinity distribution based on A-factor (see figure 2.9)*

3.1.6 Groundwater flow

To predict the possible changes in salinity variation in the groundwater it is important to know how the groundwater flows and will flow. The changes in groundwater flow will be simulated during the modelling part of this study but the current groundwater flow and especially the drivers of this flow are discussed in this section. With the knowledge of the current groundwater flow in combination with the salinity distribution the exact purpose of the model can be created. This section starts with an objective overview of the results after which the most important results are explained and coupled to conclusions in the discussions section. An overview of the filter depths of the piezometers with loggers is provided in table 3.4. Hereby the filters have a length about 3 meters and the depth is chosen in the middle of this filter.

***Table 3-4**. Filter depths of piezometers with logger devices.*

Logger	N1F1	N1F2	N3F1	N3F2	P6F1	P6F2	P11	P13	P14	P15
Filter depth [m]	12.2	24.4	7.6	24.4	6.1	22.9	16.8	7.2	4.9	36.0

3.1.6.1 Results

As explained in section 2.2.1.6 the first step in analyzing the groundwater flow is to create a map of the spatial head distribution as it is measured on the 17th of January 2018 during the dry period. It must be noted that during this section the freshwater heads will be used, as described in section 2.1.3. The distribution is shown in figure 3.14.

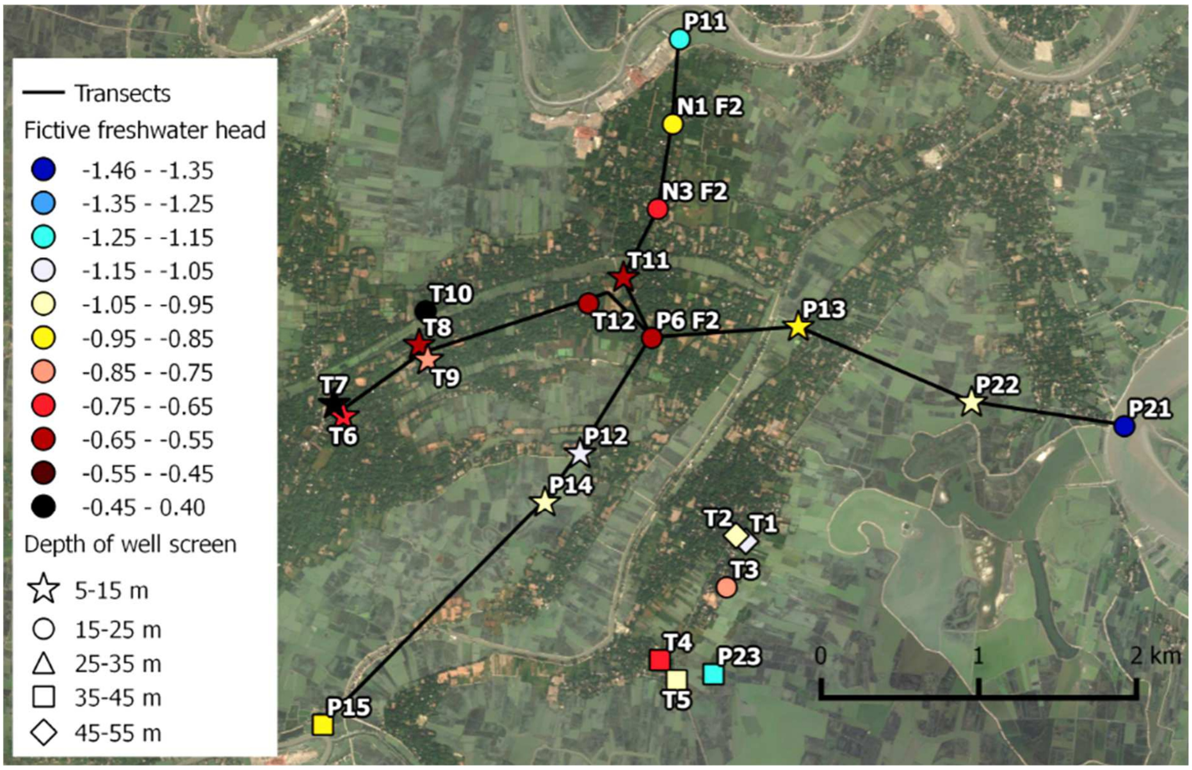

Figure 3-14. Spatial distribution of equivalent freshwater heads on the 17th of January 2018

To show the temporal variance between the wet and dry season, daily averaged logger data between August 2017 and April 2018 are plotted in figure 3.15. For this figure the three loggers in the elevated homestead area in the north (N1, N3 and P6) are compared to two loggers situated in the southern low-elevated aquacultural area (P14 and P15). A more extensive overview of all loggers starting in February 2017 and with 20-minute time intervals is presented in appendix A1.

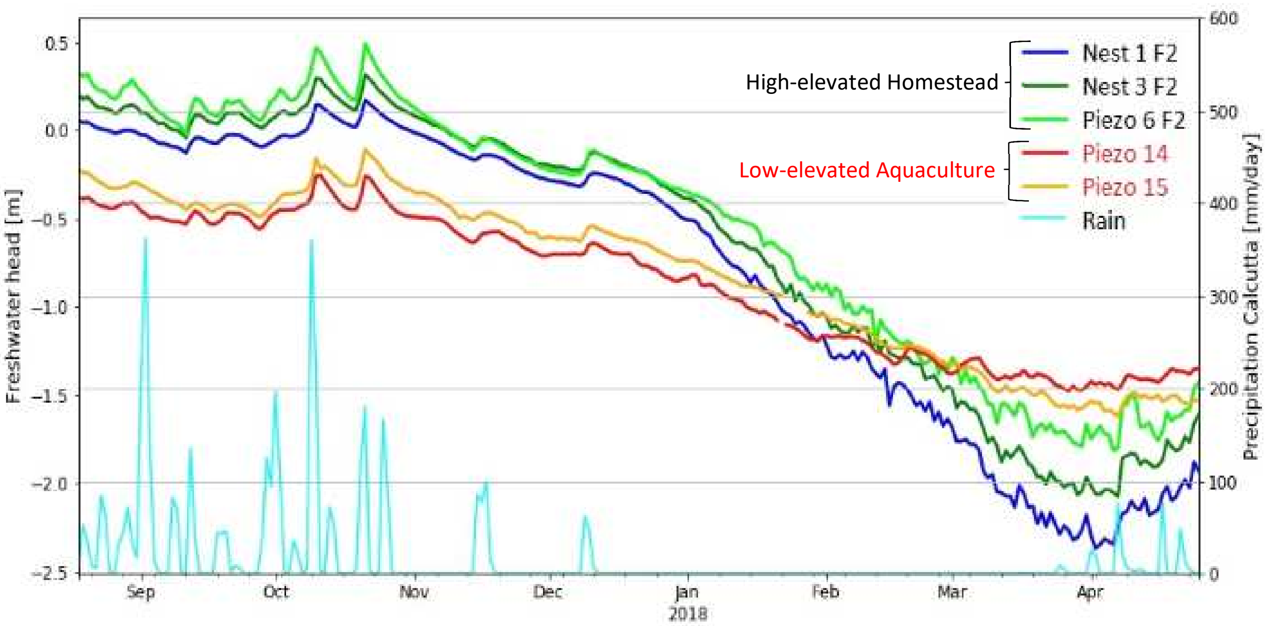

Figure 3-15 Temporal overview of part of the logger data. The black loggers written in black in the legend represent the loggers in the elevated homestead area and the ones written in red those in the low-elevated aquacultural region

It is clearly visible that the head gradient changes direction due to a larger seasonal variation in the elevated homestead area (N1 F2, N3 F2, P6) in comparison to the low-elevated aquacultural region (P14 and P15). This is emphasized in the boxplots of all logger data (figure 3.16), where all piezometers are shown, with the ones situated at lower elevation in aquacultural ponds in red.

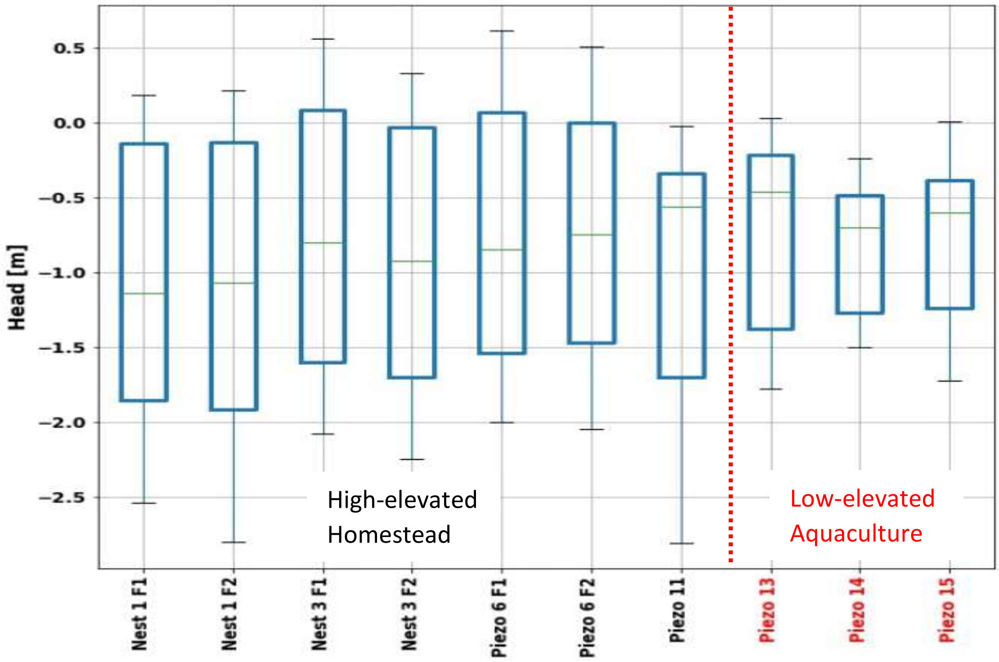

Figure 3-16 *Boxplots of all logger data for the period February 2017 to April 2018. The piezometers in red are the ones situated at lower elevation in aquacultural ponds*

It must be noted that the very low values at nest 1 and piezometer 11 in the north are expected to be caused by pumping in the vicinity. Thereby it is clear that the piezometers situated in low-elevated aquacultural regions show less seasonal variation in comparison to those on the high-elevated homestead areas. Whether this is caused by pumping, evaporation or other factors will be discussed in the following section when all results are combined.

To clarify the head data from figures 3.14 and 3.15, two cross-sectional head profiles are shown in figure 3.17 where (when available) heads from the wet period (4 October 2017) and dry period (4 April 2018) are included as well. It is important to notice that the wet season will be used to refer to the period with maximum heads (September to November) and the dry season for the period with minimum heads (April).

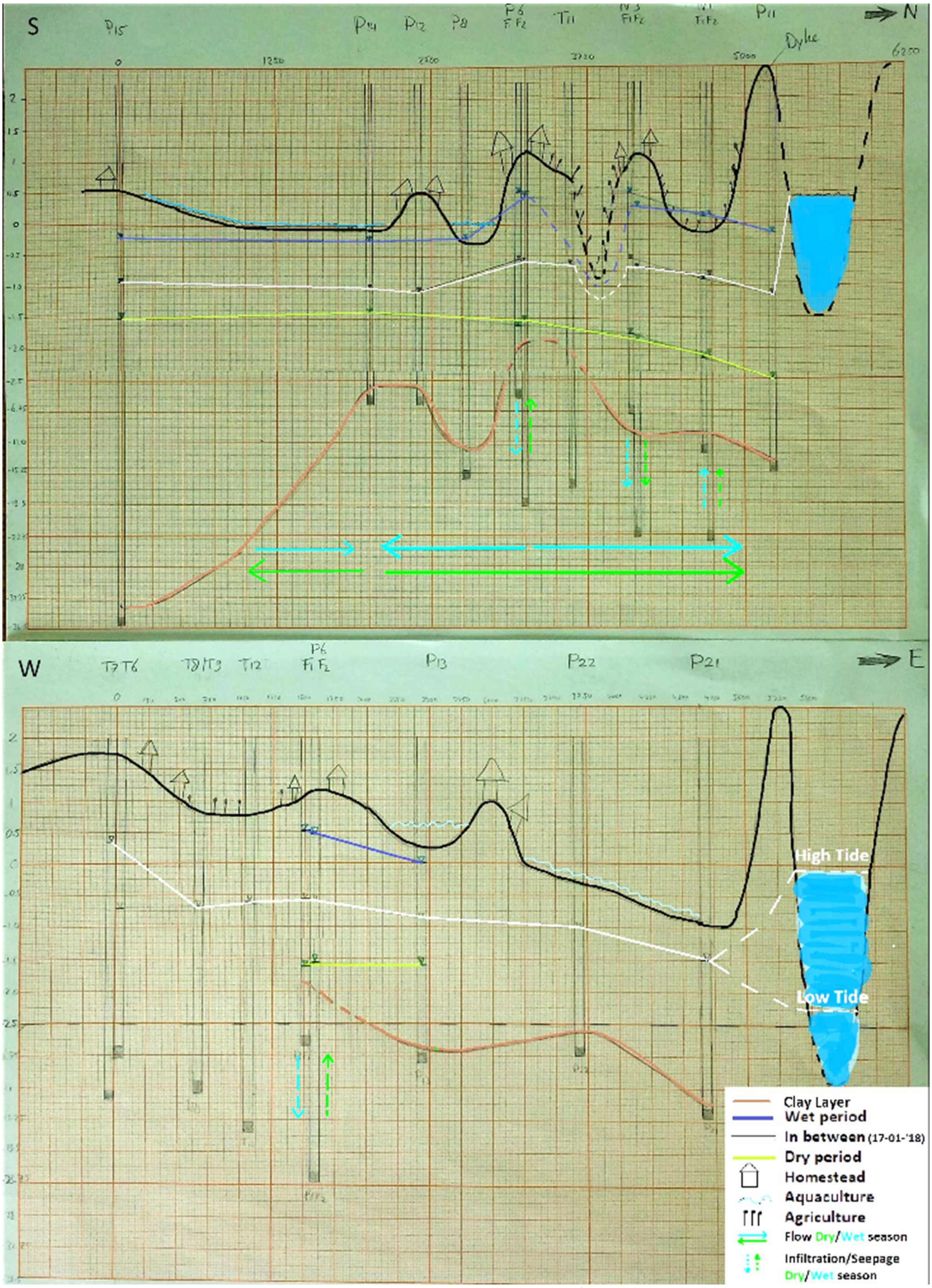

Figure 3-17 Cross-sectional profiles of head data measured in the field on the 17th of January and by be the loggers in the dry and wet period.

The lower figure shows a large head difference between tube wells T7 and T6 which are situated close to each other in the west. For the head connection T7 is chosen because a head increase in expected due to the elevation difference. For the rest of the piezometers with multiple measurements the one at similar depth compared to nearby well screens is chosen. The flow lines show seepage at agricultural regions and a reversal from infiltration (wet season) to seepage (dry season) at the elevated homestead area where P6 is situated. The river levels are estimated (northern river) or measured (eastern river) during the fieldwork procedure.

To test the possible influence of pumping, a graph of the daily variations is presented in figure 3.18. It must be noted that the daily variation is averaged over a week to make the graph better readable, the original graph with daily averages can be found in appendix A2.

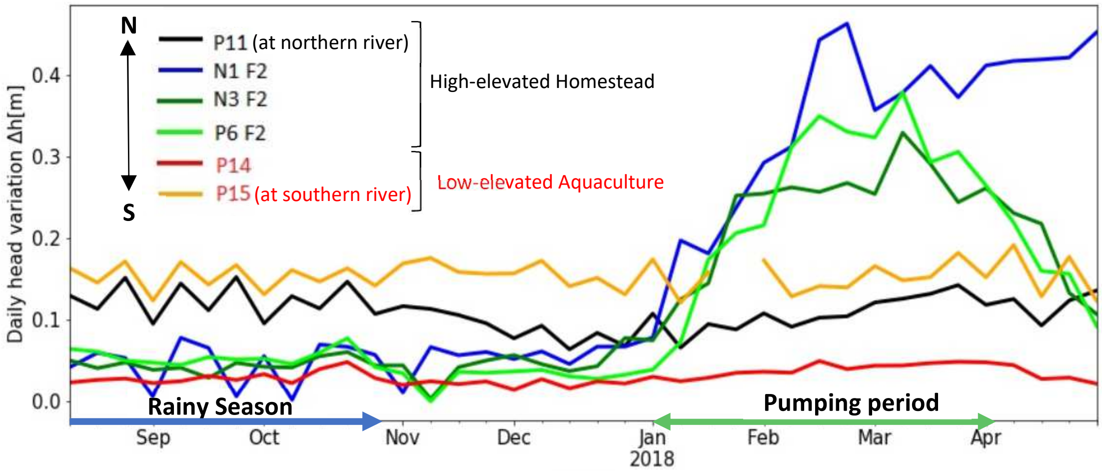

Figure 3-18. Weekly averages of daily variation of all loggers. Computed by subtracting the daily minimum from the daily maximum value before averaging all these values for one week

It is clearly visible that all loggers (except the one next to the river, P11) situated at high-elevated homestead areas show more variation during the period of pumping which generally starts in January (section 3.1.4). This will be important in the formation of conclusions when all results are combined in the following section.

Finally, extra graphs of the logger data on smaller timescales are constructed to analyze the short-term processes and the differences between the seasons, these are presented in figure 3.19 and again discussed in the following section. A distinction is made between the wet period with rain (19-21 July 2017), the wet period without rain (3-5 October 2017), the dry period with minimum head values (3-5 April 2018) and the period in between dry and wet during which the fieldwork is conducted (16-18 January 2018).

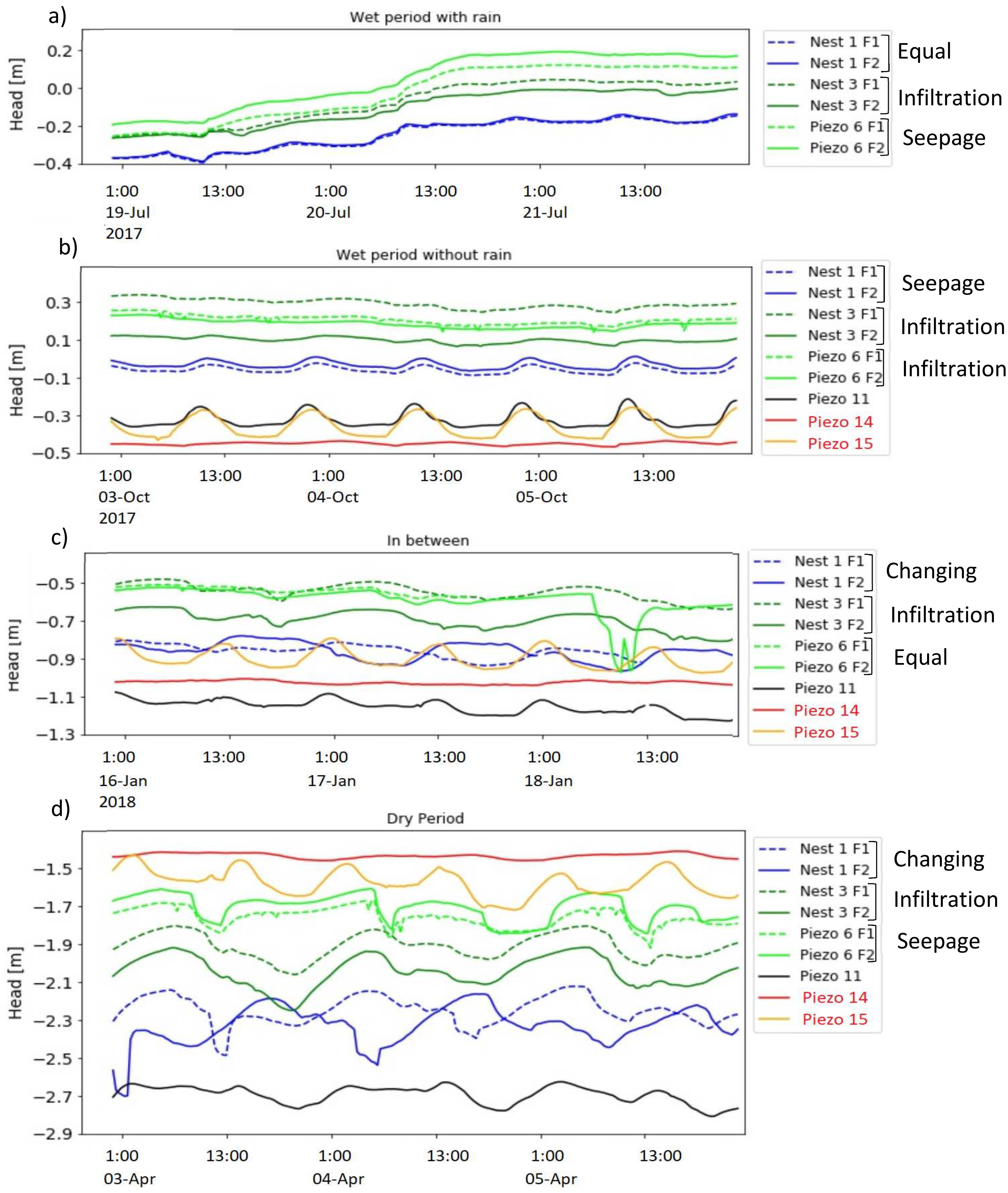

Figure 3-19 *Hydraulic head variation for 3-day periods a) in the wet season with a lot of rain b) in the wet season with 3 dry days c) between dry and wet without rain during the fieldwork and d) in the dry season. The loggers located in low-elevated qqaculture are shown in red and for locations with 2 well screen depths the vertical flow direction is indicated next to the legend*

An interesting observation is the change in vertical flow direction within the wet season at piezometer 6 on the southern side of the elevated homestead region. It is expected that the seepage during the period with rain is caused by overland flow filling the lower elevated fields in the vicinity, (see figure 3.17) this causes high pressures under the thick clay layers in these areas inducing upward flow towards P6.

The rest of the important observations from all the graphs presented in this section are summarized in table 3.5 below so they can easily be referred to during the formation of general conclusions in the discussions section. Here for each observation is denoted with a number in the column ‘#’. Thereby the ‘Dir.’ and ‘Dry/Wet’ columns indicate the direction and season to which the observation belongs.

Table 3-5 *Observations from the resulting graphs and figures.*

#	Figure(s)	Dir.	Dry/wet	Observation
1	3.14	-	Between	Decreasing head gradient from elevated homestead towards low elevated ponds; From central elevated homestead→southern and eastern aquaculture
2	3.14 & 3.17	W-E	Between	Heads at tube wells T7 and T10 in the north and west of the elevated homestead region are very high in comparison to other values on the 17th of January 2018
3	3.17	W-E	Between	Due to big difference between T7 and T6 not clear if head drops severely towards T8/T9 due to elevation or increases a bit
4	3.14 & 3.17	W-E	Between	Clear decreasing head gradient of 0.90 m from the central transect (P6) towards the eastern river (P21)
5	3.14 & 3.17	W-E	Between	Slight decreasing head gradient from central transect towards lower elevated T12, T8 and T9 in in the west
6	3.14 & 3.17	W-E	Dry+Wet	The decreasing head gradient from high elevated P6 towards the low elevated aquacultural P13 in the east reduces in the dry season
7	3.14, 3.15, 3.17	S-N	Wet	Decreasing head gradient from elevated homestead areas P6 and N3 towards low elevated aquacultural P14 in the south and to northern river (P11)
8	3.14, 3.15, 3.17	S-N	Dry	Downward head gradient implying flow from low elevated aquaculture (P14) towards elevated homestead (P6) in the north and P15 in the south. Same downward gradient from elevated N3 towards northern river (P11) as in the wet season
9	3.15 & 3.16	S-N	Dry+Wet	Head variation between dry and wet ±1m in aquaculture region (P13, P14, P15) and ±2m at high-elevated homestead (N1, N3, P6).
10	3.18	S-N	Dry+Wet	Higher daily variance in the dry season for piezometers in elevated homestead region with pumping (N1, N3 and P6) compared to the wet season. River (P11, P15) and aquacultural (P14) piezometers don’t show seasonal variance
11	3.17 & 3.19	S-N	Wet	High elevated P6 and N3 downward decreasing head (infiltration); Lower elevated agriculture N1 upward decreasing head (seepage)
12	3.19	S-N	Dry	Vertical head gradient N1 reverses during a day: shallow well head decreases during day and increases in night, deep well head vice versa, resulting in upward decreasing head (upward flow) during part of the day and downward decreasing head (downward flow) during most of the night
13	3.19	S-N	Wet	Vertical head difference in N1 is very small, slightly higher head at deep well
14	3.19	S-N	Dry+Wet	Vertical head N3 is always higher in the upper well indicating constant infiltration. This difference is lowest during rainfall events.
15	3.17 & 3.19	S-N	Dry+Wet	Vertical head distribution of P6 reverses between dry and wet. During the dry period the deepest filter has a higher head than the top well, this difference increases during daytime. In the wet period, after most of the rains the shallowest filter shows slightly higher head values.
16	3.19	S-N	Wet	Increase of about 0.2 m/day in all piezometers
17	3.19	S-N	Wet	Without rain tides clearly visible in P15, P11 and a bit in N1, N3
18	3.19	S-N	Dry	Head increase due to tides in P11 (northern river) and P15 (southern river) is less during daytime in comparison with nighttime
19	3.19	S-N	Dry	P14 shows almost no variation in the three-day period
20	3.19	S-N	Dry	Vertical head difference of N3 decreases during daytime and increases in the night

3.1.6.2 Discussion

Based on the observations drawn from the presented graphs in the previous section (table 3.5), this section first presents several conclusions with their motivation regarding the drivers behind the groundwater flow. Second, conclusive isohypses-maps for the dry period, wet period and period in between to present the expected current flow patterns are created.

Conclusion 1: Mechanical pumping is an important driver for the groundwater flow, especially in the dry season

First, logger data showed that the hydraulic head gradient and thereby expected groundwater flow on the central north-south oriented transect changes direction (obs. 8 & 15). This reversal in flow direction is due to a higher annual head variation on elevated village areas in comparison to low elevated aquacultural areas (obs. 9). This is expected to be partly caused by high pumping rates for irrigation during the dry season. High daily head variations in the elevated homestead areas (obs.10) amplify the importance of pumping since the fieldwork showed mechanical pumping not or nearly to occur in the low-elevated aquacultural regions.

Also, the decreasing head of N3 during daytime before increasing again over night (obs. 20) and the reversal of vertical head gradient of N1 (obs. 12) can be explained by extraction of water during daytime: Between 7:00 and 18:00 the hydraulic head of the shallow well (F1), which is at the same depth as the pumping wells, decreases due to pumping. To supply the demanded pumping quantity the head distribution radially changes around the pumping well, causing the head at the deep filter to increase so water can flow upward towards the well. The pumped water is then placed on top of the surface making it possible to infiltrate and cause a downward head gradient after pumping stops at night. This local difference in the head variations is an extra indication that pumping of groundwater causes the head decrease, since evaporation would be visible on a larger scale.

The fact that P14 in the aquacultural fields barely shows any daily head variations (obs. 19) also suggests the effect of evaporation to be negligible. But this could also be caused by the refilling of the aquacultural ponds with water from the river. Contrary, the larger tidal head decrease of P15 during daytime (obs. 18) is an example of possible evaporation. No pumping for irrigation is present in the region, yet still a small variation between day and night is observed. To check the driving force of the pumping, the decrease in heads is compared to potential and measured evaporation. This potential evaporation is done like *Mukherjee, Fryar, & Howell* (2007) with the method of *Malmstrom* (1969) where an average temperature of 34 ^{o}C is used for April in the following equation:

$$\text{Potential evaporation } [\frac{\text{mm}}{\text{month}}] = 40.9 \text{ x } e^{*}(\tau) \qquad \text{Equation 3.1}$$

where $e^{*}=0.611\exp(\frac{17.3\tau}{\tau+237.3})$, and τ is the average monthly temperature in ^{o}C. This method resulted in a potential evaporation of 218.45 mm/month or 7.28 mm/day. During previous fieldwork a pan was installed to measure the rain and evaporation between October 2017 and January 2018 (Naus, 2018; Appendix A3), this experiment shows a maximum evaporation rate in the beginning of January of 2.17 mm/day which is three times lower than the calculated potential evaporation rate. Dividing both these values by a sand porosity of 0.25 to obtain the representative column of water in the soil gives a potential evaporation range of 8.68 - 29.12 mm/day. This is way less than the observed daily fall in hydraulic head of 200 to 300 mm/day in the pumping area (N1, N3; figure 3.19d). This indicates that pumping is the main driver of the decrease in hydraulic head and thus flow towards higher elevated areas in the dry season.

This corresponds to previous research where a similar reverse in groundwater flow is found and attributed to pumping (Radloff et al., 2017). With respect to the previously formed hypothesis 3, the effect of the pumping is found to be higher than expected in advance since a complete shift in flow direction between dry and wet season was not expected. This could have major implications for the sustainability of the pumping which will be further explained later in this section and analyzed during the modelling part of this study.

Conclusion 2: Elevation is an important driver for groundwater flow, especially in the wet season in combination with recharge

Similar as in conclusion 1, the first indication of the driving force of elevation is the changing flow direction between dry and wet period (obs. 7 & 8). Head observations indicate flow from the high elevated homestead areas towards low elevated aqua- and agricultural regions in the wet season. This is visible in both north-south as west-east direction (obs. 1, 4, 7 and possibly 3).

Secondly, the high elevated homestead loggers P6 and N3 indicate infiltration during the wet season, while the lower elevated agricultural N1 measurements indicate seepage (obs. 11). At the high elevated N3, the elevation driver seems to stay dominant over the pumping driver since there is year-round infiltration (obs.14).

The influence of the elevation however decreases during the dry season (obs. 6) due to increased influence of pumping and the permanently ponded fields at low elevation. This causes the eastward flow to decrease in strength. Previous research (*Radloff et al.* 2017) even documented flow reversals in Bangladesh where a river performed drainage during the wet season and beginning of the dry season and supply during the dry season and beginning of the wet season. Such a complete reversal of the eastward flow is not expected in the Assasuni region since: 1) *Goswami* (2014) measured year-round flow towards the meander of the northern river in the northeast, 2) there is no extensive pumping close to the eastern river and 3) the flow towards the east is still strong during the dry season when the measurements were done (January). Nevertheless, the head difference between the elevated area on the north-south transect (P6) and aquacultural ponds to the east of it (P13) do show a weak westward flow towards the higher elevated P6 during the dry season. This is however expected to be local and not represent the overall eastward flow towards the river. But it must be noticed that this estimation regarding the flow in east-west direction is highly uncertain since P6 and P13 are the only measurements of both dry and wet season. To further confirm this estimation on west-east flow through the year, the heads of the newly placed piezometers in the east (P21 and P22) should be measured far in the dry season (end of March).

This conclusion regarding the elevation as driver corresponds with hypothesis 1 and 2 where elevation and rivers were mentioned as a driving force. However, the fact that the influence of this driving would differ so strong between the two seasons was not expected.

Conclusion 3: Infiltration on the elevated homestead area is an important process in the groundwater flow processes of the Assasuni area

As hypothesized in hypothesis 3, it is expected that infiltration influences the hydrogeological situation. Moreover, its effect is likely to be larger than believed beforehand since head values on the elevated homestead area increase with 2 meters during the 58 days of intensive precipitation (figure A1 in the appendix), resulting in a head increase of 35 mm/day. Combining this with a porosity of 0.25 indicates an average infiltration of 8.6 mm/day. Since the soils become saturated this rate can be used to check the conductivity values reported in section 3.1.4 that represent the infiltration rates (Philip, 1969). The infiltration found at I5 (24.5 mm/day),

which was concluded to be the most reliable for homestead areas, represents an infiltration velocity of 98 mm/day when it is corrected for the porosity. This is much higher than the average head increase since saturated infiltration does not constantly occur in the villages. It however does roughly correspond to the head increase of 300 mm in 1 day during days of rain (logger P6 in figure 3.19a) which represents an infiltration of 75 mm/day after correcting for porosity. This increases the certainty of the measured infiltration rate at homestead regions.
The infiltration rates at low elevated aquacultural ponding areas are expected to be lower since their seasonal variation is much less (obs. 9), infiltration measurements in the field resulted in values of zero infiltration (section 3.1.4) and the clay layer is expected to be much thicker in most low-elevated areas (section 3.1.2). The low infiltration rate is caused by deposition of fine clay in the stagnant ponds which created a very low-conductive clay layer at the bottom (Sengupta et al., 2008). However, even these regions show a head decrease of 1 m in the dry period (figure 3.15) which must be filled up during the wet season. This indicates that infiltration and lateral flow should cause a head increase of 4.3 mm/day during the wet season.
As mentioned previously in this section, the measured infiltration rate on the elevated homestead area (98 mm/day) is higher than the representative infiltration causing the measured head increase (75 mm/day). This high infiltration rate together with the expected low infiltration rate in the aquacultural ponds implies lateral flow towards these ponds to be the main source of the required head increase. The magnitude of this lateral flow is further investigated in the section regarding the modelling study.
In general, the high expected influence of infiltration (35-98 mm/day in the wet season) corresponds to the previous literature indicating that recent infiltration is a possible source of fresh water presence in the subsurface (Ayers et al., 2016; George, 2013; Worland et al., 2015).

Conclusion 4: The fact that lower elevated areas are constantly ponded could be important for the flow direction.
The fact that lower elevated areas are artificially flooded by riverine water during the complete dry season provides protection from upward suction due to evaporation in the soil. Thereby, the pressure exerted by the ponded water on the soil causes the head values to remain more constant which is visible on a daily scale at piezometer 14 (obs. 19). This contributes to a smaller falling head in the dry season (obs. 9) in aquacultural regions. Due to this lower variation in head values the flow of water from the low elevated aquacultural areas towards the high-elevated homestead areas is enhanced. However, it must be noticed that this conclusion is highly uncertain and should be investigated in further detail be means of a modelling study or comparison to a region with similar elevation but without ponding. This way it can become clear if the flow reversal would occur as well if the lower elevated areas would not consist of ponded water during the dry season and whether this would result in larger head variances due to evaporation.

Conclusion 5: The eastern and southern boundary of the Assasuni region act as no-flow boundaries
For the groundwater model, the flow at the western and southern boundary are important. Unfortunately, head measurements were not possible at the southern border and the western boundary was only analyzed by salinity measurements so this hypothesis cannot be easily confirmed. However, not much flow is expected at both borders since the south consists of a thick clay layer and is not connected to the eastern river and the west is expected to act as a water divide, like the other elevated areas, especially since the elevation is even higher. Salinity measurements (figure 3.11) show this area to consist of fresh groundwater while it is surrounded by aquacultural ponds with saline surface and groundwater. This is an extra indication of a lack

of in- or outflow since incoming flow from the west or east would have salinized this groundwater.

Conclusive flow patterns

Based on the conclusions regarding the flow drivers, three isohypses maps are created for the wet period (figure 3.21), dry period (figure 3.22) and the period in between (figure 3.20). Since elevation and pumping are expected to be the main drivers for groundwater flow, the elevation (figure 3.3) and pumping map (figure 3.10) together with head measurements are used to create the figures (as explained in section 2.2.1.6). Since head measurements are scarce in the east and west of the region during the dry and wet season these maps and flow directions are less reliable in comparison to the period in between during which the fieldwork was conducted.

The period between wet and dry consists of the most measurements which results in the most reliable isohypses-map (figure 3.20). The expected flow is driven by both pumping as well as elevation during this season. Figure 3.20 shows the pumping influence from P6 on the elevated homestead area towards the northern rice agriculture and the elevation driven flows from the high elevated homestead areas towards the low-elevated aquaculture and eastern and northern river. Of which the latter is based on data from *Goswami* (2014) where flow from the elevated area towards the meander in the northern river is reported year-round, so this flow direction will also be presented in the two other figures for dry and wet.

Regarding the wet period (figure 3.21) the expected flow from high-elevated homestead areas towards low-elevated aquacultural areas is implemented in the isohypses-map. For the central transect these flow directions are monitored by the logger data. The rest of the flow pattern estimates are based on the presented conclusions regarding the drivers of the groundwater flow and are thus less accurate. The flow from the eastern elevated area towards the eastern river is chosen to be like the situation measured in January it is very likely that the flow towards the lower elevated river increases or remains the same. The biggest difference between the measurements in January and the wet season is the lack of pumping near N3 and N1 during the wet season but it is not known if this pumping influences this eastward flow.

In the dry period (figure 3.22) pumping is expected to be the main driver of groundwater flow. The head data on the central transect confirmed this (obs. 8). Groundwater is expected to flow towards areas with pumping (figure 3.10) in the north of the western elevated homestead area and towards the central village area. In areas with no mechanical pumping, like the south of the western elevated village area, elevation driven flow is still expected. This also holds for the east of the region where no mechanical pumping is present, the flow towards the river is expected to decrease in strength since the head values of the elevated area are expected to decline more than those on the lower elevated aquacultural ponding area. The amount of this decrease in flow strength is highly uncertain and solely based on estimation and the process of reversing flow to/from a river due to groundwater pumping (Radloff et al., 2017).

The reverse in north-south directed flow is of large importance for the communities living on the elevated areas. Currently, fresh water is situated underneath these elevated regions (figure 3.13), but if the yearly northward flow due to pumping is stronger than the southward flow, this would cause salinization by the saline groundwater underneath the aquacultural ponds. Therefor it is of great importance to understand to what extent pumping is sustainable and does not cause a net yearly decrease of the freshwater reserve. This is also dependent on the eastward flow which needs further investigation together with the relation between dry northward flow and wet southward flow which is further studied in the small modelling study.

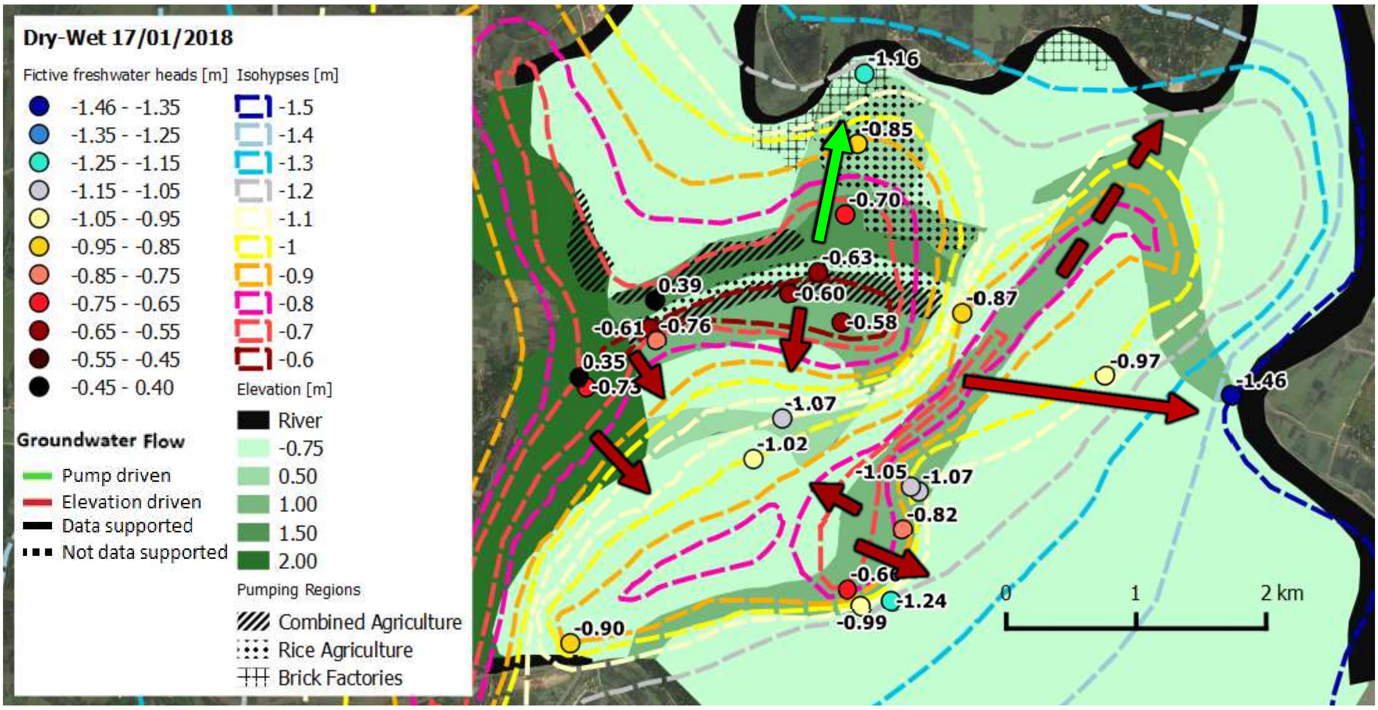

__Figure 3-20__ Isohypses map and flow directions during the period with most data (between dry and wet); the thickness of the flow lines roughly indicates the amount of groundwater flow

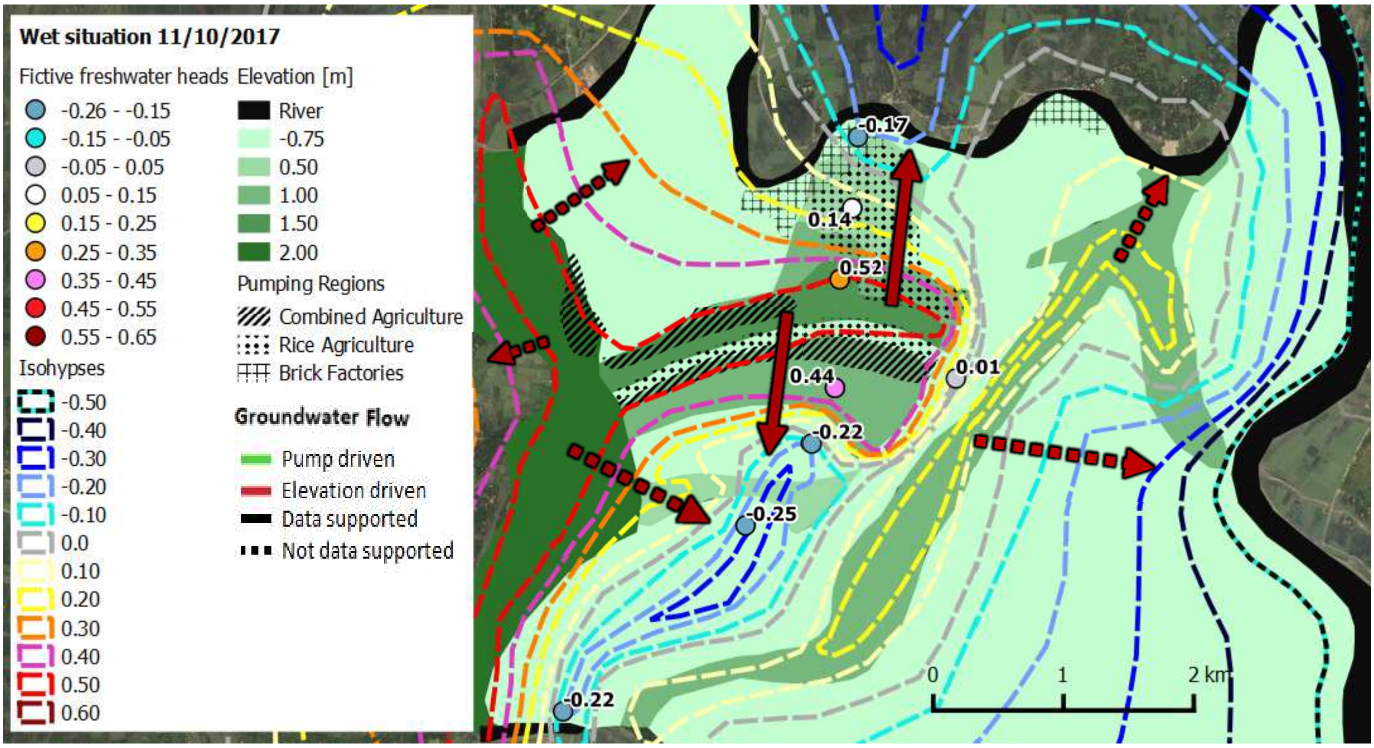

__Figure 3-21__ Isohypses map and flow directions during the wet period; the thickness of the flow lines roughly indicates the amount of groundwater flow

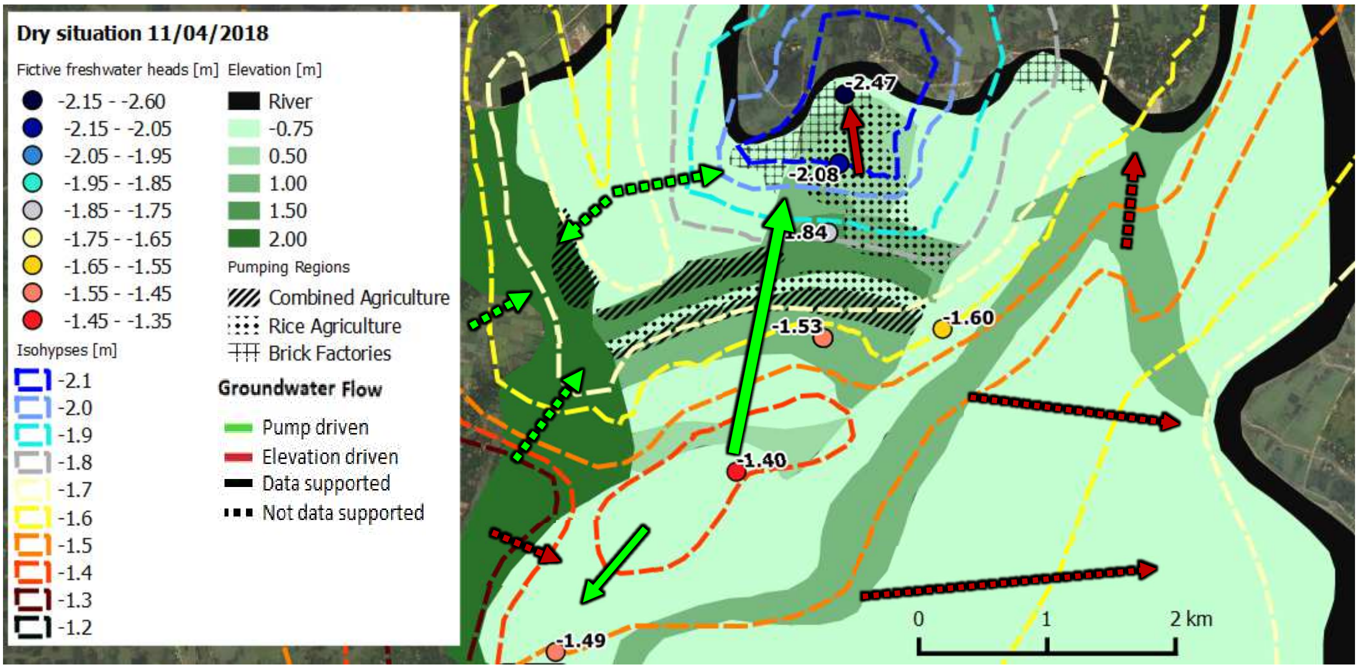

Figure 3-22 Isohypses map and flow directions during the dry period; the thickness of the flow lines roughly indicates the amount of groundwater flow

3.2 Coupling of field data to model

Before the start of this study the exact approach of the modelling study was not clear since it is highly dependent on the results obtained from the field study. Therefor this section will couple the field data to the modelling study by first emphasizing the modelling goal and second presenting the current modelling plan. This will further specify the initial research question: '*How do the current groundwater conditions evolve in the future under varying scenarios?*'

3.2.1 Modelling goal and research questions

In the previous section four conclusions regarding the groundwater flow were formed. These conclusions involved the influence of pumping, recharge by precipitation, infiltration through the clay and the importance of ponding. The goal of this brief modelling study is to test these conclusions and to quantify the relation between different processes in the dry and wet period to estimate future evolution of the salinity distribution. This results in the following research questions:

- *What are the relative contributions of pumping and recharge to the groundwater flow?*
- *To what extent do aquacultural ponds influence the groundwater flow?*
- *To what extent does possible infiltration influence the groundwater flow?*
- *At what rate does the salinity distribution change?*

3.2.2 Initial model setup

Conclusions from the fieldwork (presented in section 3.1) are used to set up the initial model. This section provides a step-by-step overview of this initial model set-up.

3.2.2.1 Grid size and model boundaries

First the extent and grid size of the model are defined. The northern and eastern river are chosen as boundaries in combination with the elevated area in the west. In the south, part of the border consists of a river and part of aquacultural ponds with a thick clay layer. The size of this region is 6.9 by 6.3 km with a total area of 27.4 km^2 within the boundaries (figure 3.23). The choice for the rivers as boundaries is obvious since they are good to model via general or constant heads, the western and southern region are suitable because they are both expected not to experience any in- or outflow (section 3.1.6).

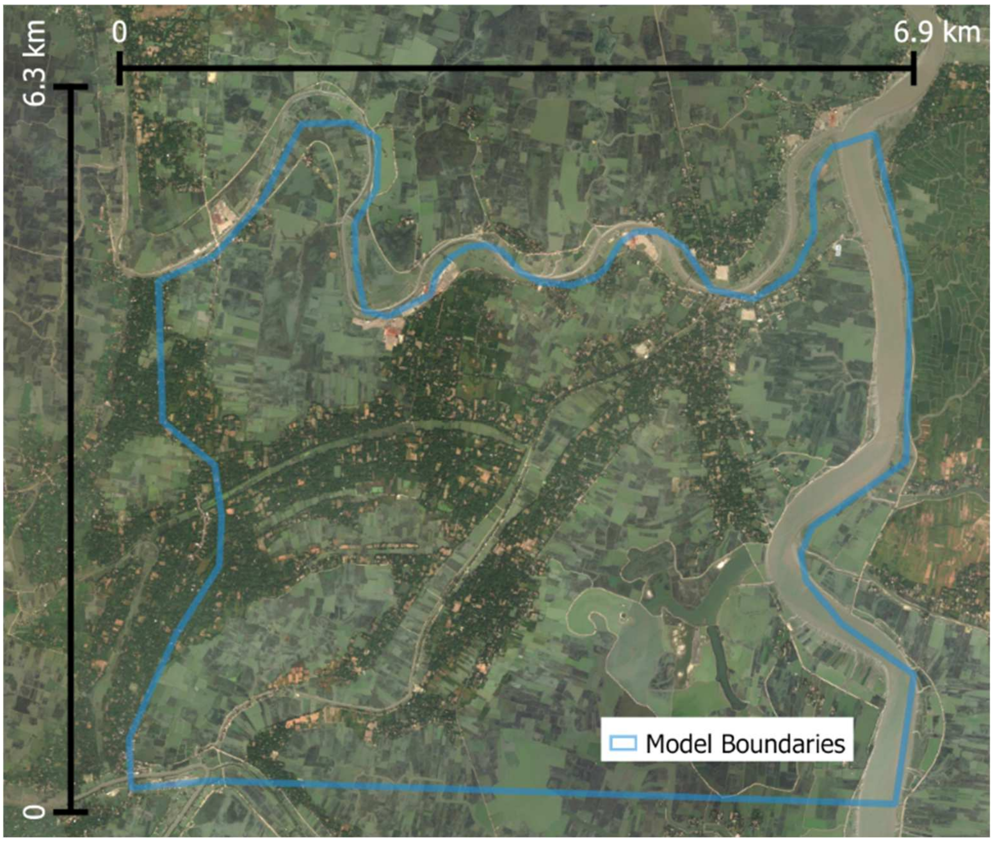

Figure 3-23. *Boundaries chosen for the model*

The depth of the model is chosen to extend to 110 meters since a regional borehole showed a clay layer to be situated at this depth (van Broekhoven, 2017). These dimensions are fit to a modelling grid of in total 58 by 56 cells and 15 layers. Hereby refinements are created over the elevated areas because these regions require larger detail. These refinements result in cell sizes of 172.5 x 175 meters in the non-refined regions and cells sizes of 53 x 50 meters in the refined regions (figure 3.24 at the end of this section). This figure also shows the vertical refinement of the 15 layers with two thin layers of 3 and 2 meters at the top, followed by 11 layers of 5 meters, 1 layer of 10 meter and 1 layer of 40 meter. This structure is chosen because very little is known about the bottom part of the model and it is only used to simulate a possible storage volume. The layers at the top must be thin because differences in initial and boundary conditions vary over small vertical distances. With this structure the model consists of 48,720 cells. The cell sizes and depths are relatively large since the model is used as a first rough representation to investigate some general processes in short time, so it is important that the model has a low processing time. Unfortunately this will decrease the accuracy of the model.

3.2.2.2 Elevation

The elevation of the top layer of the model is based on the findings in section 3.1.1. The conclusive figure provided in this section (figure 3.3) is implemented as elevation of the top layer.

3.2.2.3 Lithology and soil parameters

The lithology of the model is divided in two layers; clay on top of sand. Both layers are characterized by different soil hydraulic parameters. The thickness of the overlying clay layer through the region is implemented like presented in figure 3.7, hereby the values are rounded to be able to fit in one layer. The conductivity values discussed in section 3.1.3 are appointed to the different layers.

For the effective porosity, standard values for sand and clay are chosen, the specific yield is chosen to be equal to the effective porosity (Hendriks, 2010) and the specific storage is based on values from literature for clay and sand (Younger, 1993). All the chosen values are presented in table 3.6. The vertical conductivity values of especially clay will be analyzed during calibration since they are expected to be important for the groundwater flow.

3.2.2.4 Additional water in- and output

As discussed before (section 3.1.6), extraction via pumping and net recharge as result of precipitation are important in- and outputs of water in the model. These will be extensively varied during a sensitivity analysis. The initial values for the pumping rates in rice and combined agricultural areas are discussed in section 3.1.4. These will be assigned to the model during the dry season in the whole regions of extraction (figure 3.10) since the cell-sizes are too big to realistically represent individual pumping systems. This is done by multiplying the area of the cell with its expected daily pumping rate. The recharge will be applied to the entire surface of the model during the rainy season with an initial value of 25 mm/year since this is within ranges of values found in literature (Michael & Voss, 2009 [30-250 mm]; Mukherjee et al., 2015 [100-300 mm]; Mohammad Shamsudduha et al., 2011 [10-100 mm]) and corresponds to the value found via calibration during the previous study on the middle transect of the current region (van Broekhoven, 2017). This recharge value represents the net recharge since evaporation is not included in the model.

Table 3-6. *Overview of initial parameter applied to the model*

Parameter	Symbol	Unit	value
Width (columns)	x	meter	6700 (58 cells)
Length (rows)	y	meter	6300 (56 cells)
Depth	z	meter	110 (15 layers)
Conductivity Clay (vertical)	Kc,v	m/day	Ponds (rice and fish): 0.028 Villages: 0.6
Conductivity Clay (horizontal)	Kc,h	m/year	0.05
Conductivity Sand (vertical)	Ks,v	m/day	1.125
Conductivity Sand (horizontal)	Ks,h	m/day	11.25
Effective porosity Clay	n_c	-	0.4
Effective porosity Sand	n_s	-	0.25
Specific storage	Ss	/m	Clay: 0.005 ; Sand: 0.0005
Specific Yield	Sy	-	Clay: 0.4 ; Sand: 0.25
Net recharge	Rnet	m/day	0.00014
Pumping	Qout	m/day	Rice: 0.0106 Combined Agriculture: 0.00641

3.2.2.5 Boundary and initial conditions

As visible in figure 3.23, the boundaries of the model are partly represented by rivers and partly by elevated villages and low-lying aquacultural ponds. The boundary conditions of the western and southern borders, which are not represented by rivers are chosen as no-flow boundaries as explained in section 3.1.6. The rivers in the north, east and south are represented by constant head cells which are presented in table 3.7. The northern and southern heads are based on daily average values of piezometer 11 in the north and piezometer 15 in the south during the season of interest. For the east, a difference of 1.2 meter in comparison to the northern river was measured during the fieldwork, this was implemented in the model.

Table 3-7. *Initial head values of the rivers*

River	Wet head	Dry head
North	-0.3	-2.7
East	-2.0	-4.4
South	-0.4	-1.5

The southern river is situated in the clay (depth of 5 meter in clay thickness of 12 to 35 meters). The northern river only touches sand in the meander in the east (northwest of P24) where the clay thickness is modelled equal to the river depth (5 meters). And the eastern river is connected to the sandy aquifer in the meander near in the middle of the river where the clay thickness is about 5 and the river depth around 10 meters. It must be noted that the tidal changes are not incorporated in the model because this would require too much temporal detail and it was not measured during the fieldwork.

The bottom of the model is modelled as a no-flow boundary since it consists of a clay layer that separates two aquifers of which the exchange is expected to be low and irrelevant for this study. The top of the model inside the boundaries is partly assigned with variable head-cells (village areas and agriculture) and partly by constant head-cells (aquacultural areas) because these regions are represented by constantly filled ponds. During the dry season these aquacultural ponds are irrigated with the river water by opening sluices which can also be done during the rainy period if the water level in the aquacultural ponds drops. An initial head value of 0 meter is assigned to these aquacultural ponds because it is not possible to know the exact heads and this way a water level of 75 cm is represented in the aquacultural ponds which is like the levels observed in the field. Figure 3.24 shows an overview of the model with its boundary types at the surface with the different cell sizes in the horizontal (top) as well vertical plane (bottom).

To define an initial head distribution for both the dry and wet simulation the isohypses maps (figure 3.21 and 3.22) are used. Since the dry simulation starts at the end of the wet period the initial situation of the dry simulation is constructed by fixing the wet isohypses map to the top 35 meters of the models before running the model in steady state to fill up the lower 75 meters. This is done because field measurements showed minimum difference within the upper 35 meters. For the wet simulation the same is done with the dry isohypses map.

The initial salinity variation through the model is extensively discussed in section 3.1.5. This distribution that represents the presented chloride concentrations (figure 3.13) is applied to the SEAWAT-model.

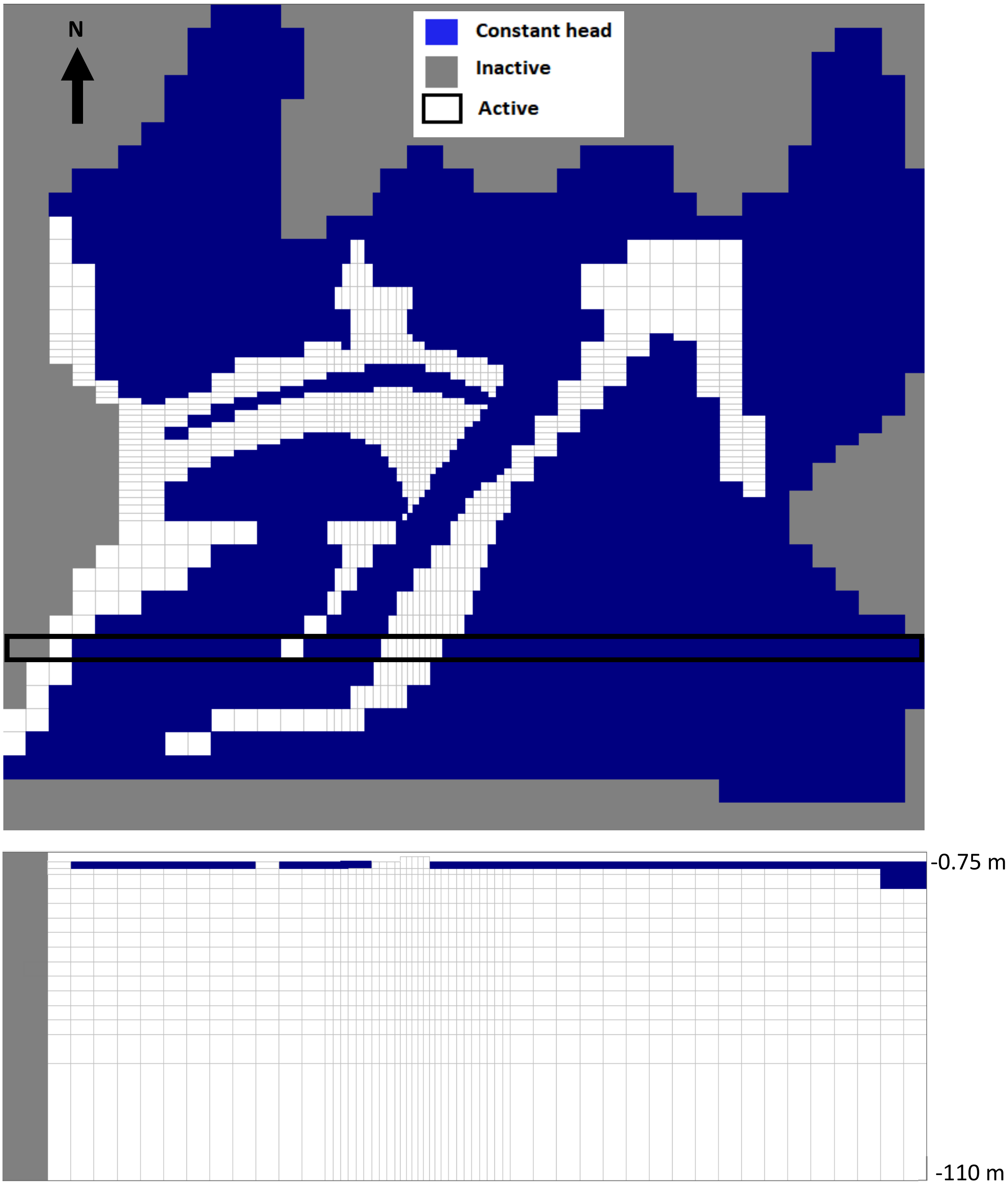

Figure 3-24*. Top: Surface of the Modflow model with in blue the constant head cells, grey the inactive cells and in white the active cells. Bottom: Cross section of the indicated row to present the different layer thicknesses.*

3.3 Model

3.3.1 Calibration and model performance

Since there was not much time for the modelling study the calibration was only limited. Only the general flow directions (section 3.1.6) were aimed to model since the logger data showed to be difficult and time consuming to reproduce. The results of this brief calibration are shown in table 3.8. The increase in recharge is severe but was necessary to reproduce the flow from high elevated homestead areas to low elevated aquaculture. The 250 mm/year is still within the ranges found in literature (see section 3.2.2.4).

Table 3-8. Parameter changes after calibration

Parameter	Change	Season
Vertical conductivity	Multiplied by 4	Wet+Dry
Recharge	From 25 to 25 mm/year	Wet
Eastern river head	From -4.4 to -3.5 m	Dry

It must be noted that modelling the transition between the dry and wet period did not work, so in the rest of this report the model is regarded as simulating a month of the dry period with minimum head values and pumping in March or a month in the wet period with maximum head values and recharge in October. Figure 3.25 shows the performance of the model is poor in terms of simulating the correct head values on the transect.

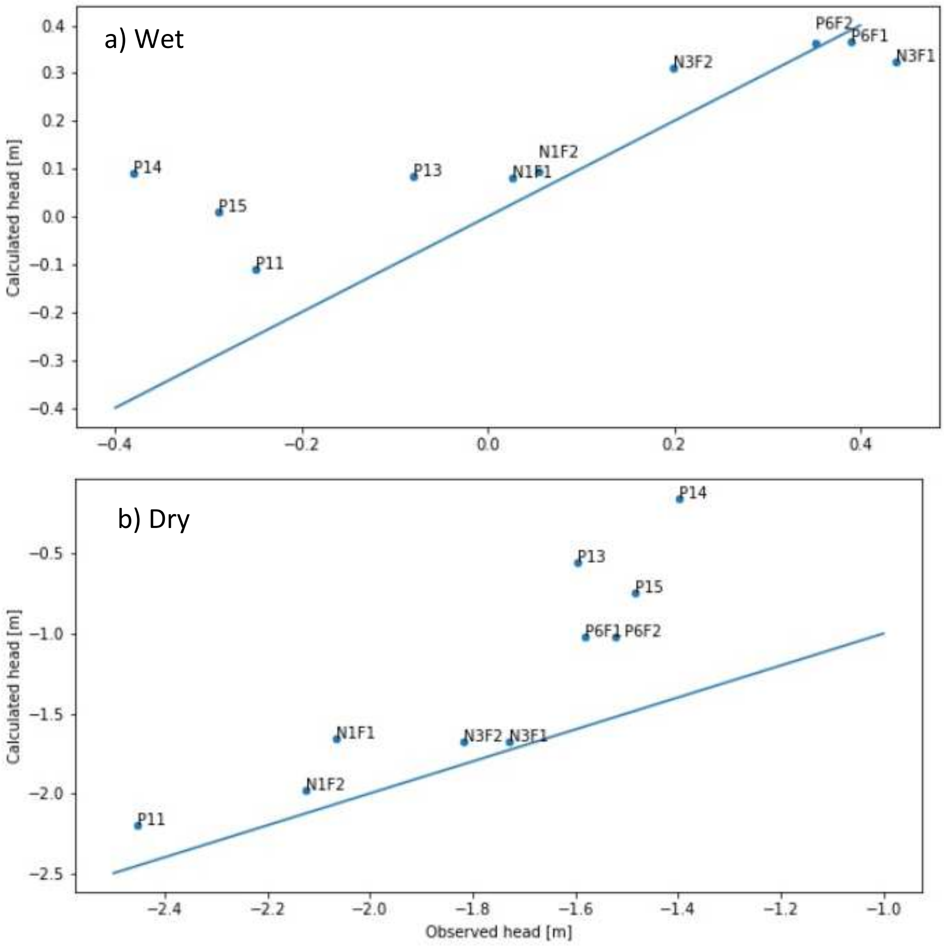

Figure 3-25 Observed head versus calculated head for the loggers in the last month of a) the wet period and b) the dry period

Nevertheless, in general the sequence of the data is correct. Only the southern piezometer heads (P14 and P15) are calculated too high during the wet period, but the expected flow from the northern elevated area (P6 and N3) towards the lower aquacultural ponds (P14) is still visible. During the analysis of the model it must be kept in mind that many of the head differences in especially the dry period are exaggerated.

To show the general model performance, figure 3.26 shows the lateral head distribution of layer 6 which is at a depth of 25 to 30 meters. The calculated flow velocities are indicated with arrows and will be further discussed in section 3.3.2.2. They are derived from calculations with the head differences and velocity vectors calculated by SEAWAT (appendix A-4).

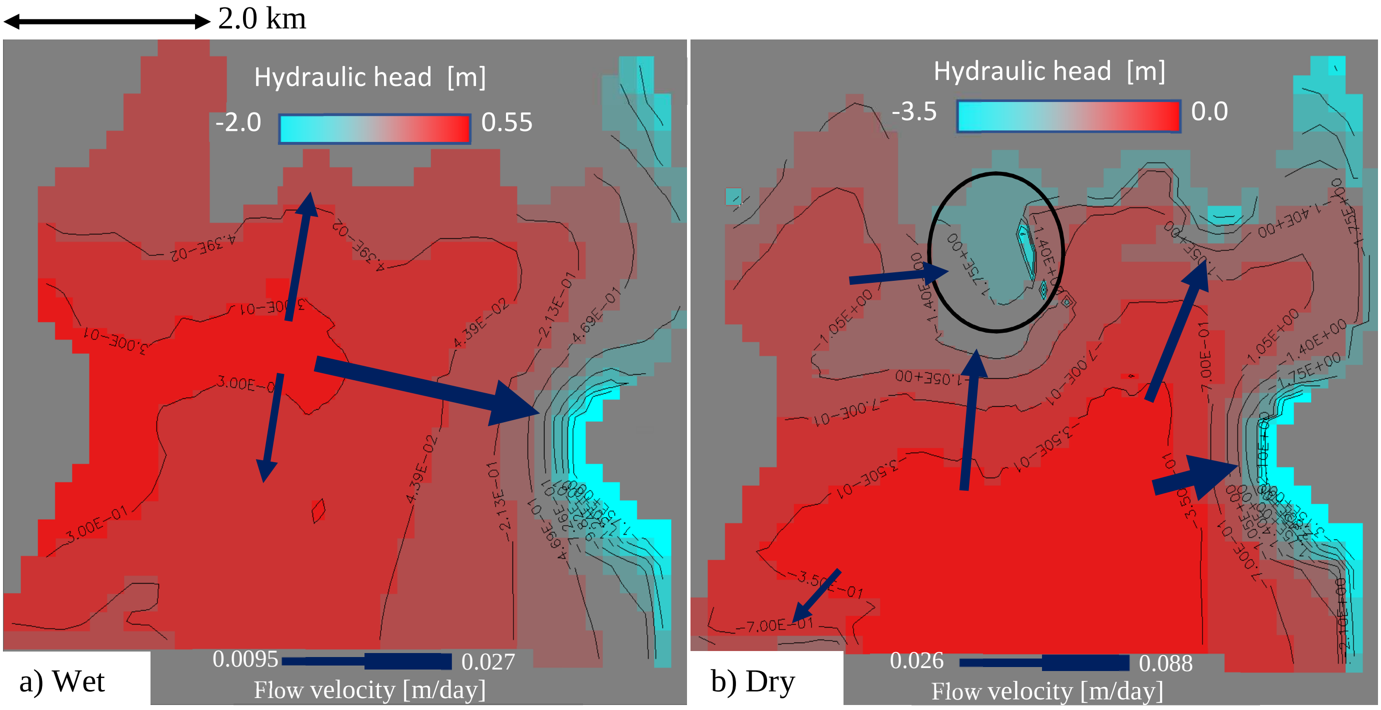

Figure 3-26 *Head distribution of layer 6 calculated in PMWIN by SEAWAT in a) wet period and b) dry period. The circle indicates the area of most severe pumping and the arrows show the flow vectors where the thickness indicates the speed.*

During the wet season, the flow from the higher elevated homestead areas situated in the center and west of the region towards the aquacultural ponds surrounding them is evident. The flow from the small elevated areas more to the east is not visible at this depth. During the dry season, the flow from the aquacultural ponded areas towards the area of pumping in the north is clearly visible. The head distribution indicates flow from all directions towards the pumping region. In both situations the river in the east shows to influence the flow severely as was concluded from the fieldwork and induced by the low constant heads. Since this shows to be a sufficient representation of the flow system that is concluded from the field work this model is used to answer the research questions.

3.3.2 Model outcomes

This section will present the results obtained by the modelling study. These results will be discussed to answer the research questions and couple the model to the real situation.

3.3.2.1 Results

First the general water balance of the dry and wet model is regarded (table 3.9). It is important to notice the severe difference in outflow via wells during the dry period and inflow via recharge in the wet period (factor 1.76), even though the recharge is set at 250 mm/year which is high in the range of reasonable values. The difference is induced by the constant head cells representing the aquacultural ponds. Recharge applied to these cells is not recorded as input to the model since the constant head cells do not change because of recharge. The total recharge added to the model is 38,346 m^3/day (0.0014 m/day x 27.39x10^6 m^2) which is much higher than the wells in this simulation. Thereby the water balance indicates larger fluxes during the dry season in comparison with the wet season, these are further analyzed during a sensitivity analysis.

Table 3-9. Water balance wet and dry model. Values in m^3/day for the whole model domain.

	Constant head **In**	Constant head **Out**	Constant head **(In-Out)**	Recharge **In**	Wells **Out**
Wet	12,500	21,100	-8,600	8,560	-
Dry	49,700	34,600	15,100	-	15,100

To compare the concluded flow from fieldwork with the modelled flow, head profiles of the two models are presented in north-south direction and east-west direction (figure 3.28). The locations of these profiles are like those during the fieldwork study (see figure 3.27). The flow lines drawn in the figures are based on head differences and velocity vectors calculated by SEAWAT (figure A5 in appendix).

Figure 3.28 clearly represents the differences in flow behavior between the two simulation periods. Both transects show more local head variation during the wet period in comparison to the dry period. The head profiles in the wet period are strongly induced by the constant head cells (aquacultural ponds and rivers) that act as the drainage basin for the area. In the wet model these local head variations are visible up to about 70 meters depth. For the dry period this highly depends on the location. In the north (figure 3.28b) pumps are situated at 10 meters depth causing the infiltrated pond water to flow directly to the pumps. This prevents the head to further increase with depth. In the same figure in the south, head variations up to 70 meters are visible due to the constant head ponds. On the west-east transect (figure 3.28c) no mechanical pumping occurs, this causes the influence of the constant head ponds to increase on the local scale. Nevertheless, the driving force of the eastern river is so big in this situation that it exceeds the ponding influence.

To test these influences of the different in- and output fluxes on the groundwater flow in the north-south direction the flux between two created domains (figure 3.27) is regarded. The width of this domain is chosen because the loggers are situation within this area and the division between A and B is to separate the higher homestead area in A from the mainly aquacultural ponded area in B.

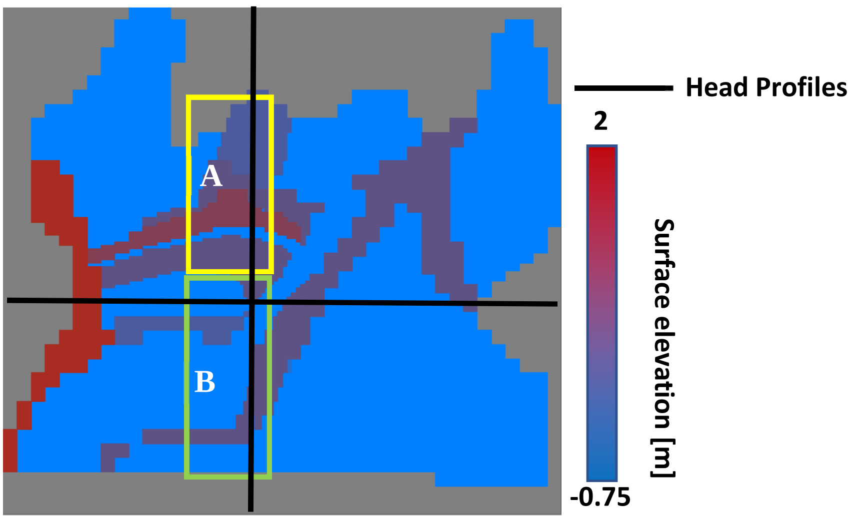

Figure 3-27 Domains used to analyze the flow in north-south direction with the surface elevation of the model as background.

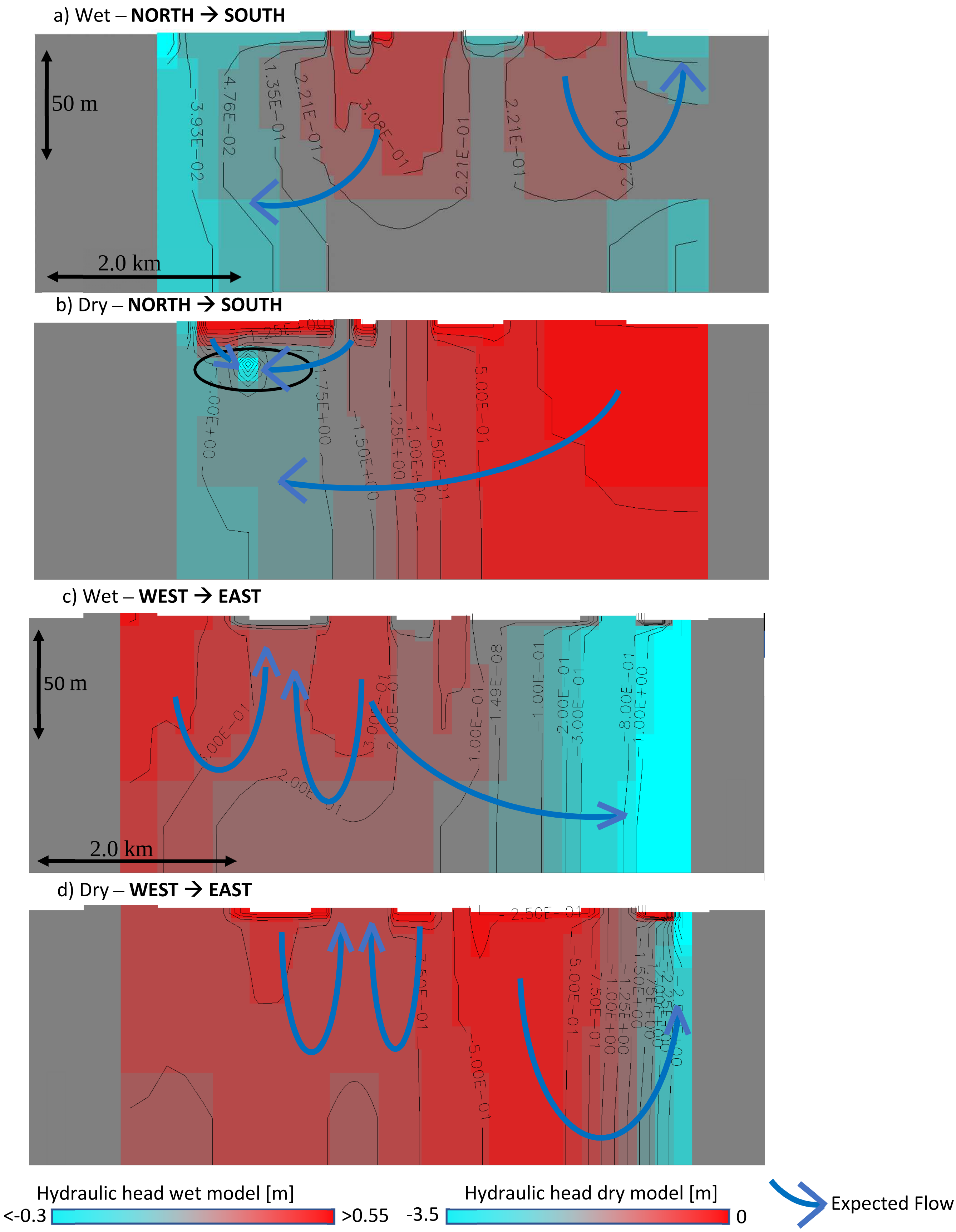

__Figure 3-28__ Cross sectional head profiles of the wet (a and c) and dry (b and d) model. The black circle again indicates an area of mechanical pumping. The scale of b is the same as a and of d the same as c.

Flow from A towards B is regarded as positive in this analysis where the aquacultural ponds, recharge, pumping and vertical clay conductivity representing the ease of infiltration are varied within reliable ranges. Aquacultural ponds are regarded between values of -1 and 1 m while the others are varied relatively to their standard condition in the calibrated model (table 3.10).

***Table 3-10**. Absolute values used in the sensitivity analysis of the models*

Relative	Recharge [mm/year]	Pumping [m/year]		Vertical conductivity clay [m/day]	
		Rice	*Other*	*Homestead*	*Ponds*
0.04	10	-	-	-	-
0.2	50	0.38	0.23	0.12	0.0056
0.6	150	1.15	0.70	0.36	0.0168
1.0	250	1.91	1.16	0.6	0.028
1.2	300	2.29	1.39	0.72	0.0336
1.6	-	3.06	1.86	0.96	0.0448
2.0	-	3.82	2.32	1.2	0.056

The results of the sensitivity analyses for both models are shown in figure 3.29. The relative flow in comparison with the standard simulation is plotted so the two models can be compared. The absolute flow towards the north during the dry season is severely higher (1671 m^3/day) than the southward flow during the wet season (279.9 m^3/day).

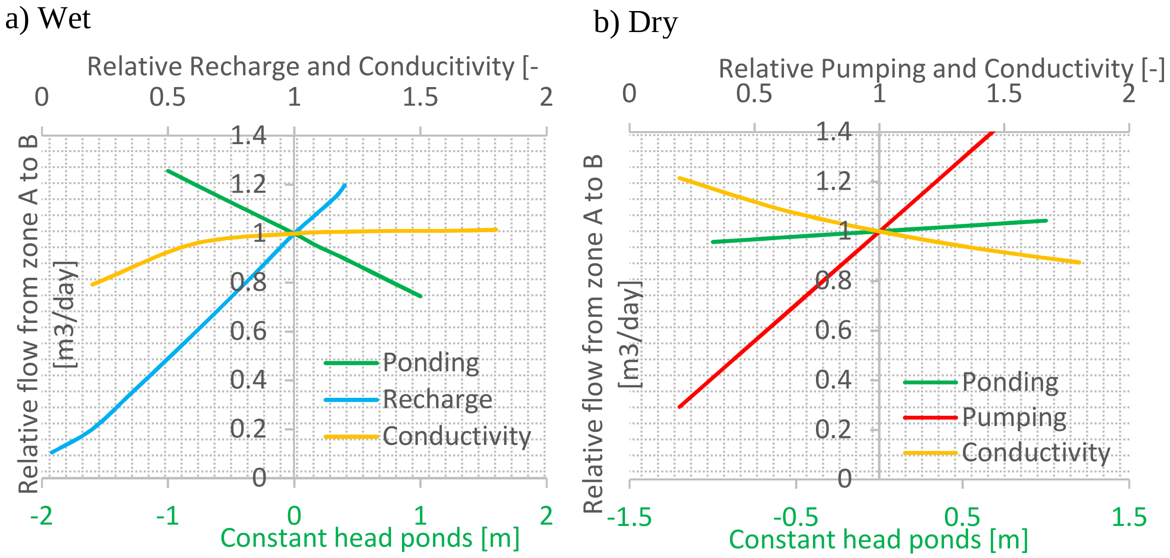

***Figure 3-29** Results of the sensitivity analysis regarding the flow between zone A and B for a) the wet model and b) the dry model*

The wet period clearly shows to me most sensitive to recharge which logically increases the southward flow. Ponding on the other hand decreases the flow because the flow in the model is driven by the drainage of the constant lower head in the aquacultural ponds while non-constant cells increase due to infiltration. The relative importance of the conductivity is only significant for low values. This indicates that infiltration limits the flow for low conductivity values, if these increase the drainage of the aquacultural ponds becomes the main driver in the model. During the dry period the pumping is most important as expected with higher pumping rates logically increasing the northward flow. This sensitivity to pumping in the dry season is comparable to the sensitivity to recharge during the wet season. Contrary to the wet period, the ponding shows a positive and the conductivity a negative correlation. For the aquacultural ponds this is easily explained as they act as a supplier of water in the region. The negative influence of the vertical conductivity is found to be induced by an increase in direct infiltration from the surface towards the pumping in the region of pumping itself. This decreases the demand of water from the south.

Last, the model is used to roughly calculate flow velocities in the dry and wet period in the north-south direction to get a feeling of the distances travelled by water in 1 year. This is done by taking the head differences (dh) and distance (dx) between P14 in the aquacultural area and P6 in the elevated homestead area to calculate the flow velocity v [m/day]:

$$v = -k \frac{dh}{dx}\frac{1}{n} \quad \text{[Equation 3.2]}$$

Where k is horizontal conductivity (11.25 m/day for sand in the model) and n the porosity (0.25 for sand in the model). For the wet season a head difference of 0.272 m results in a flow velocity of 0.0098 m/day and for the dry season a head difference of 1.181 m results in a flow velocity of 0.042 m/day. This indicates maximum flow distances of about 7.5 meters in the dry situation which explains why the salinity distribution with minimum cell size 50x50 meters does not change over the modeling periods. The flow velocities and their implications for future salinity variations will be further analyzed in the discussions section.

3.3.2.2 Discussion

In this discussion, the results presented in the previous section will be coupled to the field situation and used to answer the four research questions for the modelling study. Thereby possible improvements of the model will be discussed.

1) *What are the relative contributions of pumping and recharge from precipitation to the groundwater flow?*

Before regarding the contributions of precipitated recharge and pumping to the groundwater flow, first the contribution to the complete system is discussed. As reported in the previous section the amount of pumped water per day is much higher than the amount of recharge from precipitation added to the model because the constant headed aquacultural pond cells do not receive any recharge. This is comparable to the real situation in which part of the aquacultural ponds are filled with riverine water via sluices and flooding. Nevertheless, the contribution of the precipitation to aquacultural ponds is expected to be much higher than indicated by the model, meaning that the total volume of net recharge in the model is underestimated with respect to the daily input of net recharge. This daily input however is on the high end of the possible range. Thereby, the duration of pumping is only four months, where precipitation occurs on the variable basis for eight months. In the case of the modelled values this would indicate a total input of fresh precipitated recharge of 2.09 million m^3 per year (8,560 m^3/day x 30.5 days/month x 8 months). The total amount of pumped water in the model for four months is 1.84 million m^3/year (15,100 m^3/day x 30.5 days/month x 4 months). This would indicate fresh recharge of the aquifer to be more than the subtraction. But this is not possible to conclude from only these results. To further test this, the model should be constructed with more detailed timescales and varying amounts of pumping and net recharge through time.

The model does show pumping to be the main driver during the dry season and recharge during the wet season. This confirms fieldwork conclusion 1 regarding the pump-driven flow in the dry season.

2) To what extent do aquacultural ponds influence the groundwater flow?

The sensitivity analysis (figure 3.29) together with the cross-sectional profiles (figure 3.28) and water balance (table 3.9) clearly showed the importance and role of ponding during both the dry as well as the wet model. This major influence of ponding via recharge and drainage, of which the recharge effect is found in literature as well (Harvey et al., 2006), confirms conclusion 4 of the fieldwork regarding the influence of aquacultural ponds on the groundwater flow. Since the amount of pond water is strongly varied through the year because farmers often decide to let part of the aquacultural ponds remain dry for a period of several months the model probably overestimates this ponding effect. More information on the behavior of regional farmers regarding their aquacultural ponds is necessary to improve the modelling performance. Satellite data could be useful for this kind of study.

Since the aquacultural ponds are filled with river water during the dry season and a combination of river and precipitated water in the wet season, the salinity of the ponds is expected to be highly variable through the year with saline water in the dry season and fresh to brackish water in the wet season. As the model shows the aquacultural pondwater to infiltrate during the dry season, it is expected that ponding increases the salinity of the groundwater. The fact that the water balance (table 3.9) shows very high in- and output of constant head cells increases the expected salinization effect of aquacultural ponds in the model. These rates are however highly uncertain and the model should be improved before concluding anything.

Interestingly, the drainage effect of the aquacultural ponds seems to be higher than the infiltration effect (figure 3.29). This process was not expected to be so important before the modelling study and could be interesting to further investigate during future research.

3) To what extent does possible infiltration influence the groundwater flow?

As stated before, the model shows severe rates of infiltration during both the wet and the dry period. This infiltration is however self-induced by applying high rates of vertical conductivity to the model making it difficult to draw conclusions regarding the infiltration from the model. Nevertheless, the fact that the conductivity values that were concluded from the fieldwork had to be increased with a factor 4 to improve the modelling results (section 3.3.1) does indicate a strong importance. Thereby, the sensitivity analysis (figure 3.29) clearly shows a decrease of influence with increasing vertical conductivities, indicating vertical conductivity and thus infiltration to be a limiting factor in the groundwater flow, especially during the wet season. This is expected to be an important effect in the real situation as well since aquacultural pondwater is a significant source of recharge and the infiltration of ponds becomes limited due to the formation of a layer with very low conductivit. If the reliability of the model would be improved by implementing more detailed recharge, pumping and aquacultural ponding information, the infiltration could be studied in more detail. For now, the model together with the fieldwork results imply the infiltration to be more than was expected beforehand (hypothesis 3) which confirms fieldwork conclusion 3.

4) At what rate does the salinity distribution change?

To estimate changes in salinity distribution the flow velocity is calculated for the model (figure 3.26) and the fieldwork measurements. Figure 3.26 shows the flow towards the eastern river to be the most dominant direction in both the dry and wet season. However, this is highly uncertain since no loggers were present in the east and the head values are based on static measurements during the start of the dry season (Januray 2018). Therefor the north-south directed flow is discussed by regarding the flow velocity between piezometer 6 on the elevated homestead area and piezometer 14 in the aquacultural area. It must be noted that the model does not show any salinity variations during the period of 180 day for both models. The calculated flow velocities (as explained in previous section) are presented in table 3.11.

Table 3-11. *Calculated flow distances of the groundwater for model and measurements*

		Date	Calculated velocity [m/day]	Duration [months]	**Total annual distance [m/year]**
WET	Model	-	0.0098	8	**2.39**
	Loggers	09/10/2017	0.0263	8	**6.41**
DRY	Model	-	0.042	4	**5.12**
	Logger	11/04/2018	0.0040	4	**0.488**

These results emphasize the discrepancy between the modelled and the measured results. The model indicates a net flow of 2.73 meters/year towards the northern elevated homestead area where the logger data indicate a net flow of 5.92 meters/year towards the southern aquacultural ponds. The measured head data from the loggers are assumed to be more reliable since the model consists of many uncertainties. It is remarkable however that the relatively large amount of pumped water in comparison to recharge does not induce a severe flow to the north compared to the logger data. This net yearly southward flow indicated by the logger data implies that the current pumping does not induce salinization of the fresh water under the elevated homestead area and the pumping rates are sustainable. Thereby it is important to keep in mind that this is only the flow in one direction while the model shows flow from the east and west as well (figure 3.26). Regardless of the exact magnitudes of the flow it can be concluded that net flow rates and thus displacement of saline water are in the order of several meters per year. With minimum cell sizes of 50 by 50 meters this explains why no salinity change is visible after 1 year. The net rate is not extremely fast but as infiltration of saline water via aquacultural ponds occurs at distances of only 50 meters from irrigation or drinking water pumps this is enough to cause salinization of fresh water that is used for pumping. Whether the current pumping rate is indeed sustainable as the logger measurements on the north-south transect indicate should be investigated in more detail by extending the number of loggers or increasing the performance of the model. This could be done by decreasing the cell sizes and smoothening the interfaces of different chloride concentrations. But for now, it is expected that the pumping does not cause the fresh water reserve to be salinized by aquacultural water. This is contrary to hypothesis 4 (section 1.4) since the influence of pumping on salinity was expected to be higher before the start of this study.

4. Conclusions and recommendations

The first aim of this research was to understand and map the current hydrogeological situation of the Assasuni region. Secondly it is intended to predict the influence of this current situation regarding the future salinity distribution.

First, this study has confirmed that elevation, clay thickness and salinity are connected as was stated in *Naus (2018)*. This implies that the clay layer is generally thin under elevated areas and thick under low elevated areas with exception of regions where former river systems eroded the thick clay layer. Elevated areas are protected from saline flooding which results in fresh groundwater due to infiltration of fresh rainwater. Low-elevation regions with thin clay layers on the other hand contain saline groundwater due to infiltration of water from saline flooding. Thick clay layers at low elevation protect the groundwater from saline infiltration and result in brackish groundwater. This connection was first stated by *Naus (2018)* based on a transect in the same region and confirmed in this study of the complete Assasuni region. Since the Assasuni region consists of many different elevation and land use types this theory can be upscaled to larger areas to predict salinity and lithology with only information on the elevation. This is highly important to save time during future research.

Second, the fieldwork results showed a reversal of the groundwater flow, where flow from the elevated north to the low-elevated south in the wet season reverses during the dry season. During the wet season this flow is driven by elevation and recharge with high amounts of precipitation and no pumping. During the dry season extensive amounts of pumping for irrigation become important and exceed the elevation differences as main driver. Pumping proved to be an important driver since large local differences were visible and the calculated potential evaporation was to small induce the observed daily fall in hydraulic head. This groundwater extraction causes severe seasonal hydraulic head variations in the elevated regions near agricultural fields with pumping. Since low-elevated aquacultural fields in the Assasuni region do not contain any irrigation pumping and receive riverine water to fill the ponds, the seasonal head variation is smaller. This difference causes the reversal in groundwater flow which is shown by logger data. This flow reversal is an important and unexpected conclusion since it implies the possibility of freshwater to be salinized due to pumping. Regarding the overall goal of predicting the performance of MAR-systems this is important to regard in future studies.

To quantify this flow, a representative model is set up. The performance of the model was limited to correctly representing the overall flow conditions but it presented some important insights in the flow behavior. First it confirms the importance of ponding in the low-elevated aquacultural region and the induced infiltration through the low-conductive clay. Second, it emphasized the importance of determining the exact quantity of fresh rainwater being recharged to the aquifer in comparison to the pumped water; within the ranges of representative recharge and pumping they alternated in causing net in- and output. This relation is important to determine to what extent pumping does not cause net yearly salinization of the freshwater reserve.

Regarding flow velocities and the future salinity distribution, fieldwork results in the north-south direction on the central transect indicate a net yearly flow from the fresh elevated area towards the low saline area, indicating that the current pumping is sustainable. Contrary, the model with large pumping quantities in comparison to recharge results in a net flow velocity of 2.73 m/year towards the elevated area indicating the pumping not to be sustainable. This difference emphasizes the importance of correctly estimating and applying the recharge and pumping rates to the model. For the current situation, the fieldwork conclusion is regarded as more reliable. But this only regards the flow in one direction and a change in recharge/pumping ratio can reverse the net flow direction and thus sustainability of the pumping as visible in the model. In general, the salinity distribution with the current flow conditions is expected to remain more less constant in the near future since flow velocities are in the range of several meters per year. Off course, this is prone to climate changes inducing larger dry spells with more pumping and an increase in intensity of precipitation events decreasing the infiltrating recharge due to increased runoff. But even with this climatic change the expected net flow from fresh to saline waters will first decrease making the system less dynamic. If the system becomes salinizing this has severe implications for the population since many elevated homestead regions with fresh water are situated near saline aquacultural fields.

For future research it is first recommended to use the current model as basis and improve it by increasing the amount of stress periods so recharge and pumping can gradually be applied to the system. This way the transition between the dry and wet period can be modelled and used as calibration since an extensive spatial head distribution in this period is obtained during the fieldwork. Secondly, a smaller gridsize would improve the model results since pumping could be applied more specifically and flow will be calculated in more detail. Thirdly, more information regarding the aquacultural ponding would be useful for the model as this research showed it to be a significant factor. Satellite data could indicate the range and timing of aquacultural ponds being filled with saline river water which would again improve the modelling performance. Last, it would be useful to better investigate the flow in the west-east direction since most information currently focusses on the north-south transect. This transect does contain all processes in the region but the influence of the eastern river is expected to be much higher and important for the groundwater flow of the region. A similar transect of loggers could be used for this by placing only 2 extra piezometers in the west. This information of eastward flow is important to better understand the relation between aquacultural ponding, elevation and pumping to determine the sustainability of the latter.

Since no knowledge regarding the groundwater flow was available before the start of this study the discovered reversal in flow direction is expected to be an important contribution to further research. Even though the current situation looks sustainable this study showed the human influence of both the use of aquacultural ponds and pumping for irrigation to possibly cause salinization of the freshwater reserve.

References

Acacia Water & Dhaka University. (2015b) Spatial data base for MAR application in Khulna District. Technical Report No. 4. Geology Department, Dhaka University.

Acacia Water. (2015). MAR-UNICEF for drinking water. Retrieved April 3, 2018, from http://en.acaciawater.com/nw-29143-7-3578307/nieuws/mar-unicef_for_drinking_water.html

Acacia Water, & Dhaka University. (2015). *Spatial data base for MAR application in Khulna District. Technical Report No. 4*.

Adhikary, S. K., Das Gupta, A., & Babel, M. S. (2011). Modeling groundwater flow and salinity intrusion by advective transport in the regional unconfined aquifer of southwest Bangladesh. *Proceedings of the 3rd International Conference of European Asian Civil Engineering Forum*, (EACEF 2011), 20–22.

Auerbach, L. W., Goodbred, S. L., Mondal, D. R., Wilson, C. A., Ahmed, K. R., Roy, K., … Ackerly, B. A. (2015). Flood risk of natural and embanked landscapes on the Ganges-Brahmaputra tidal delta plain. *Nature Climate Change*, *5*(2), 153–157. https://doi.org/10.1038/nclimate2472

Ayers, J. C., Goodbred, S., George, G., Fry, D., Benneyworth, L., Hornberger, G., … Akter, F. (2016). Sources of salinity and arsenic in groundwater in southwest Bangladesh. *Geochemical Transactions*, *17*(1), 4. https://doi.org/10.1186/s12932-016-0036-6

Bot, B. (2011). *Grondwaterzakboekje*. Rotterdam: Bot Raadgevend Ingenieur.

FAO. (1959). *Soil survey of the Ganges-Kobadak area*.

Fitts, C. R. (2002). *Groundwater science*. *Elsevier*.

Future Deltas. (2016). Project: Exploring the potential of Managed Aquifer Recharge in Bangladesh. Retrieved April 3, 2018, from https://www.uu.nl/en/futuredeltas/project-exploring-the-potential-of-managaged-aquifer-recharge-in-bangladesh

George, G. J. (2013). *Characterization of salinity sources in southwestern Bangladesh evaluated through surface water and groundwater geochemical analysis*. Graduate School of Vanderbilt University.

Goswami, S. (2014). *Surface and Groundwater Interactions in Four River Systems of Satkhira District*. Dhaka University.

Harvey, C. F., Ashfaque, K. N., Yu, W., Badruzzaman, A. B. M., Ali, M. A., Oates, P. M., … Ahmed, M. F. (2006). Groundwater dynamics and arsenic contamination in Bangladesh. *Chemical Geology*, *228*(1–3 SPEC. ISS.), 112–136. https://doi.org/10.1016/j.chemgeo.2005.11.025

Hendriks, M. (2010). *Introduction to physical hydrology*. Oxford University Press.

Horneman, A., van Geen, A., Kent, D. V., Mathe, P. E., Zheng, Y., Dhar, R. K., … Ahmed, K. M. (2004). Decoupling of As and Fe release to Bangladesh groundwater under reducing conditions. Part I: Evidence from sediment profiles. *Geochimica et Cosmochimica Acta*, *68*(17), 3459–3473. https://doi.org/10.1016/j.gca.2004.01.026

Malmstrom, V. (1969). A new approach to classification of climate. *J Geogr*, *68*, 351–357. https://doi.org/10.1080/00221346908981131

Michael, H. A., & Voss, C. I. (2009). Controls on groundwater flow in the Bengal Basin of India and Bangladesh: Regional modeling analysis. *Hydrogeology Journal*, *17*(7), 1561–1577. https://doi.org/10.1007/s10040-008-0429-4

Mukherjee, A., Fryar, A. E., & Howell, P. D. (2007). Regional hydrostratigraphy and groundwater flow modeling in the arsenic-affected areas of the western Bengal basin, West Bengal, India. *Hydrogeology Journal*, *15*(7), 1397–1418. https://doi.org/10.1007/s10040-007-0208-7

Mukherjee, A., Fryar, A. E., & Thomas, W. A. (2009). Geologic, geomorphic and hydrologic framework and evolution of the Bengal basin, India and Bangladesh. *Journal of Asian Earth Sciences*, *34*(3), 227–244. https://doi.org/10.1016/j.jseaes.2008.05.011

Mukherjee, A., Saha, D., Harvey, C. F., Taylor, R. G., Ahmed, K. M., & Bhanja, S. N. (2015). Groundwater systems of the Indian Sub-Continent. *Journal of Hydrology: Regional Studies*, *4*, 1–14. https://doi.org/10.1016/j.ejrh.2015.03.005

Naus, F. (2018). Evolution of the groundwater salinity in Southwest Bangladesh : A detailed case study. *Unpublished*.
Neumann, R. B., Polizzotto, M. L., Badruzzaman, A. B. M., Ali, M. A., Zhang, Z., & Harvey, C. F. (2009). Hydrology of a groundwater-irrigated rice field in Bangladesh: Seasonal and daily mechanisms of infiltration. *Water Resources Research*, *45*(9), 1–14. https://doi.org/10.1029/2008WR007542
NWO. (2016). Delta-MAR: Governance and hydrogeological prerequisites for sustainable water suply through MAR systems in urbanizing deltas, applied to Bangladesh. Retrieved April 3, 2018, from https://www.nwo.nl/onderzoek-en-resultaten/onderzoeksprojecten/i/70/10970.html
Oude Essink, G. H. P. (2001). Density Dependent Groundwater Flow - Salt Water Intrusion and Heat Transport. *Utrecht University*, 1–6.
Oude Essink, G. H. P., van Baaren, E. S., & de Louw, P. G. B. (2010). Effects of climate change on coastal groundwater systems: A modeling study in the Netherlands. *Water Resour. Res.*, *46*(October), W00F04. https://doi.org/10.1029/2009wr008719
Philip, J. R. (1969). Theory of Infiltration. https://doi.org/10.1016/B978-1-4831-9936-8.50010-6
Radloff, K. A., Zheng, Y., Stute, M., Weinman, B., Bostick, B., Mihajlov, I., … van Geen, A. (2017). Reversible adsorption and flushing of arsenic in a shallow, Holocene aquifer of Bangladesh. *Applied Geochemistry*, *77*, 142–157. https://doi.org/10.1016/j.apgeochem.2015.11.003
Rotzoll, K., Gingerich, S. B., Jenson, J. W., & El-Kadi, A. I. (2013). Estimating hydraulic properties from tidal attenuation in the Northern Guam Lens Aquifer, territory of Guam, USA. *Hydrogeology Journal*, *21*(3), 643–654. https://doi.org/10.1007/s10040-012-0949-9
Sengupta, S., Mcarthur, J. M., Sarkar, A., Leng, M. J., Ravenscroft, P., Howarth, R. J., & Banerjee, D. M. (2008). Do ponds cause arsenic-pollution of groundwater in the Bengal Basin? An answer from West Bengal. *Environmental Science and Technology*, *42*(14), 5156–5164. https://doi.org/10.1021/es702988m
Shahid, S. (2011). Impact of climate change on irrigation water demand of dry season Boro rice in northwest Bangladesh. *Climatic Change*, *105*(3–4), 433–453. https://doi.org/10.1007/s10584-010-9895-5
Shamsudduha, M., Chandler, R. E., Taylor, R. G., & Ahmed, K. M. (2009). Recent trends in groundwater levels in a highly seasonal hydrological system: The Ganges-Brahmaputra-Meghna Delta. *Hydrology and Earth System Sciences*, *13*(12), 2373–2385. https://doi.org/10.5194/hess-13-2373-2009
Shamsudduha, M., Taylor, R. G., Ahmed, K. M., & Zahid, A. (2011). The impact of intensive groundwater abstraction on recharge to a shallow regional aquifer system: Evidence from Bangladesh. *Hydrogeology Journal*, *19*(4), 901–916. https://doi.org/10.1007/s10040-011-0723-4
van Beers, W. F. J. (1983). *The Auger hole method - A field measurement of the hydraulic conductivity of soil below the water table*. Wageningen: International Institute for Land Reclamation and Improvement/ILRI.
van Broekhoven, F. (2017). *Spatial Variability of Salinity in Groundwater in Coastal Southwest Bangladesh Frank van Broekhoven*. University of Utrecht.
Worland, S. C., Hornberger, G., & Goodbred, S. L. (2015). Source, transport, and evolution of saline groundwater in a shallow Holocene aquifer on the tidal deltaplain of southwest Bangladesh, 8331–8361. https://doi.org/10.1002/2014WR015773.Received
Younger, P. L. (1993). Simple generalized methods for estimating aquifer storage parameters. *Quarterly Journal of Engineering Geology and Hydrogeology*, *26*(2), 127–135. https://doi.org/10.1144/GSL.QJEG.1993.026.02.04

Appendix

A1– a) Logger data for the period from February 2017 to April 2018 with logger measurements per 20 minutes and b) Daily average logger data for the period August 2017 to April 2018

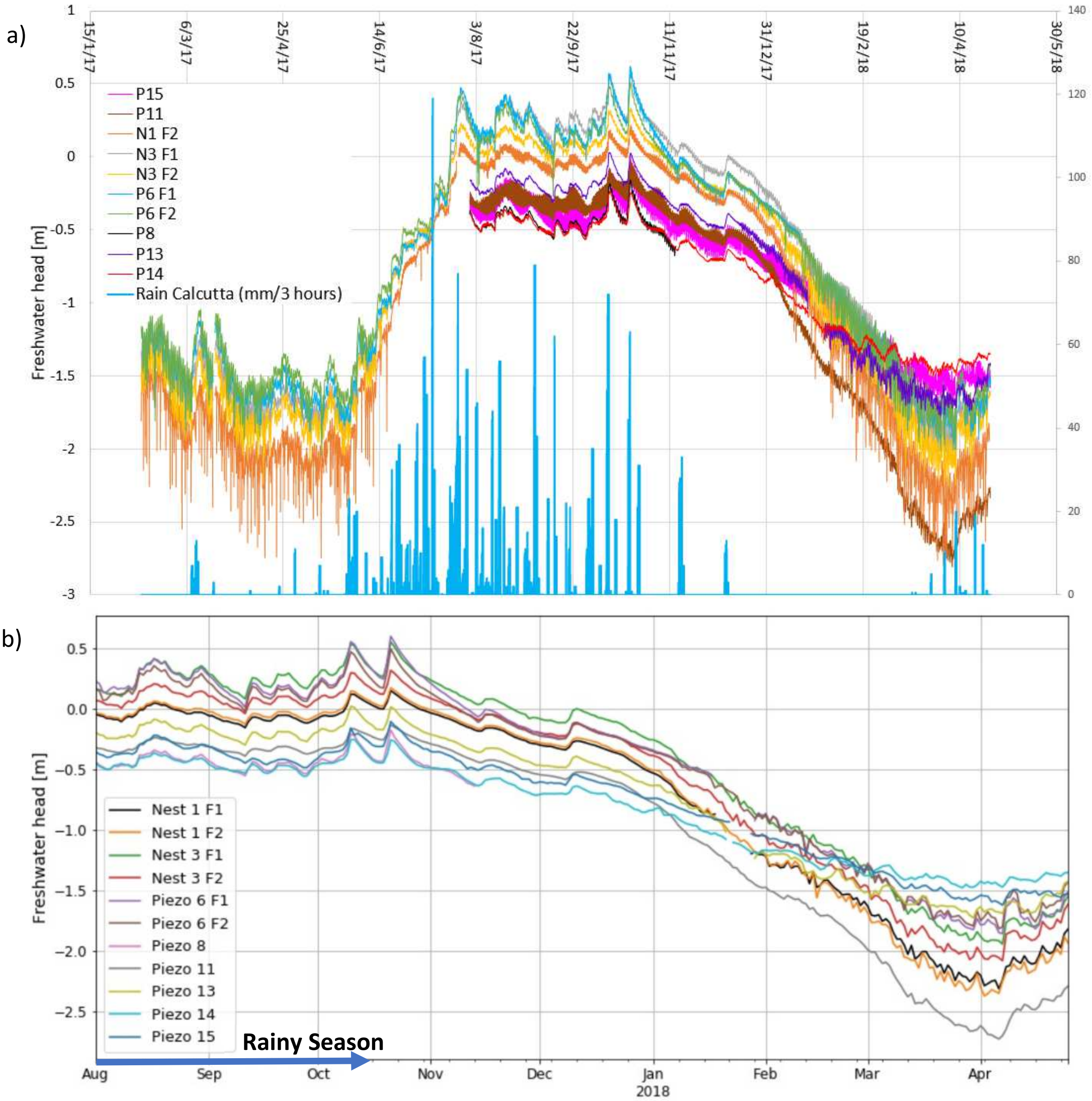

A2 – Daily variation with all loggers: Daily maximum-daily minimum

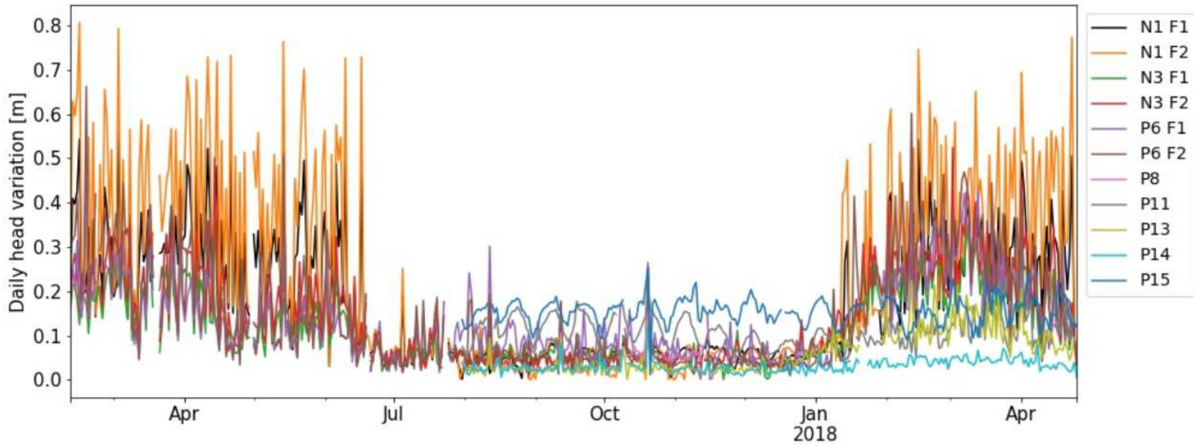

A3 – Pan experiment (Naus, 2018)

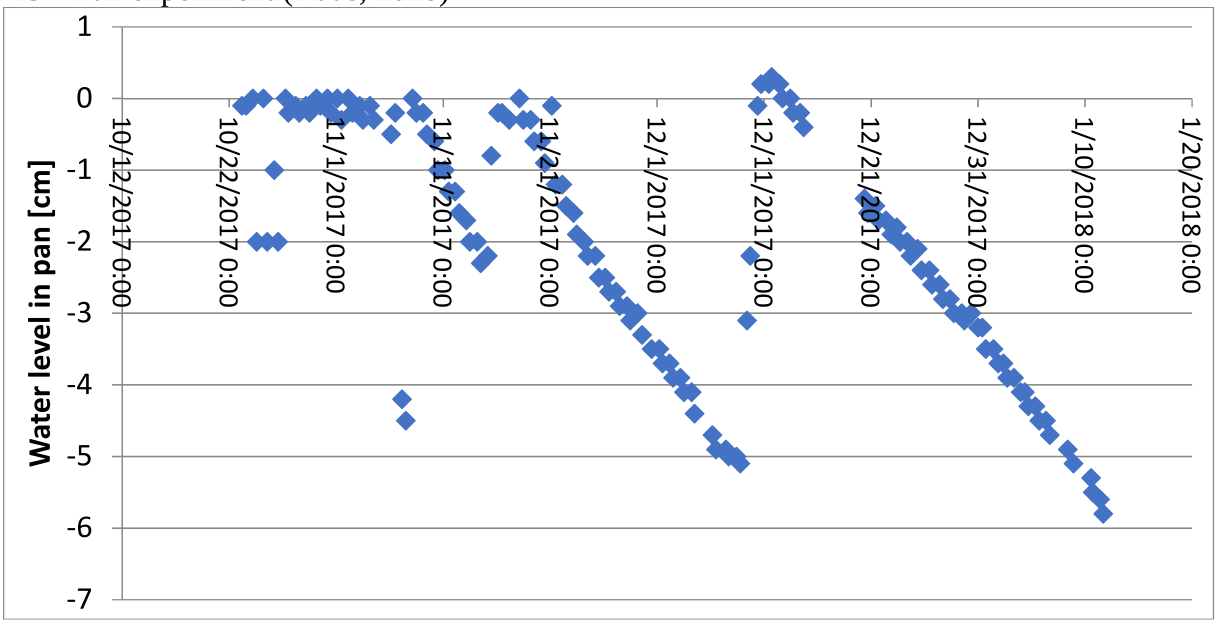

A4 – Calculated velocity vectors and hydraulic heads by SEAWAT [Layer 5]

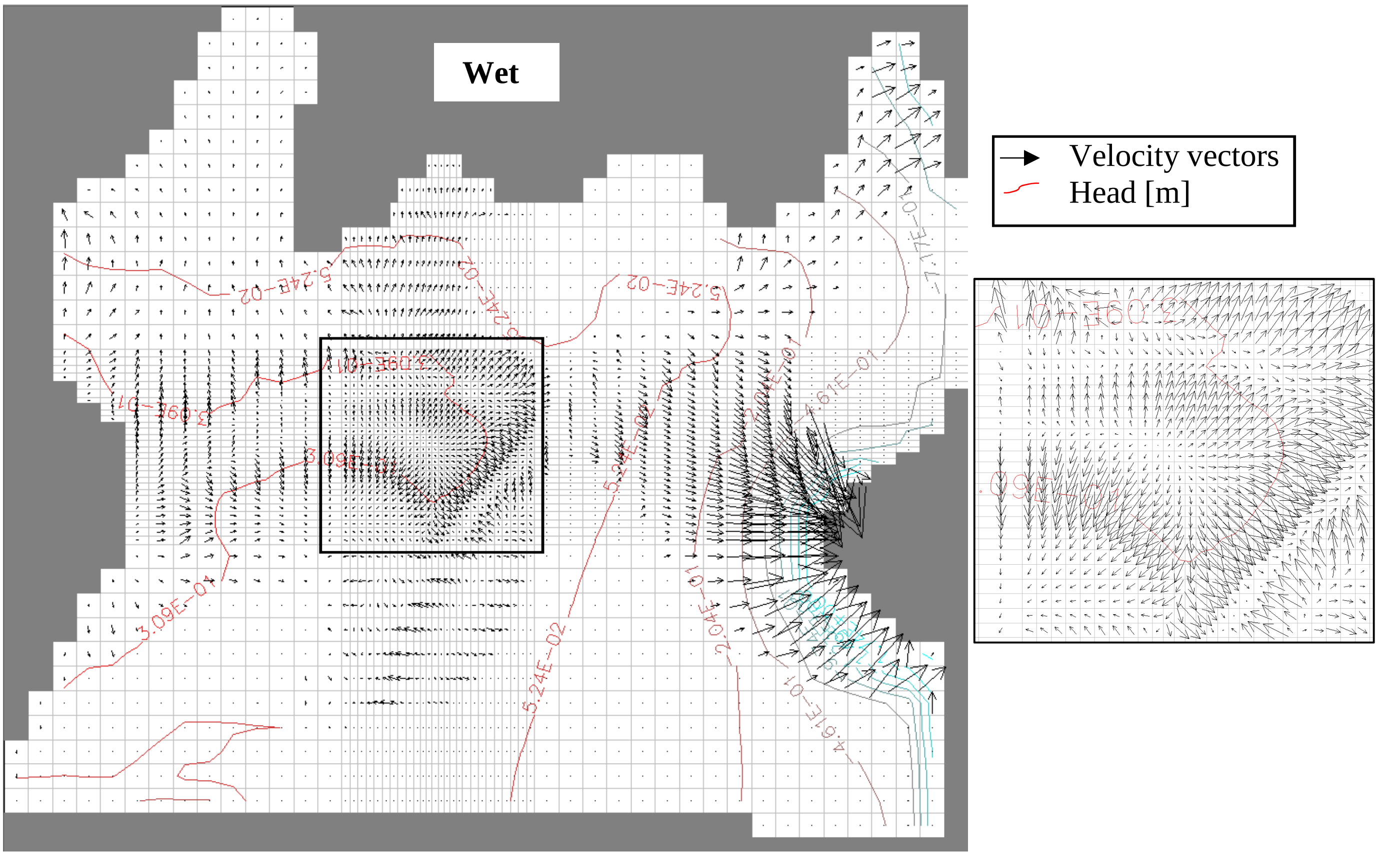

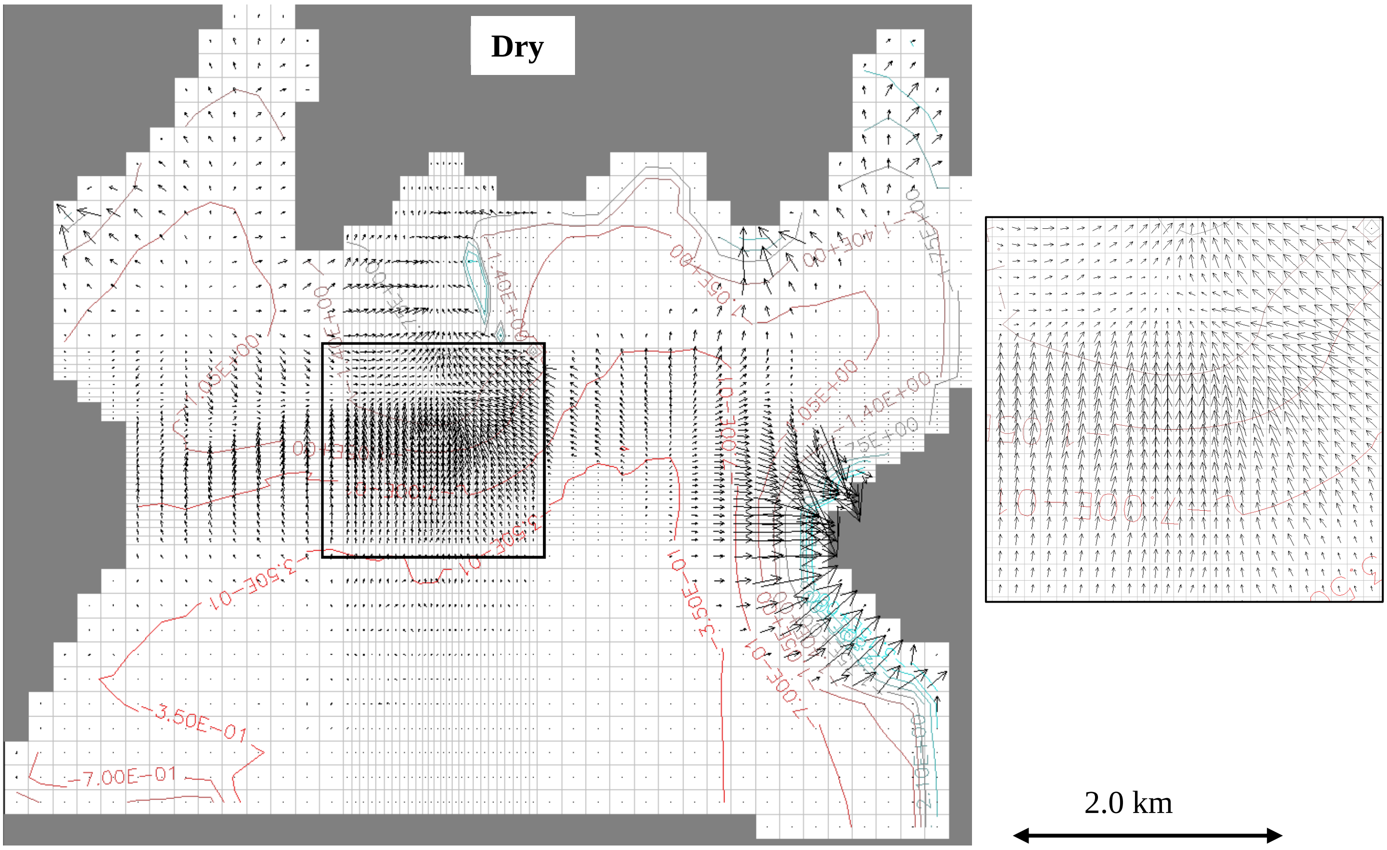

A5a – Calculated velocity vectors by SEAWAT for the North-South column 32

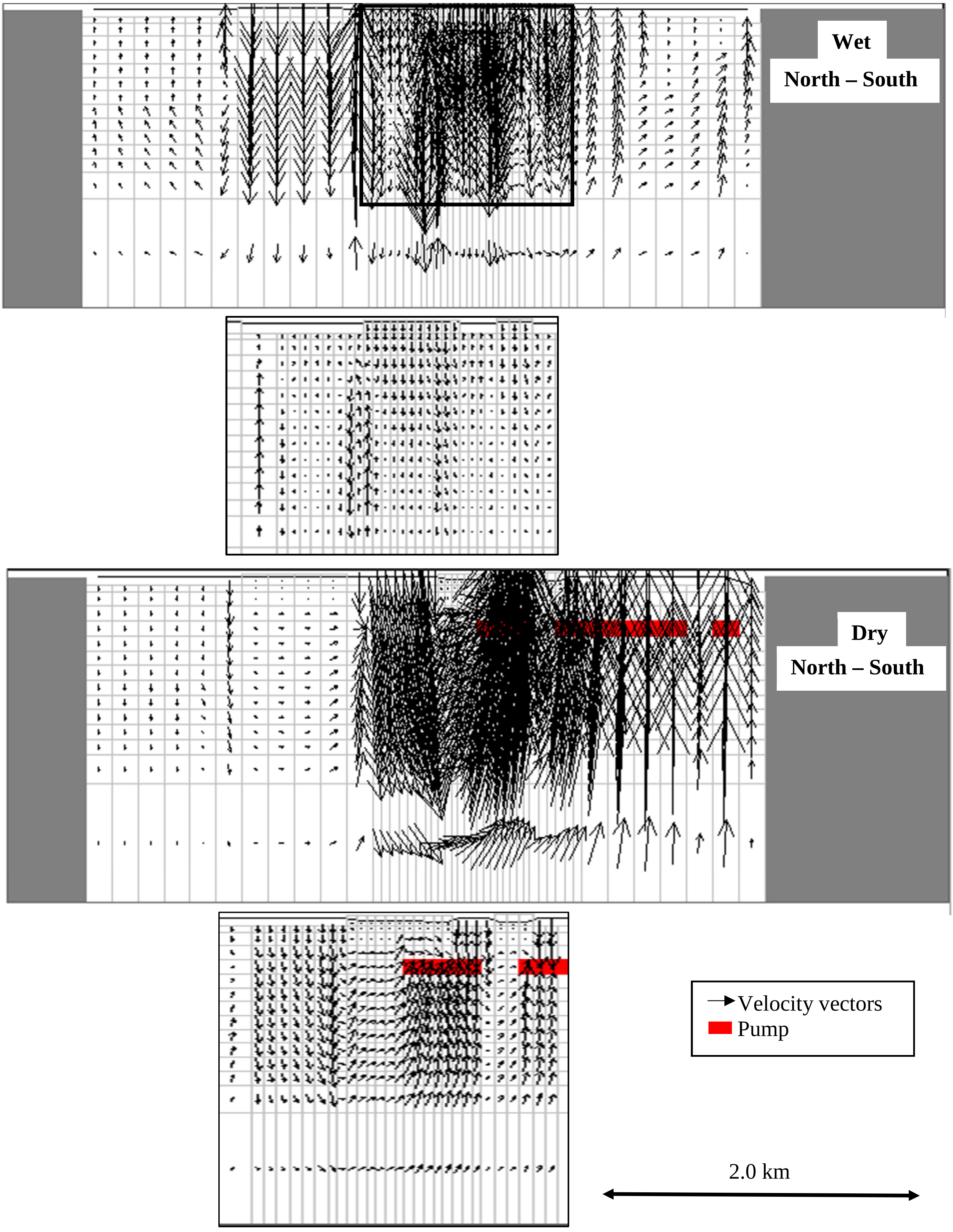

A5b – Calculated velocity vectors by SEAWAT for the West-East row 32